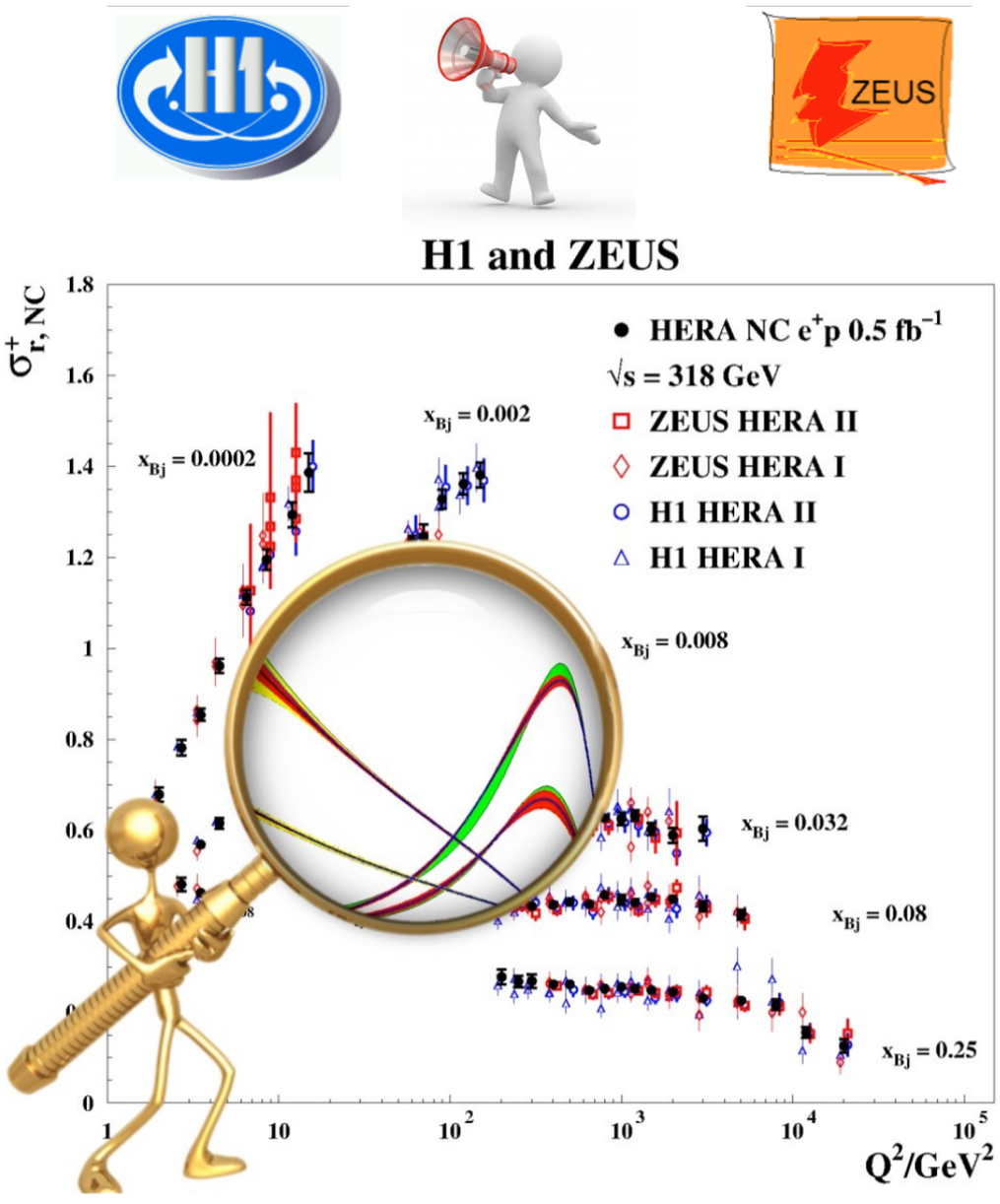

courtesy of K. Wichmann

Latest results on QCD at HERA

E. Tassi
for the H1 and ZEUS collaborations

QCD@Work - International Workshop on QCD Theory and Experiment

27-30 June 2016, Martina Franca, Italy

Outline

- HERA and structure of the proton
- NC and CC inclusive DIS cross sections
- QCD DGLAP (and EW) Analyses and proton's PDFs
- Charm and jet production

HERA and structure of the proton

HERA data are our main source of knowledge on proton structure as quantified in term of **proton's parton distribution functions (PDFs)**

Precise knowledge of PDFs is crucial in QCD and for the LHC Physics Programme:

➔ stringent tests of the Standard Model (often PDF uncertainty main limiting factor)

➔ searches of Physics Beyond the SM (need to control QCD Background)

Combination of the complete H1 and ZEUS inclusive measurements needed in order to provide the most precise input to QCD/DGLAP analyses

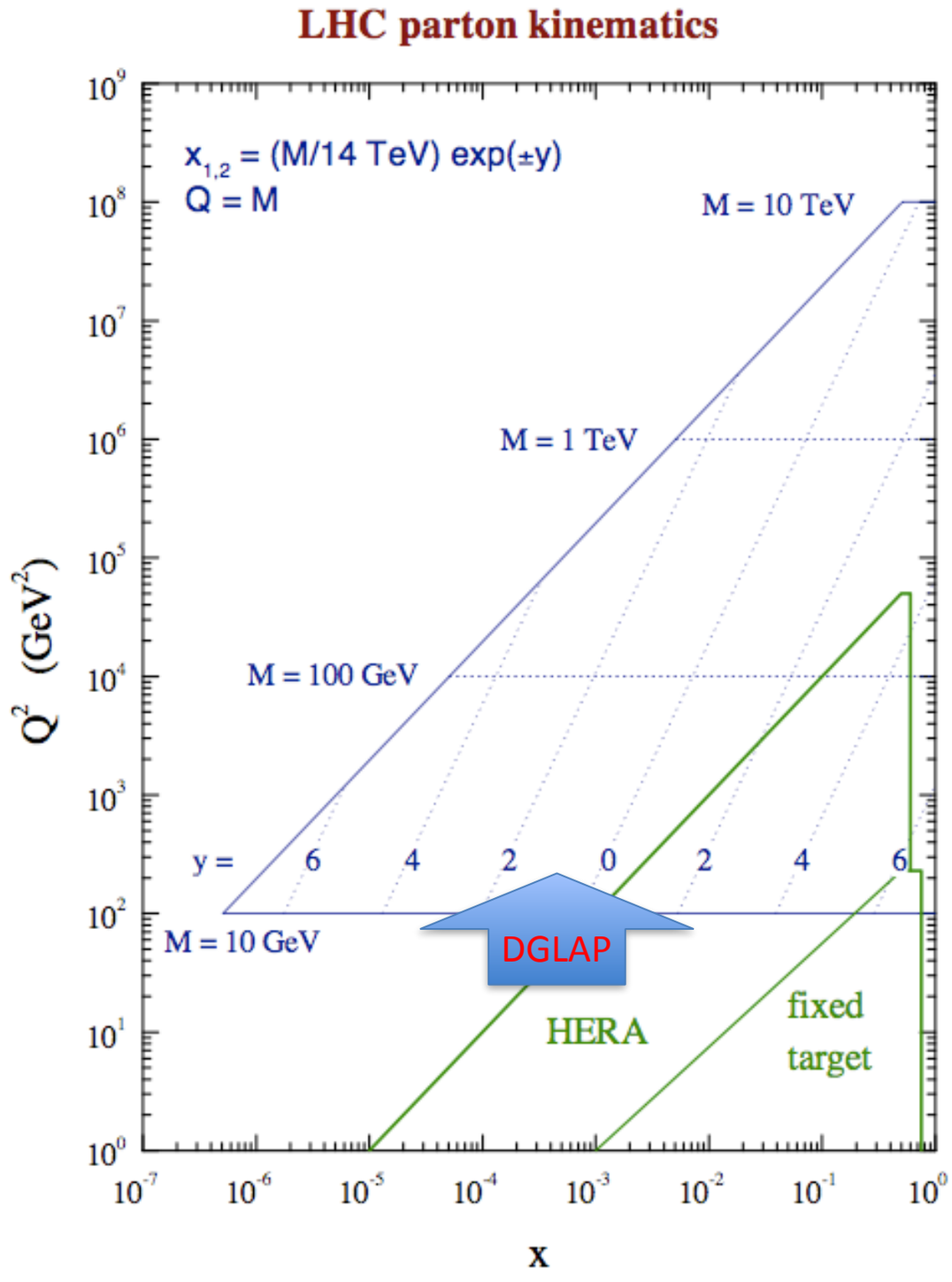

HERA Operation

HERA-I (1992-2000)
Ee=27.6 GeV
Ep=820 & 920 GeV
L_{int} ~ 130 pb^{-1} per experiment
Mostly e^+p

HERA-II (2003-2007)
Ee=27.6 GeV
Ep=920 GeV
L_{int} ~ 360 pb^{-1} per experiment
Longitudinally polarized lepton beams
Similar amounts of e^+p and e^-p

Low Energy Run 2007
Ee=27.6 GeV
Ep=460 & 575 GeV
Runs at reduced $\sqrt{s}$:
225 GeV (LER), 252 (MER) GeV
Dedicated F_L measurements

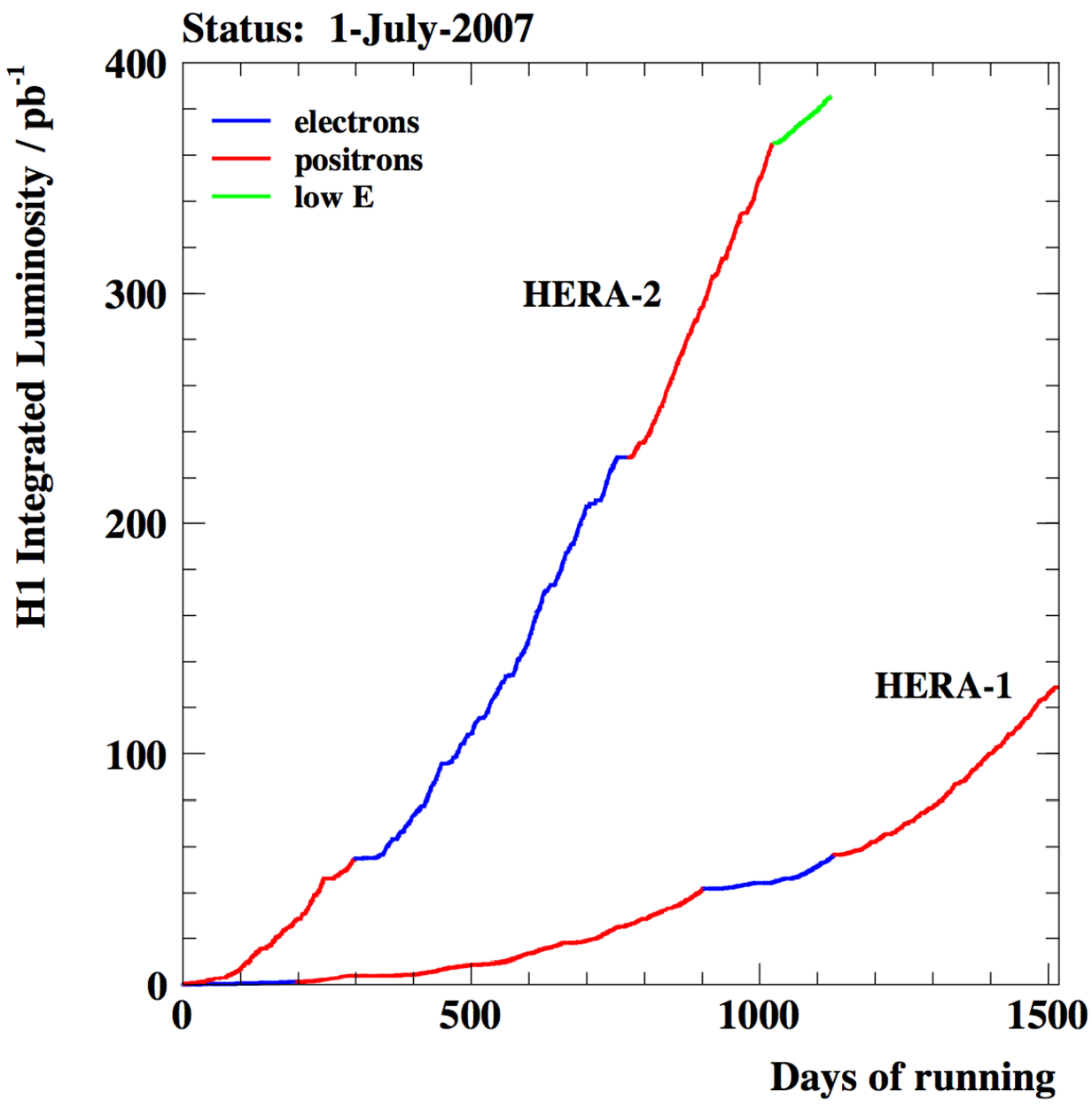

1 fb^{-1} Integrated lumi, H1+ZEUS

DIS processes and cross sections

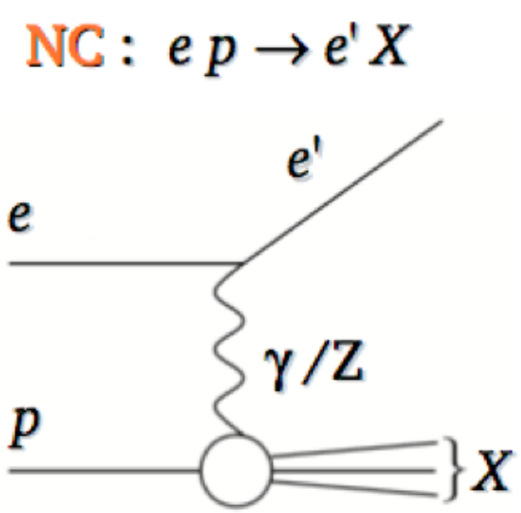

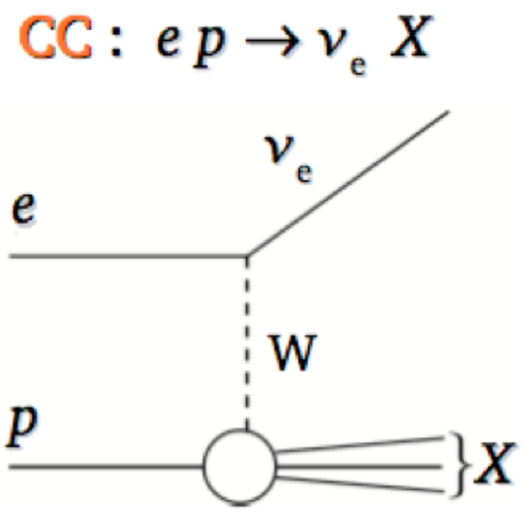

Kinematic variables:

- Virtuality exchanged boson

$$Q^2 = -q^2 = -(k - k')^2$$

- Bjorken scaling variable

$$x = \frac{Q^2}{2p \cdot q}$$

"Reduced" Cross sections

NC:

$$\sigma^{\pm}_{r,\mathrm{NC}} = \frac{d^2\sigma^{e^{\pm}p}_{\mathrm{NC}}}{dxdQ^2} \cdot \frac{Q^4 x}{2\pi\alpha^2 Y_+} = F_2 \mp \frac{Y_-}{Y_+} xF_3 - \frac{y^2}{Y_+} F_L$$

CC:

$$\sigma^{\pm}_{r,\mathrm{CC}} = \frac{d^2\sigma^{e^{\pm}p}_{\mathrm{CC}}}{dxdQ^2} \cdot \frac{2\pi x}{G_F^2} \left[\frac{M_W^2 + Q^2}{M_W^2}\right]^2 = \frac{1}{2}\left(Y_+ W_2^{\pm} \mp Y_- x W_3^{\pm} - y^2 W_L^{\pm}\right)$$

with $\quad Y_{\pm} = 1 \pm (1-y)^2$

DIS processes and cross sections

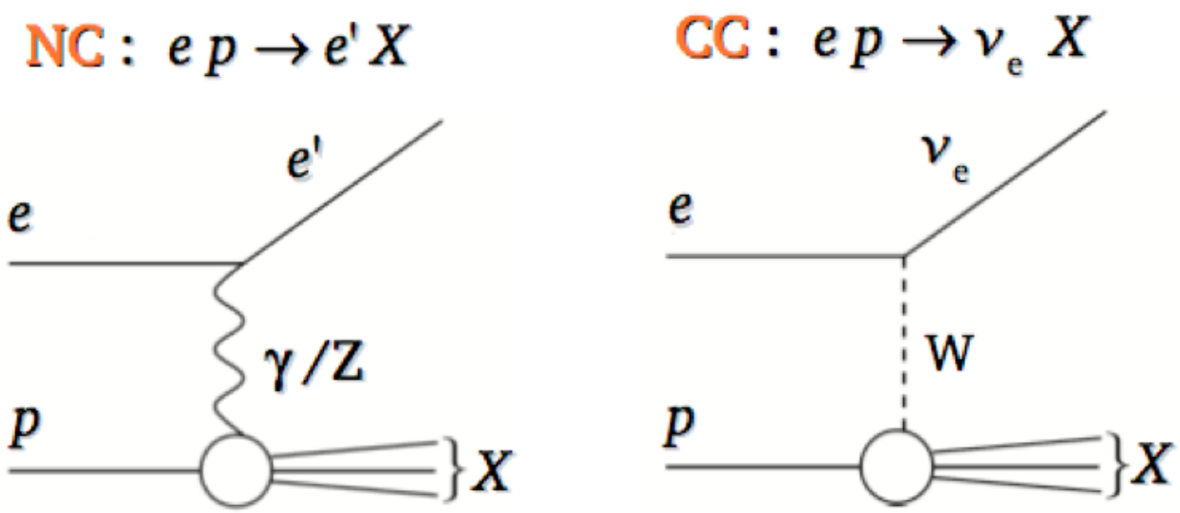

Kinematic variables:

- Virtuality exchanged boson

$$Q^2 = -q^2 = -(k - k')^2$$

- Bjorken scaling variable

$$x = \frac{Q^2}{2p \cdot q}$$

Structure Functions, PDFs and DGLAP evolution equations (LO, NLO and NNLO):

$$x^{-1} F_2(x, Q^2) = \sum_{i=q,g} \int_x^1 \frac{d\xi}{\xi} C_{2,i}\left(\frac{x}{\xi}, \alpha_s(\mu^2), \frac{\mu^2}{Q^2}\right) f_i(\xi, \mu^2)$$

$$\frac{d}{d \ln \mu^2} f_i(\xi, \mu^2) = \sum_k \left[P_{ik}(\alpha_s(\mu^2) \otimes f_k(\mu^2)) \right](\xi)$$

Combination procedure and combined results

for additional details see EPJ C75(2015)580 [arXiv:1506.06042]

Combination: Data sets

The HERA Legacy

Data Set		x_{Bj} Grid from	to	Q^2[GeV^2] Grid from	to	$\mathcal{L}$ pb^{-1}	e^+/e^-	$\sqrt{s}$ GeV	x_{Bj},Q^2 from equations	Ref.
HERA I E_p = 820 GeV and E_p = 920 GeV data sets										
H1 svx-mb [2]	95-00	0.000005	0.02	0.2	12	2.1	e^+p	301, 319	13,17,18	[3]
H1 low Q^2 [2]	96-00	0.0002	0.1	12	150	22	e^+p	301, 319	13,17,18	[4]
H1 NC	94-97	0.0032	0.65	150	30000	35.6	e^+p	301	19	[5]
H1 CC	94-97	0.013	0.40	300	15000	35.6	e^+p	301	14	[5]
H1 NC	98-99	0.0032	0.65	150	30000	16.4	e^-p	319	19	[6]
H1 CC	98-99	0.013	0.40	300	15000	16.4	e^-p	319	14	[6]
H1 NC HY	98-99	0.0013	0.01	100	800	16.4	e^-p	319	13	[7]
H1 NC	99-00	0.0013	0.65	100	30000	65.2	e^+p	319	19	[7]
H1 CC	99-00	0.013	0.40	300	15000	65.2	e^+p	319	14	[7]
ZEUS BPC	95	0.000002	0.00006	0.11	0.65	1.65	e^+p	300	13	[11]
ZEUS BPT	97	0.0000006	0.001	0.045	0.65	3.9	e^+p	300	13, 19	[12]
ZEUS SVX	95	0.000012	0.0019	0.6	17	0.2	e^+p	300	13	[13]
ZEUS NC [2] high/low Q^2	96-97	0.00006	0.65	2.7	30000	30.0	e^+p	300	21	[14]
ZEUS CC	94-97	0.015	0.42	280	17000	47.7	e^+p	300	14	[15]
ZEUS NC	98-99	0.005	0.65	200	30000	15.9	e^-p	318	20	[16]
ZEUS CC	98-99	0.015	0.42	280	30000	16.4	e^-p	318	14	[17]
ZEUS NC	99-00	0.005	0.65	200	30000	63.2	e^+p	318	20	[18]
ZEUS CC	99-00	0.008	0.42	280	17000	60.9	e^+p	318	14	[19]
HERA II E_p = 920 GeV data sets										
H1 NC $^{1.5p}$	03-07	0.0008	0.65	60	30000	182	e^+p	319	13, 19	[8][1]
H1 CC $^{1.5p}$	03-07	0.008	0.40	300	15000	182	e^+p	319	14	[8][1]
H1 NC $^{1.5p}$	03-07	0.0008	0.65	60	50000	151.7	e^-p	319	13, 19	[8][1]
H1 CC $^{1.5p}$	03-07	0.008	0.40	300	30000	151.7	e^-p	319	14	[8][1]
H1 NC med Q^2 *y.5	03-07	0.0000986	0.005	8.5	90	97.6	e^+p	319	13	[10]
H1 NC low Q^2 *y.5	03-07	0.000029	0.00032	2.5	12	5.9	e^+p	319	13	[10]
ZEUS NC	06-07	0.005	0.65	200	30000	135.5	e^+p	318	13,14,20	[22]
ZEUS CC $^{1.5p}$	06-07	0.0078	0.42	280	30000	132	e^+p	318	14	[23]
ZEUS NC $^{1.5}$	05-06	0.005	0.65	200	30000	169.9	e^-p	318	20	[20]
ZEUS CC $^{1.5}$	04-06	0.015	0.65	280	30000	175	e^-p	318	14	[21]
ZEUS NC nominal *y	06-07	0.000092	0.008343	7	110	44.5	e^+p	318	13	[24]
ZEUS NC satellite *y	06-07	0.000071	0.008343	5	110	44.5	e^+p	318	13	[24]
HERA II E_p = 575 GeV data sets										
H1 NC high Q^2	07	0.00065	0.65	35	800	5.4	e^+p	252	13, 19	[9]
H1 NC low Q^2	07	0.0000279	0.0148	1.5	90	5.9	e^+p	252	13	[10]
ZEUS NC nominal	07	0.000147	0.013349	7	110	7.1	e^+p	251	13	[24]
ZEUS NC satellite	07	0.000125	0.013349	5	110	7.1	e^+p	251	13	[24]
HERA II E_p = 460 GeV data sets										
H1 NC high Q^2	07	0.00081	0.65	35	800	11.8	e^+p	225	13, 19	[9]
H1 NC low Q^2	07	0.0000348	0.0148	1.5	90	12.2	e^+p	225	13	[10]
ZEUS NC nominal	07	0.000184	0.016686	7	110	13.9	e^+p	225	13	[24]
ZEUS NC satellite	07	0.000143	0.016686	5	110	13.9	e^+p	225	13	[24]

H1 & ZEUS have now published all their inclusive measurements (1992-2007)

- HERA-I
- HERA-II measurements at high-Q^2
- HERA-II measurements at reduced $\sqrt{s}$

$0.6 \times 10^{-6} < x_{Bj} < 0.65$, $0.045 < Q^2 < 50000$ GeV^2

41 data sets are combined:

- NC & CC cross sections
- e^+p and e^-p scattering
- 4 different $\sqrt{s}$ (318, 301, 252 and 225 GeV)

2927 data points

1307 combined points

In typical cases 3 to 6 measurements contribute to a combined result

NC e^+p accuracy reaches ~1%

The usage of different reconstruction techniques and the differences in the strengths of the detector components of the two experiments lead to a substantial reduction of the systematic uncertainties of the combined cross sections.

Combination: Grids

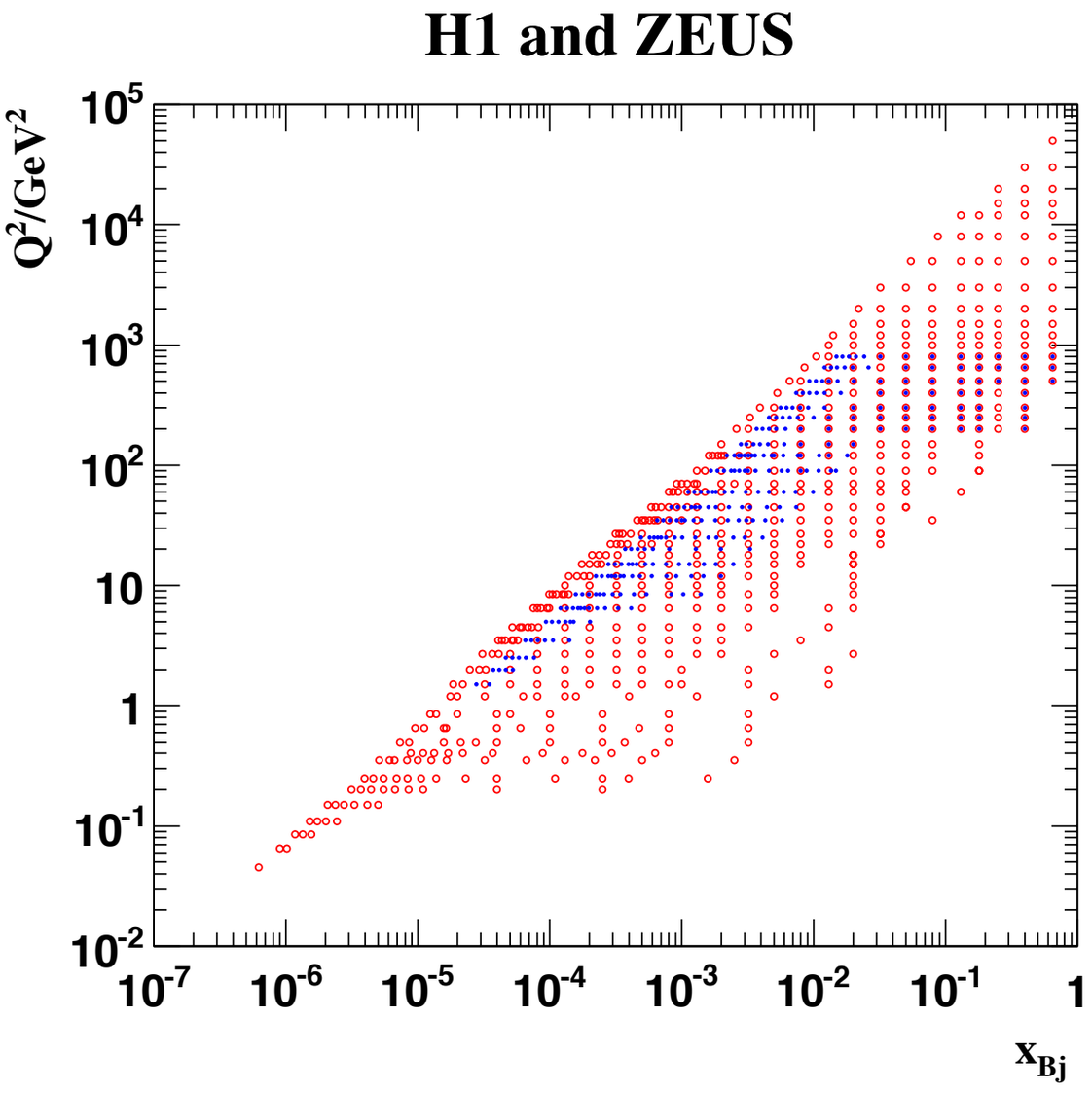

Data are combined onto a common x,Q^2 grid
Two grids are used:

- Inclusive grid for cross sections at $\sqrt{s}$ = 301, 318 GeV
- Fine-x_{BJ} grid for lower $\sqrt{s}$ measurements

Original measurements swum to the nearest grid point, via linear interpolation:

$$\sigma(x_{grid}, Q^2_{grid}) = \frac{\sigma_{model}(x_{grid}, Q^2_{grid})}{\sigma_{model}(x_{meas}, Q^2_{meas})} \cdot \sigma_{meas}(x_{meas}, Q^2_{meas})$$

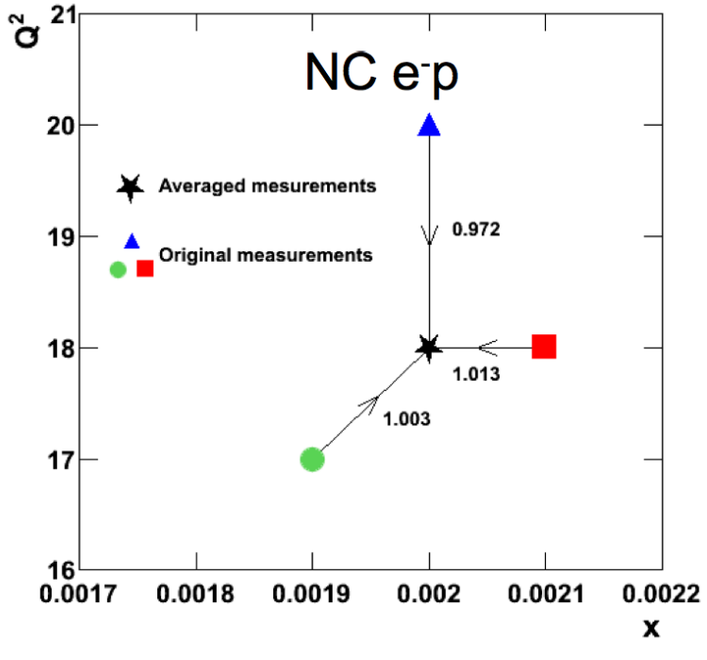

Combination: Pulls

H1 and ZEUS

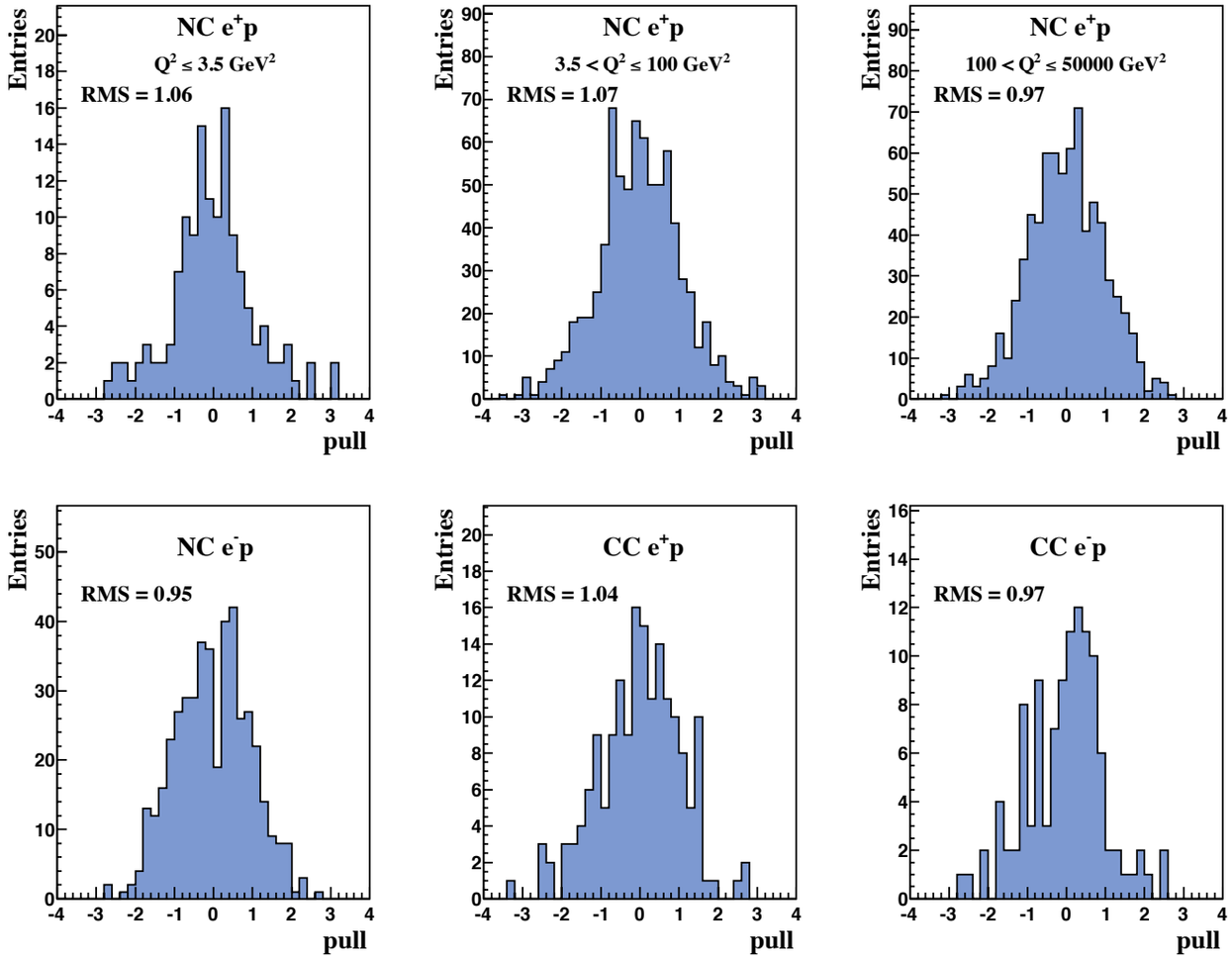

χ^2 of the combination:

$$\frac{\chi^2}{d.o.f} = \frac{1687}{1620}$$

Pull definition:

$$p^{i,k} = \frac{\mu^{i,k} - \mu^{i,ave}\left(1 - \sum_j \gamma_j^{i,k} b_{j,ave}\right)}{\sqrt{\Delta_{i,k}^2 - \Delta_{i,ave}^2}}$$

For each process pulls centred at zero with ~ unit width

Combination: Results

NC e±p , √s =318 GeV

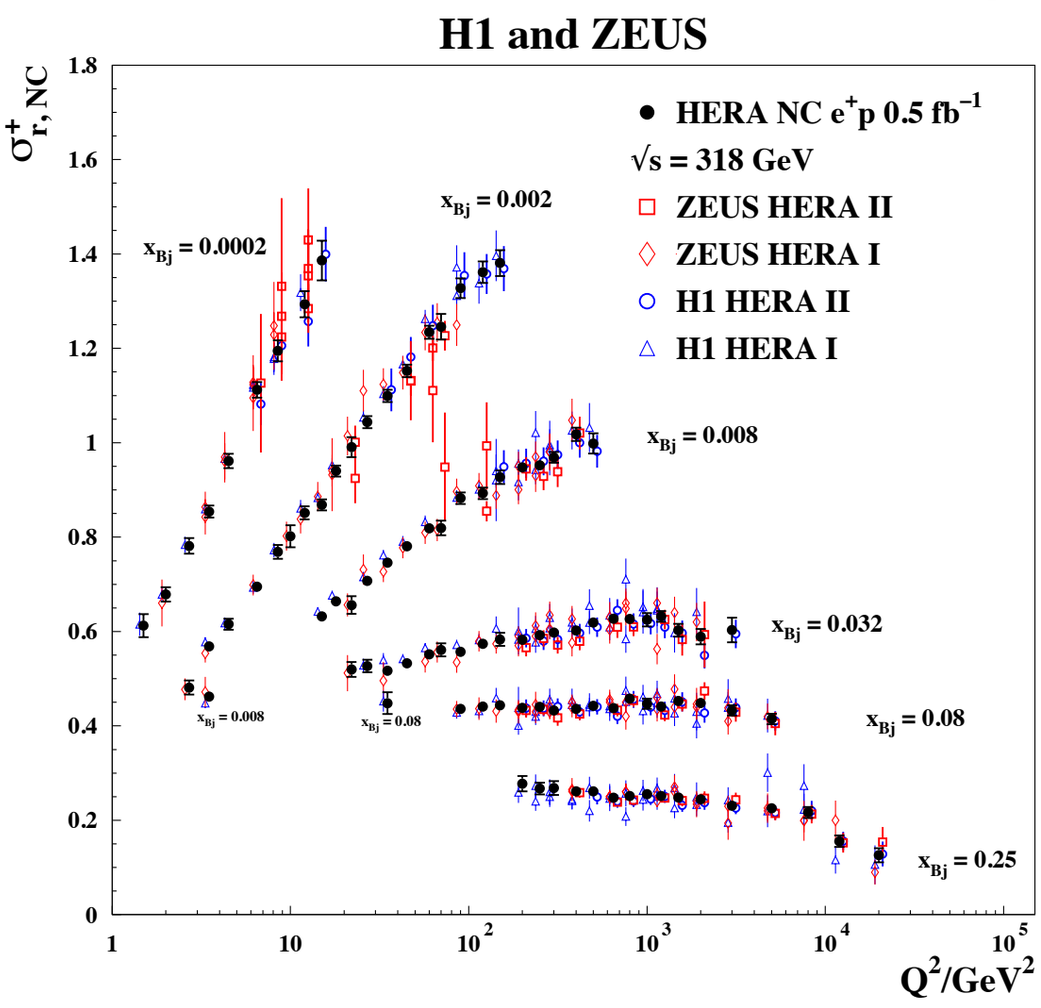

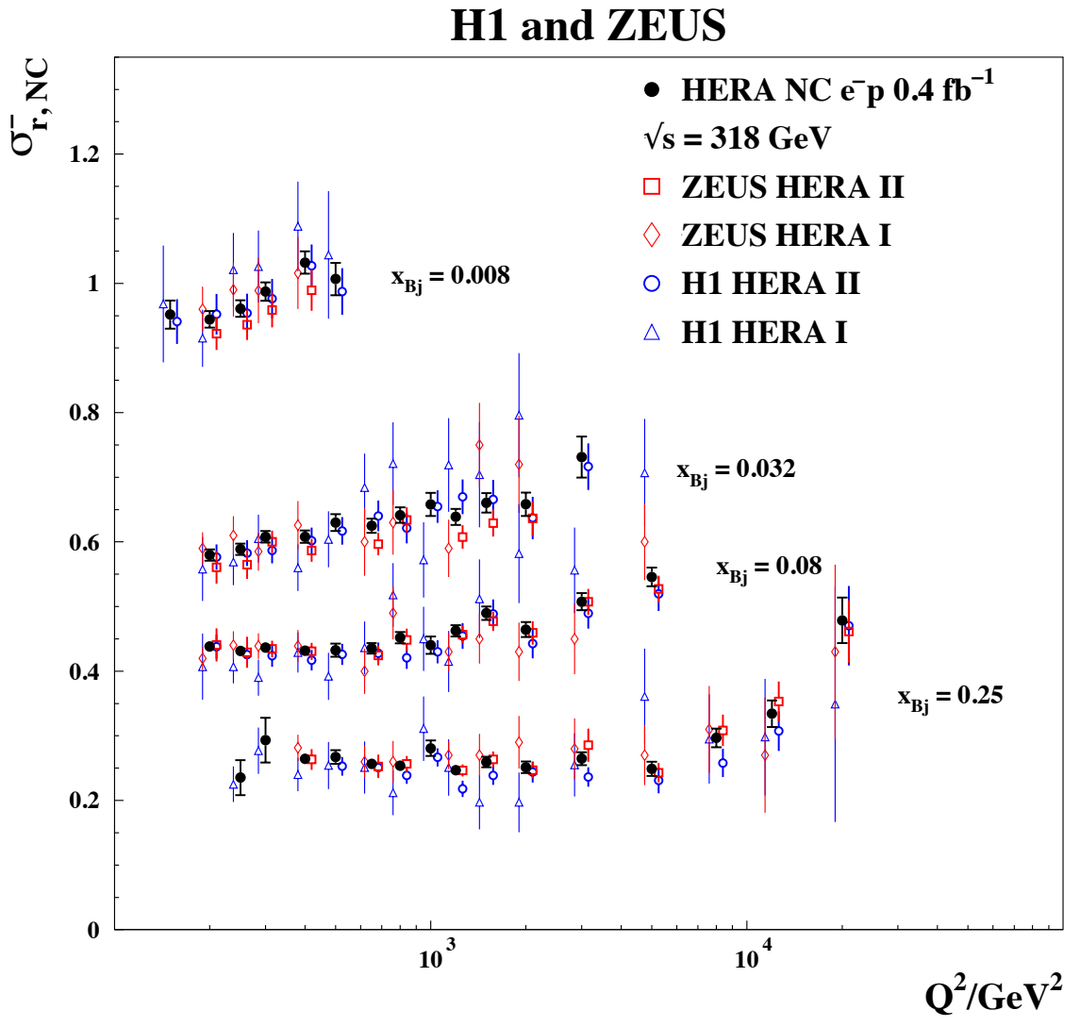

The precision of the data allows the detailed study of the scaling violations

N.B. only a few representative x_{Bj} bins are shown

Combination: Results

NC e±p , √s =318 GeV

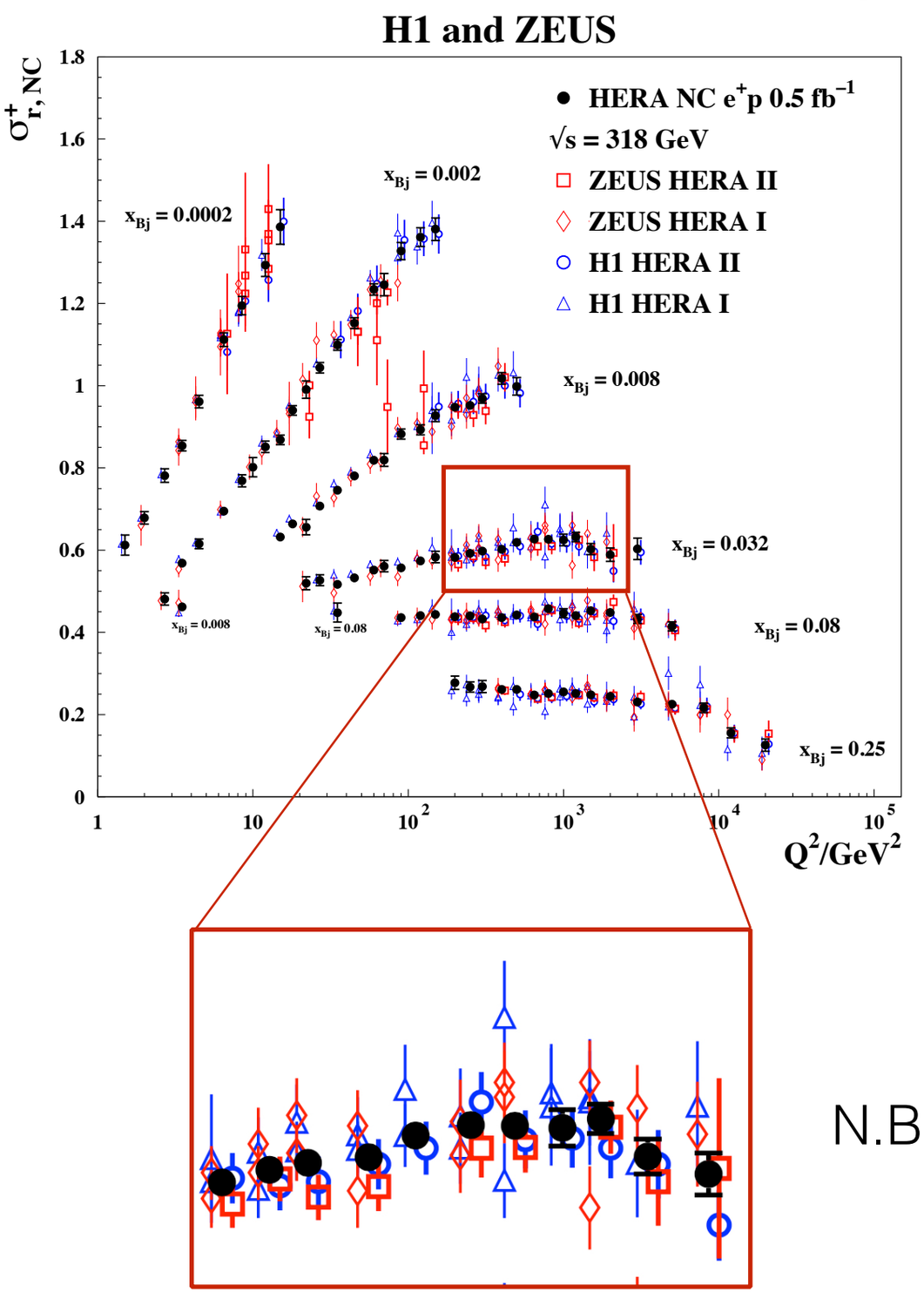

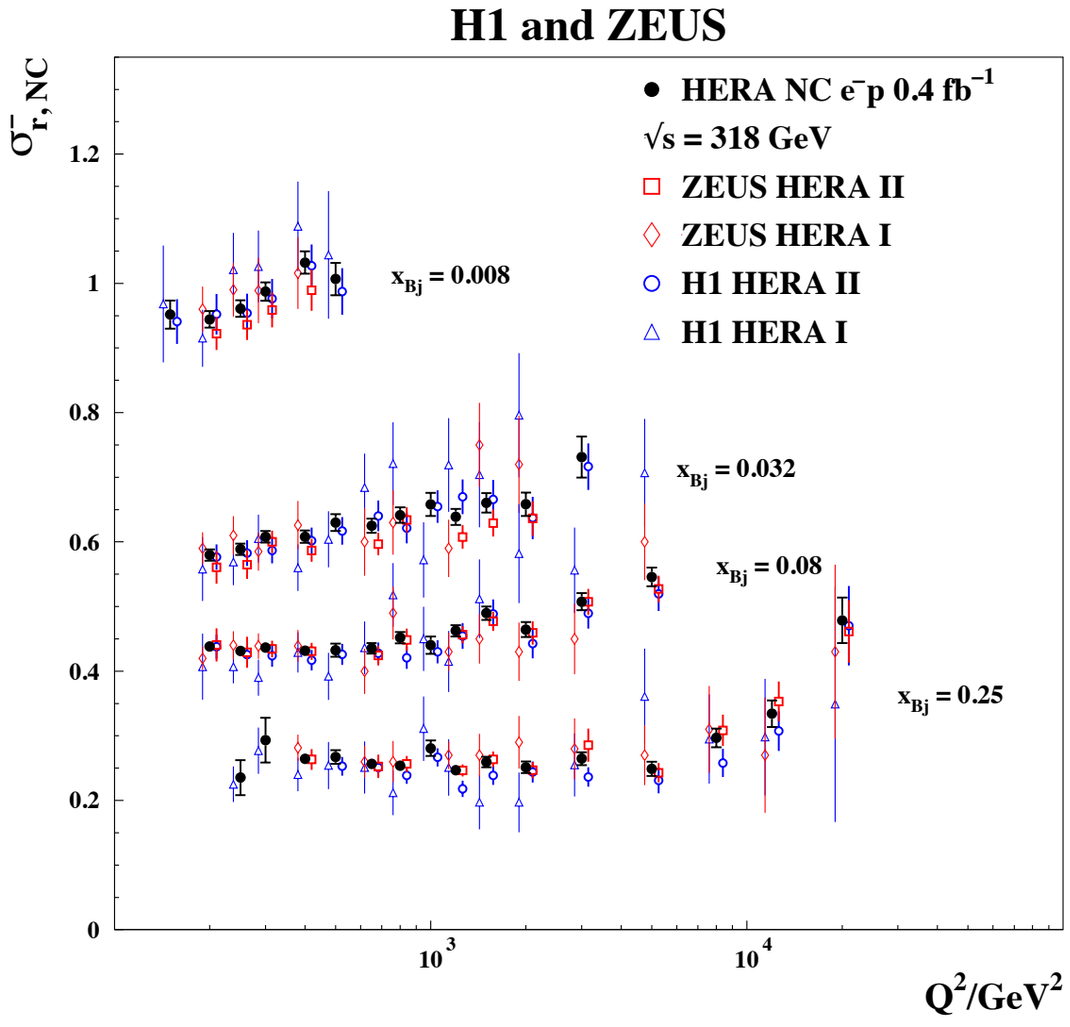

N.B. only a few representative x_{Bj} bins are shown

Combination: Results

Very low Q^2 and low x_{Bj} data $\sqrt{s}$ =300, 318 GeV

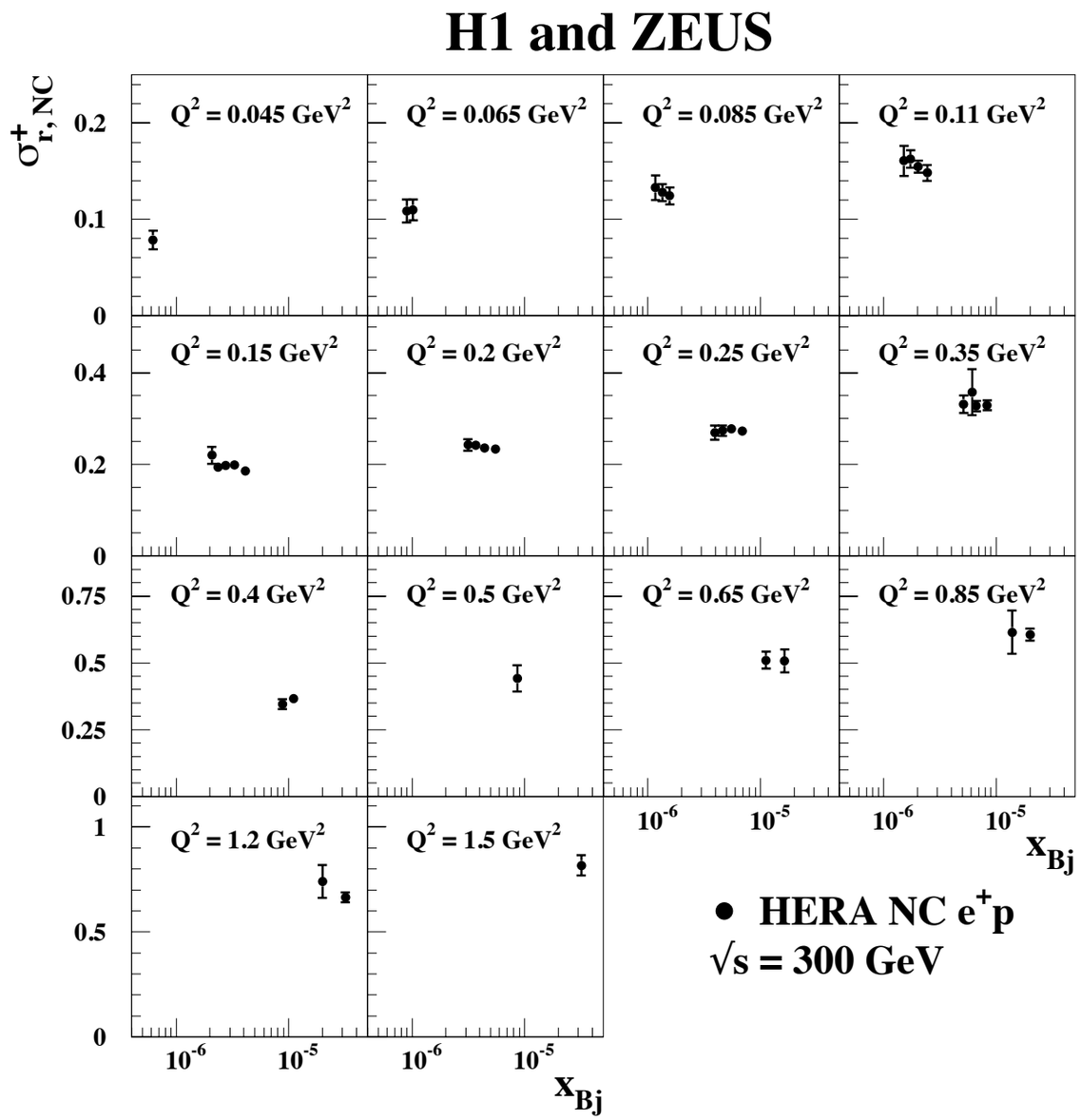

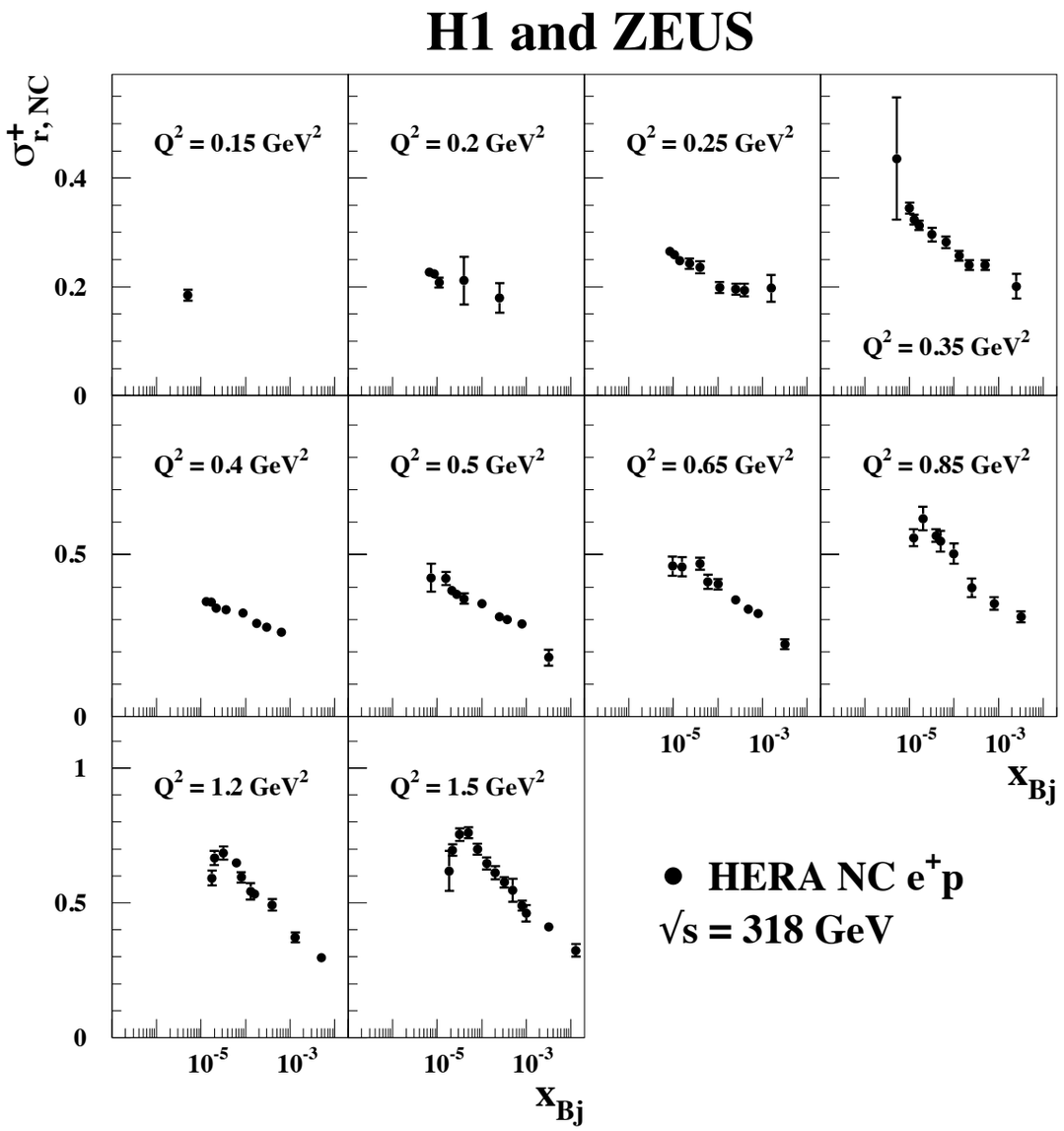

- A very important data sample for QCD studies at low-Q^2 and low-x_{Bj}
- Interesting also for dipole/saturation models and higher-twist studies

QCD Analysis and HERAPDF2.0 PDFs

for additional details see arXiv:1506.06042

HERAPDF2.0: Settings DGLAP Analysis

- QCD fits performed within the HERAFitter framework
- DGLAP Analysis based only on HERA data
- PDFs parameterised at the starting scale μ_{f0} =1.9 GeV^2:

$$xf(x) = Ax^B(1-x)^C(1+Dx+Ex^2)$$

- Final analytical form (14 params) obtained via parameter scan:

$$\begin{aligned}
xg(x) &= A_g x^{B_g}(1-x)^{C_g} - A'_g x^{B'_g}(1-x)^{C'_g}, \\
xu_v(x) &= A_{u_v} x^{B_{u_v}}(1-x)^{C_{u_v}}\left(1+E_{u_v}x^2\right), \\
xd_v(x) &= A_{d_v} x^{B_{d_v}}(1-x)^{C_{d_v}}, \\
x\bar{U}(x) &= A_{\bar{U}} x^{B_{\bar{U}}}(1-x)^{C_{\bar{U}}}\left(1+D_{\bar{U}}x\right), \\
x\bar{D}(x) &= A_{\bar{D}} x^{B_{\bar{D}}}(1-x)^{C_{\bar{D}}}.
\end{aligned}$$

This additional term was added to increase the flexibility of xg(x) as x approaches zero. Used in the variant fit HERAPDF2.0AG

- Heavy Flavours: Roberts-Thorne VFNS (RTOPT) and two FF Schemes (other VFNS also studied: ACOT and FONNL)
- Fits performed at LO, NLO and NNLO and for Q^2_{min}=3.5 and 10 GeV^2
- Detailed study of PDFs uncertainties: experimental, model and parameterisation

HERAPDF2.0: Uncertainties

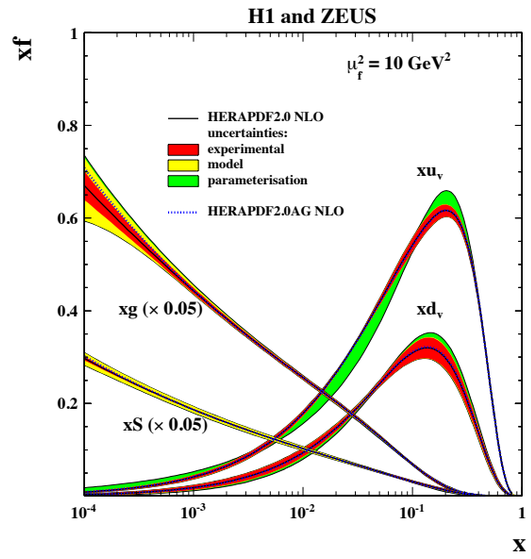

Three different uncertainty components are considered

Experimental uncertainties

Consistent data sets ➔ use Hessian Method with $\Delta\chi^2=1$
(Cross checked with a MC method based on pseudo data sets (replicas))

Model Uncertainties

The following variations are considered:

Variation	Standard Value	Lower Limit	Upper Limit
$Q^2_{\min}$ [GeV^2]	3.5	2.5	5.0
$Q^2_{\min}$ [GeV^2] HiQ2	10.0	7.5	12.5
M_c(NLO) [GeV]	1.47	1.41	1.53
M_c (NNLO) [GeV]	1.43	1.37	1.49
M_b [GeV]	4.5	4.25	4.75
f_s	0.4	0.3	0.5

Parameterisation uncertainties:

1. Addition of the parameters D and E in the parameterisation formula:

$$xf(x) = Ax^B(1-x)^C(1+Dx+Ex^2)$$

2. Variation of the starting scale μ_{f0}:

μ_{f_0} [GeV]	1.9	1.6	2.2

Variants of the HERAPDF2.0 PDFs

The following variants of the HERAPDF2.0 PDFs have been released and will soon be available on LHAPDF (https://lhapdf.hepforge.org)

HERAPDF2.0 (NLO,NNLO, Q^2_{min}=3.5 GeV^2) "Default PDF set"

- Data: combined HERA NC and CC inclusive cross sections
- HF Scheme: ROPT
- $\alpha_s(M_Z^2)$=0.118
- Grid with different $\alpha_s(M_Z^2)$ values (in the range [0.110-0.130] in steps of 0.01) are also released

HERAPDF2.0HiQ2 (NLO,NNLO) "High-Q^2 version"

- as HERAPDF2.0 but with Q^2_{min}= 10 GeV^2

HERAPDF2.0AG (LO,NLO,NNLO, Q^2_{min}=3.5 GeV^2) "Alternative Gluon"

- Data: combined HERA NC and CC inclusive cross sections
- Use an alternative gluon parameterisation
- HF Scheme: ROPT
- $\alpha_s(M_Z^2)$=0.130 (LO) and $\alpha_s(M_Z^2)$=0.118 (NLO,NNLO)

HERAPDF2.0FF (NLO, Q^2_{min}=3.5 GeV^2) "FF Schemes"

- Data: combined HERA NC and CC inclusive cross sections
- HF Schemes: Use two alternative (**FF3A** and **FF3B**) Fixed-Flavour schemes
- $\alpha_s(M_Z^2)^{Nf=3}$=0.106573 equivalent to $\alpha_s(M_Z^2)^{Nf=5}$=0.118(FF3A) and $\alpha_s(M_Z^2)$=0.118 (FF3B)

HERAPDF2.0Jets (NLO, Q^2_{min}=3.5 GeV^2) "Charm and Jets"

- Data: combined HERA NC and CC inclusive cross sections and selected HERA charm and jet production measurements
- HF Schemes: ROPT
- free $\alpha_s(M_Z^2)$ or $\alpha_s(M_Z^2)$=0.118

HERAPDF2.0: χ^2 and Q^2_{min} Study

HERAPDF	Q^2_{min}[GeV^2]	χ^2	d.o.f.	χ^2/d.o.f
2.0 NLO	3.5	1357	1131	1.200
2.0HiQ2 NLO	10.0	1156	1002	1.154
2.0 NNLO	3.5	1363	1131	1.205
2.0HiQ2 NNLO	10.0	1146	1002	1.144
2.0 AG NLO	3.5	1359	1132	1.201
2.0HiQ2 AG NLO	10.0	1161	1003	1.158
2.0 AG NNLO	3.5	1385	1132	1.223
2.0HiQ2 AG NNLO	10.0	1175	1003	1.171
2.0 NLO FF3A	3.5	1351	1131	1.195
2.0 NLO FF3B	3.5	1315	1131	1.163
2.0Jets $\alpha_s(M_Z^2)$ fixed	3.5	1568	1340	1.170
2.0Jets $\alpha_s(M_Z^2)$ free	3.5	1568	1339	1.171

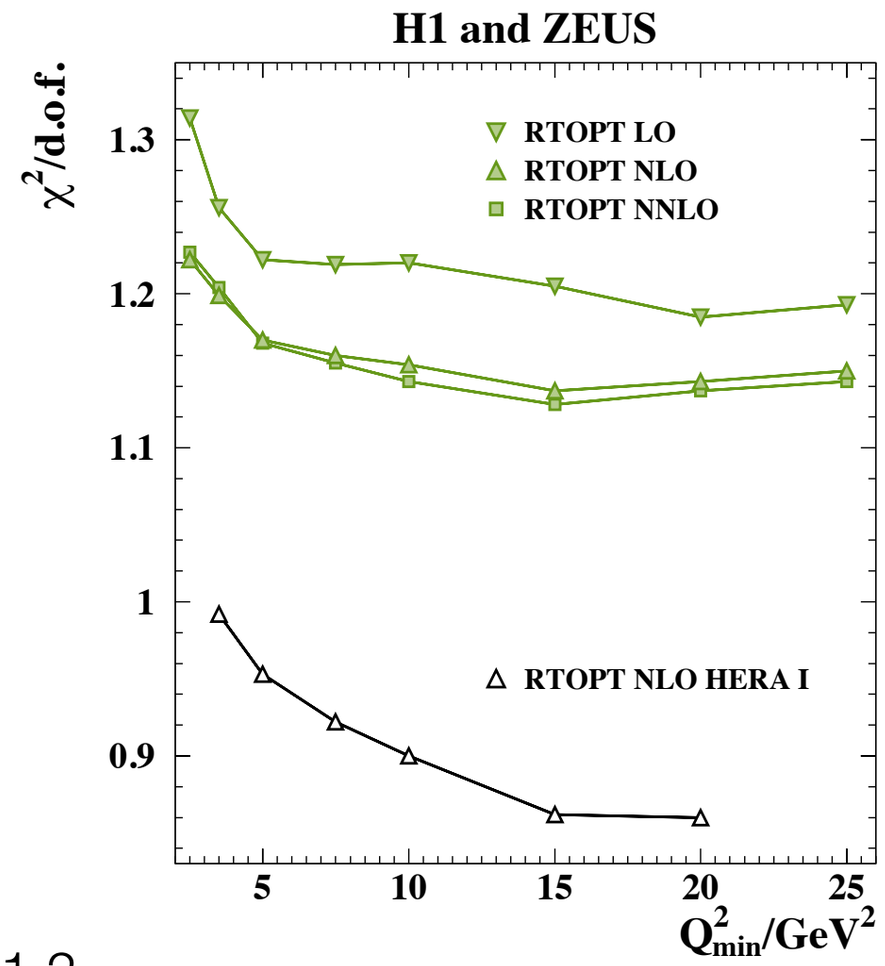

- The χ^2/d.o.f for the HERAPDF2.0 fits are typically ~ 1.2
  - somewhat larger w.r.t. to HERA-I fits (for which we had values ~1)
  - the increase is due to low-Q^2 (Q^2<15 GeV^2) and high-Q^2 (Q^2> 150 GeV^2) data

- The dependence of χ^2/d.o.f was investigated
  - the χ^2/d.o.f decreases until Q^2 ~10-15 GeV^2 both at NLO and NNLO; a trend also observed in HERA-I fits.
  - a Q^2_{min} cut at 10 GeV^2 improves marginally the quality of the fit

HERAPDF2.0: NLO and NNLO PDFs

NLO

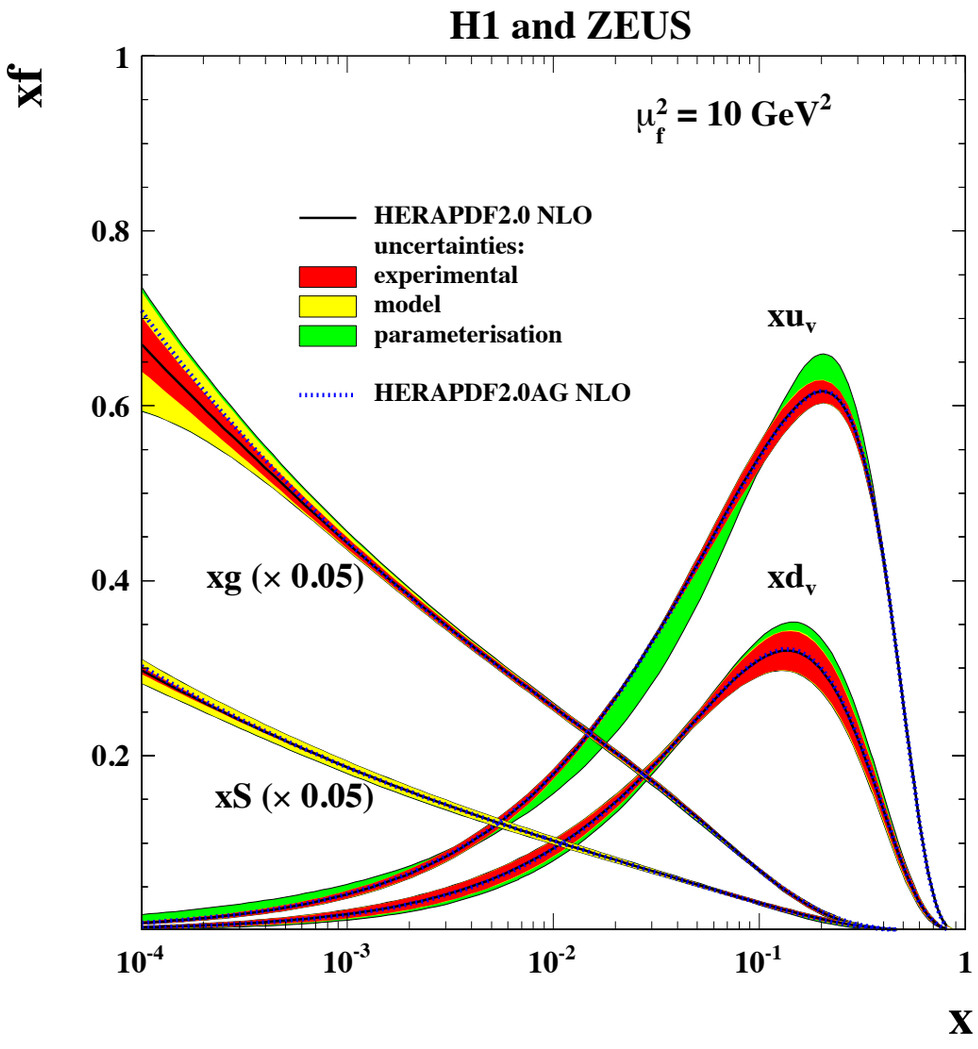

NNLO

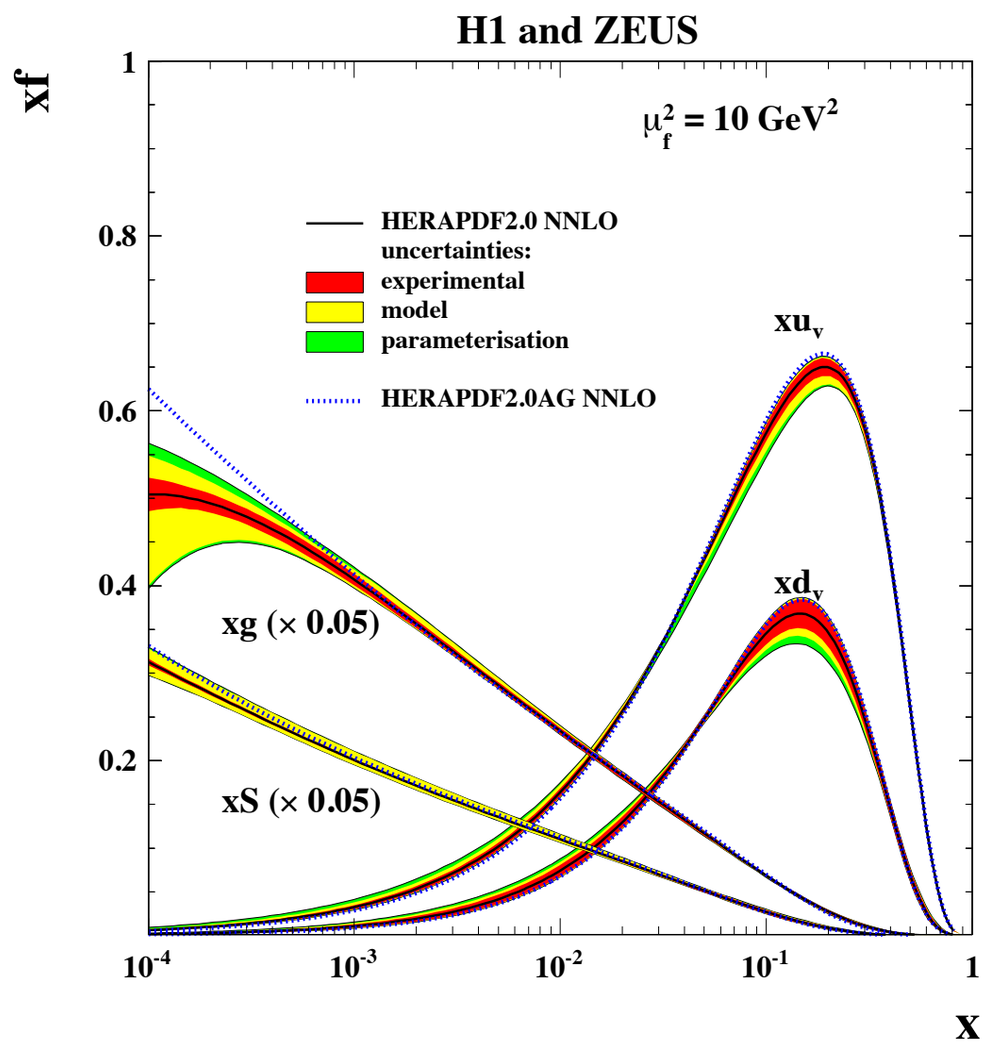

NNLO vs NLO:
- gluon ceases to rise at low-x
- sea at low-x somewhat steeper w.r.t. NLO

HERAPDF2.0: Comparison to HERAPDF1.0 and 1.5

NLO

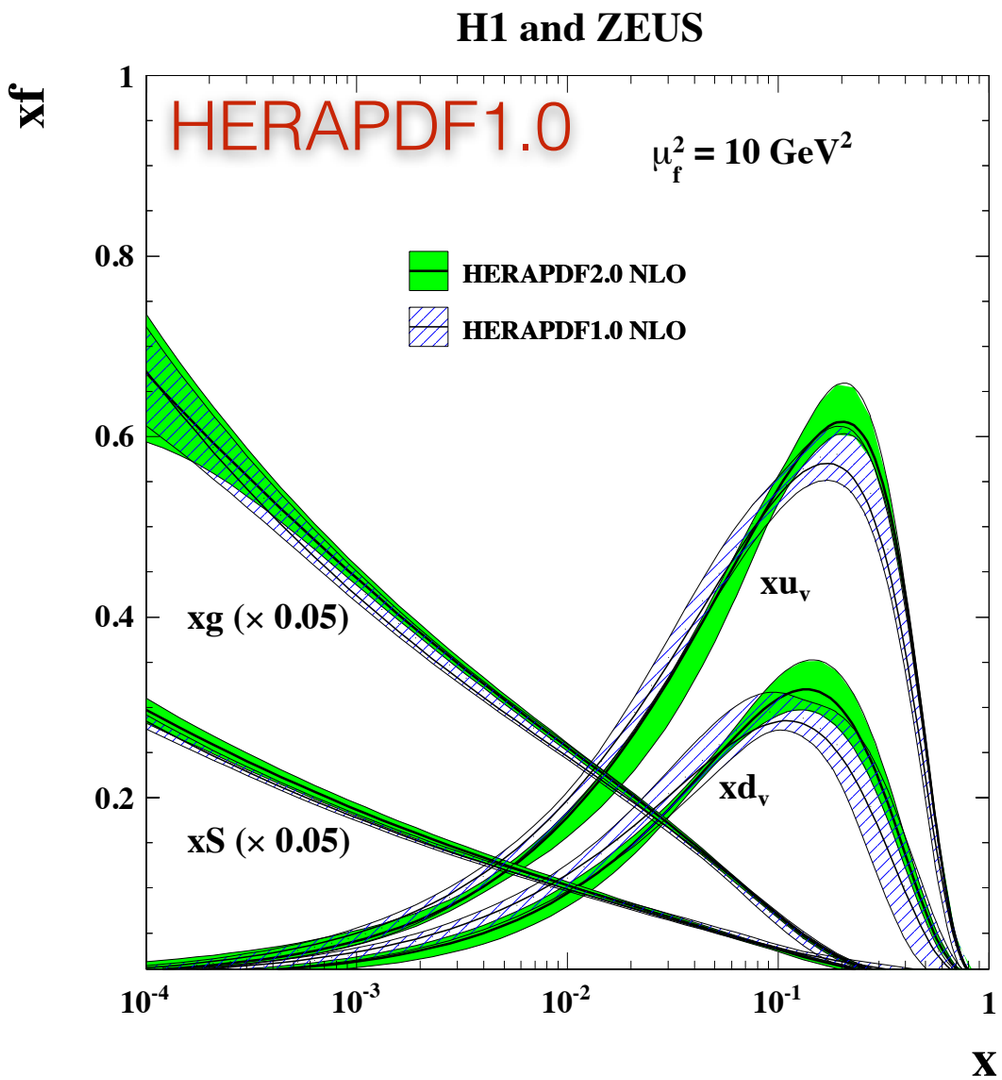

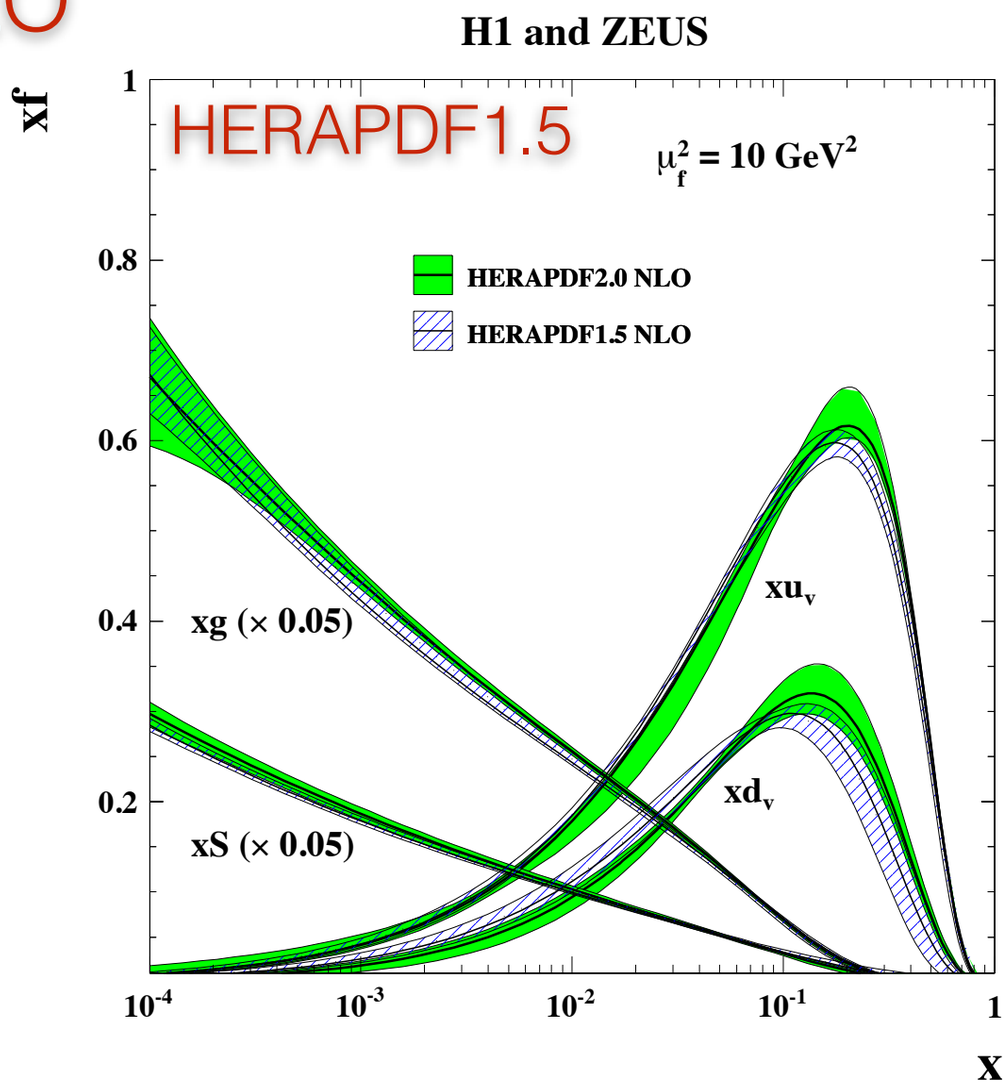

- Large reduction of the uncertainties w.r.t. to previous releases
- A little harder shape for the valence distributions
  (see backup slides for a close comparison in the high-x region)

Comparison to inclusive HERA data

for additional details see arXiv:1506.06042

Comparison to inclusive HERA data

NC e^+p $\sqrt{s}$ =318 GeV

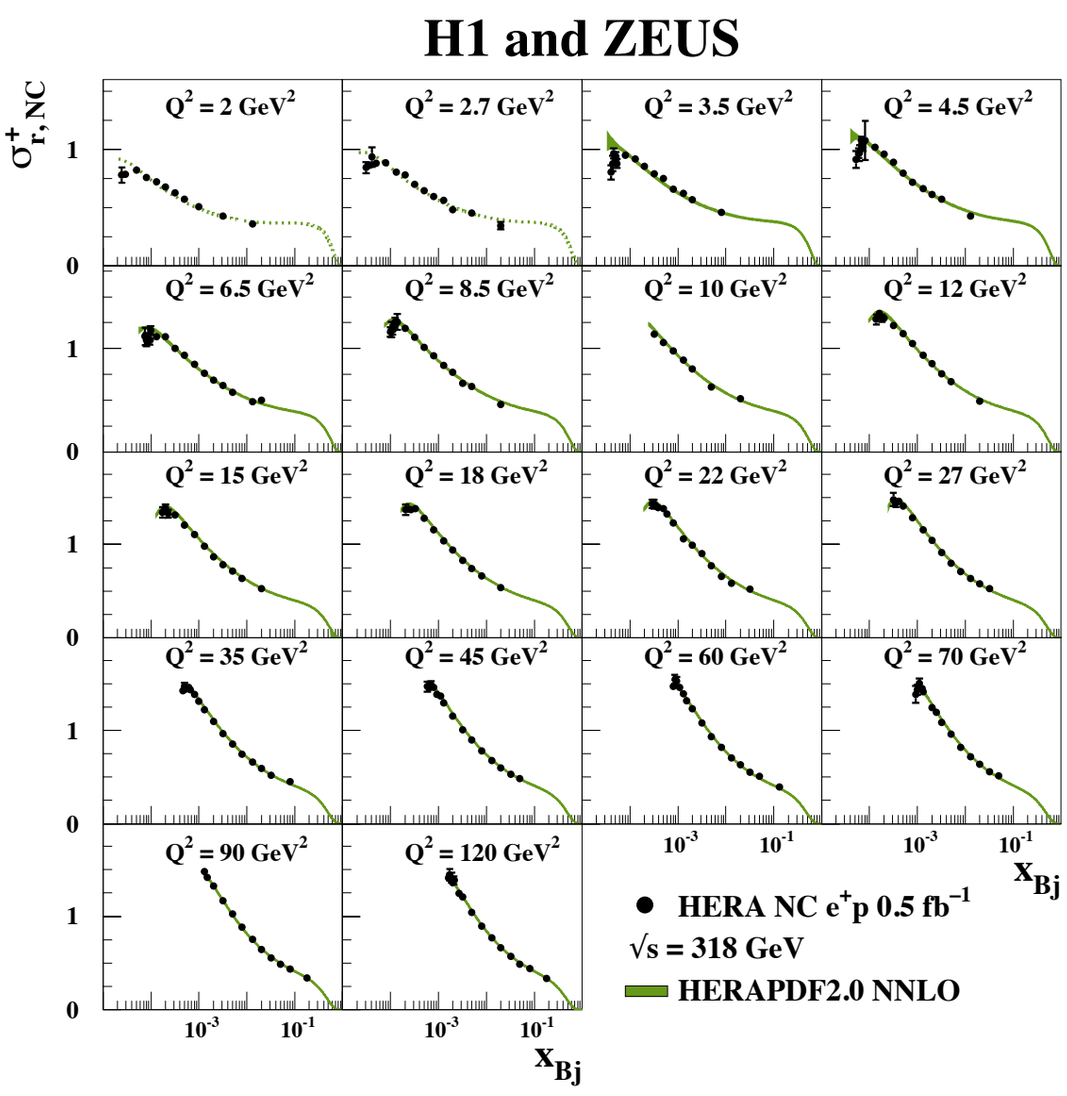

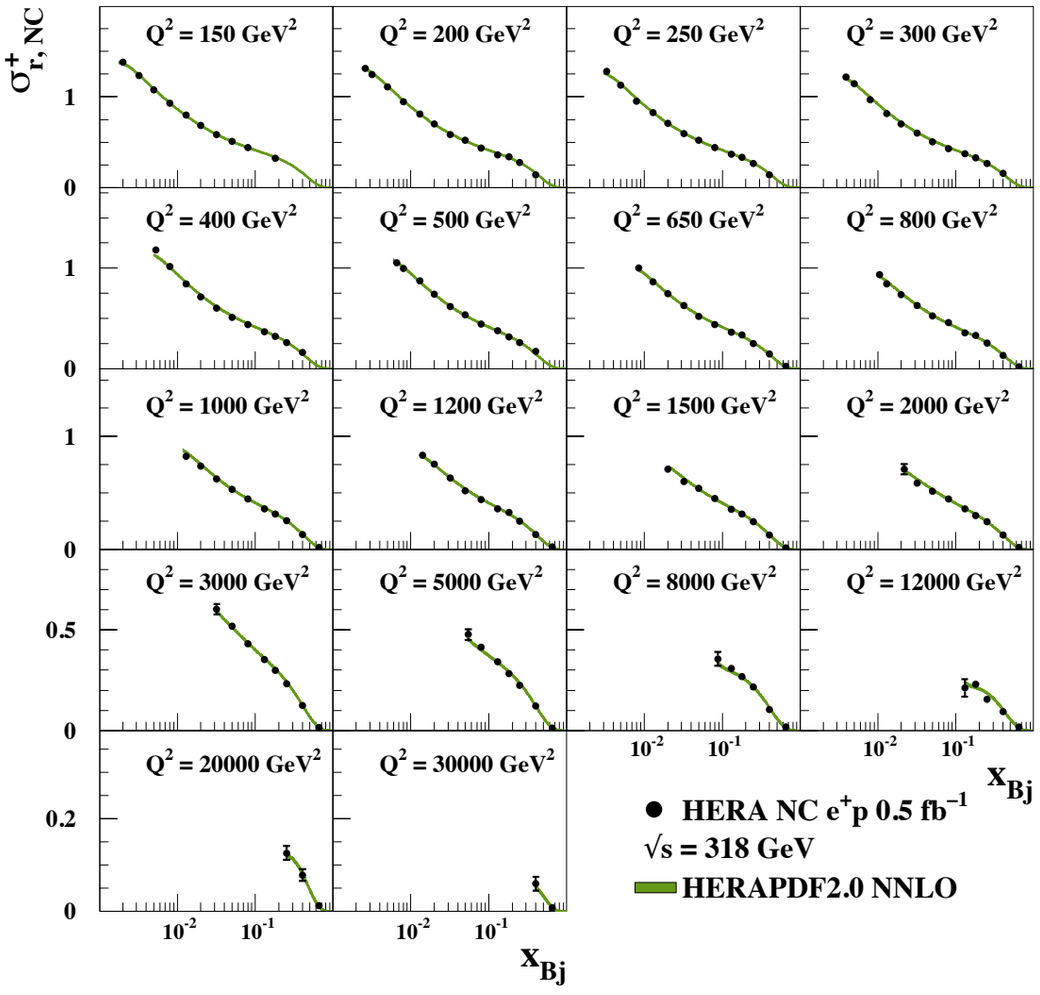

- Very good description for Q^2>10 GeV^2
- At low x,Q^2 the turnover of σ_r (due to F_L) is not well described (see backup slides for additional studies)

Comparison to inclusive HERA data

NC e^+p $\sqrt{s}$ =318 GeV

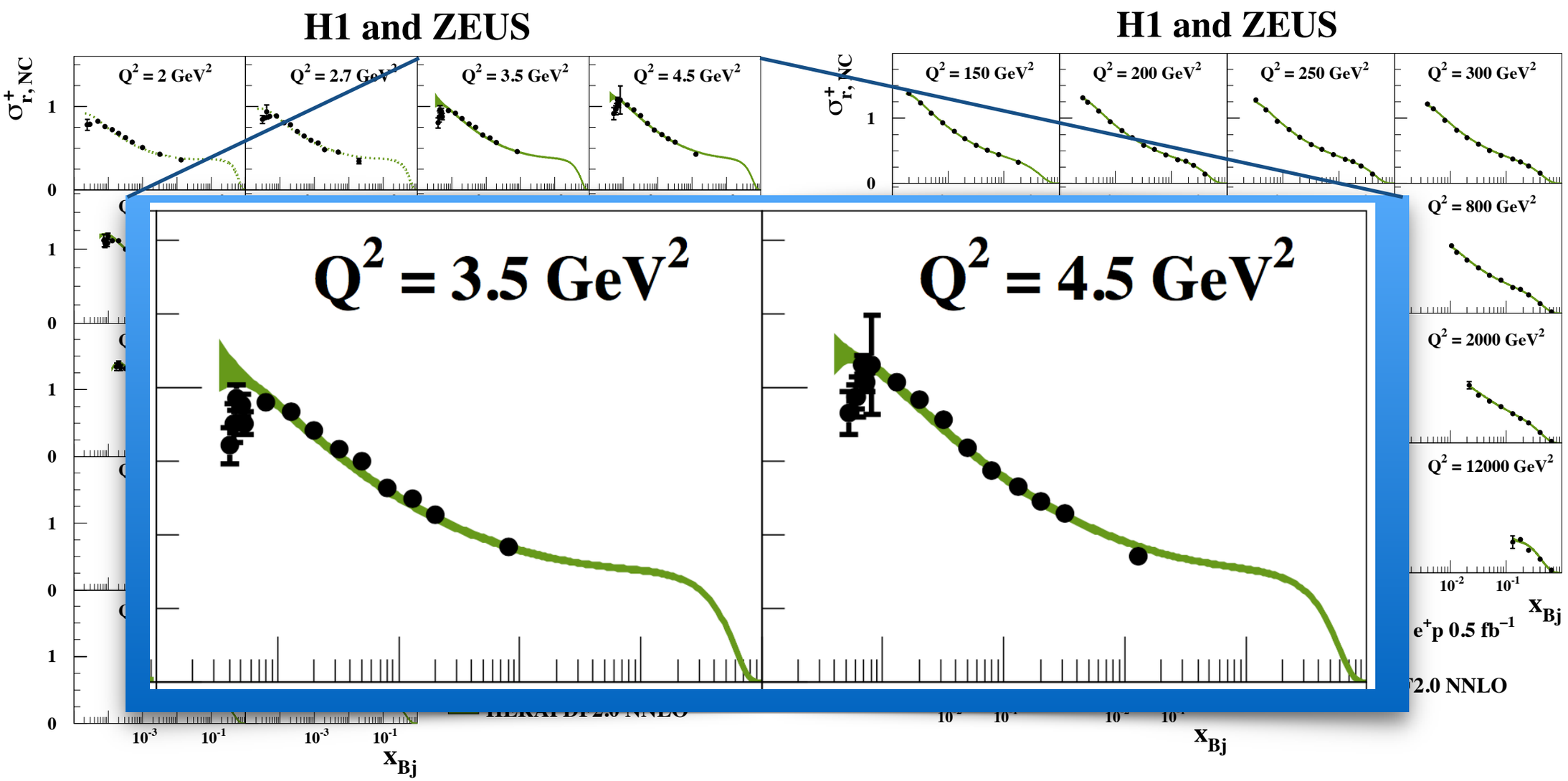

- Very good description for Q^2>10 GeV^2
- At low x,Q^2 the turnover of σ_r (due to F_L) is not well described (see backup slides for additional studies)

Comparison to inclusive HERA data

NC e^+p $\sqrt{s}$ =318 GeV

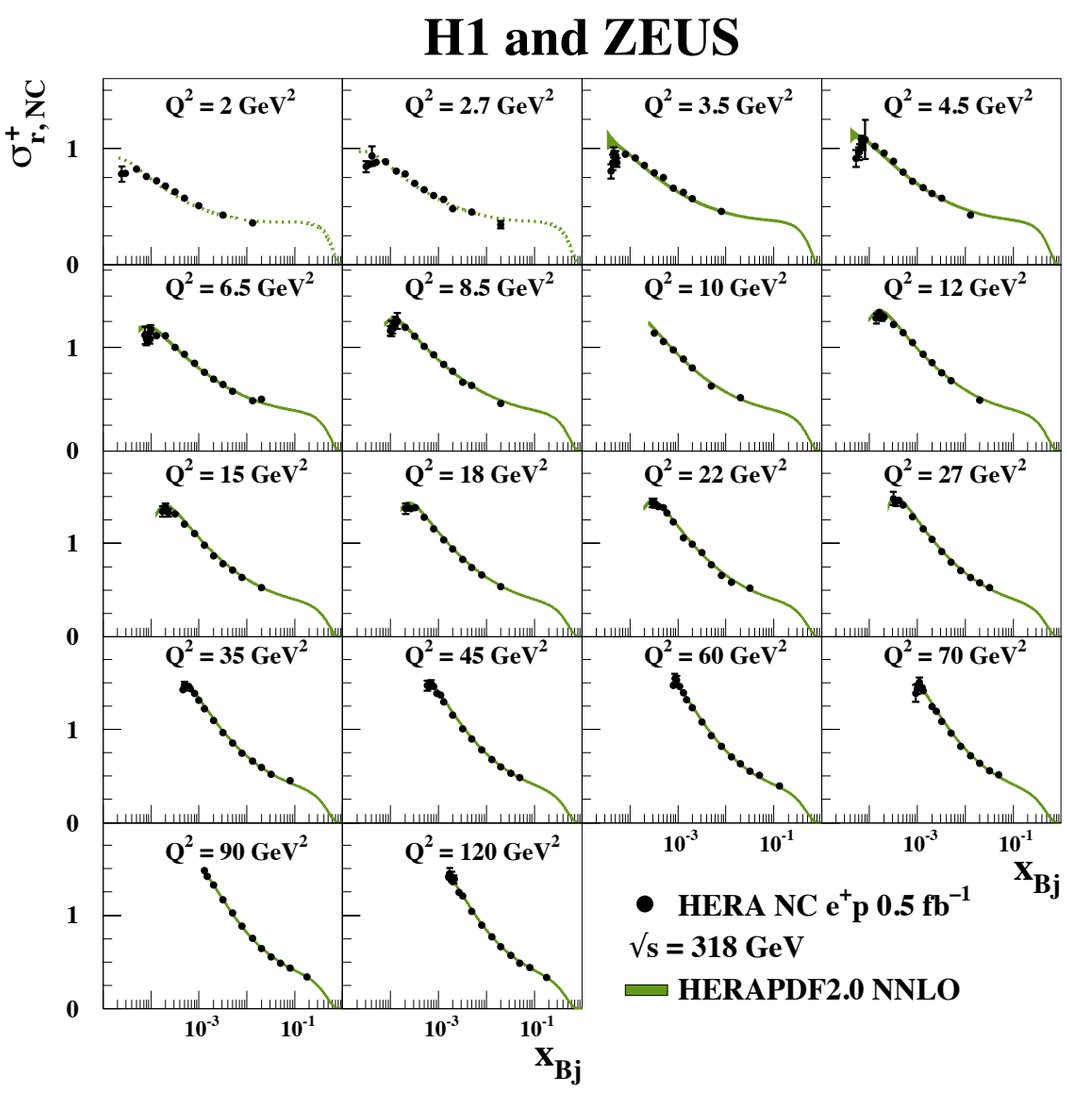

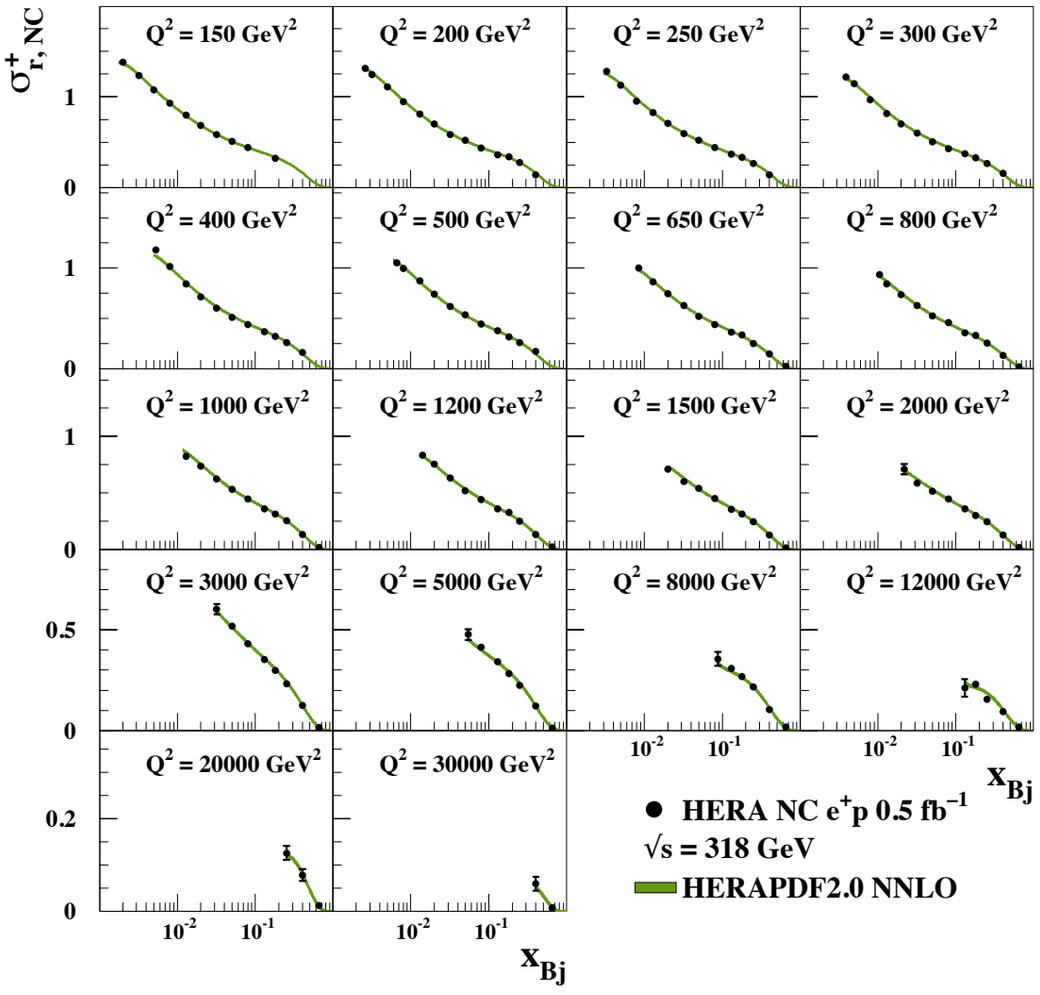

- The high Q2 cross sections allow to test compositeness and set an upper limit on quark radius $R_q < 0.43 \times 10^{-18}$ (95%CL)

ZEUS: Phys. Lett. B 757 (2016) 468 [arXiv:1604.01280]

Scaling violations

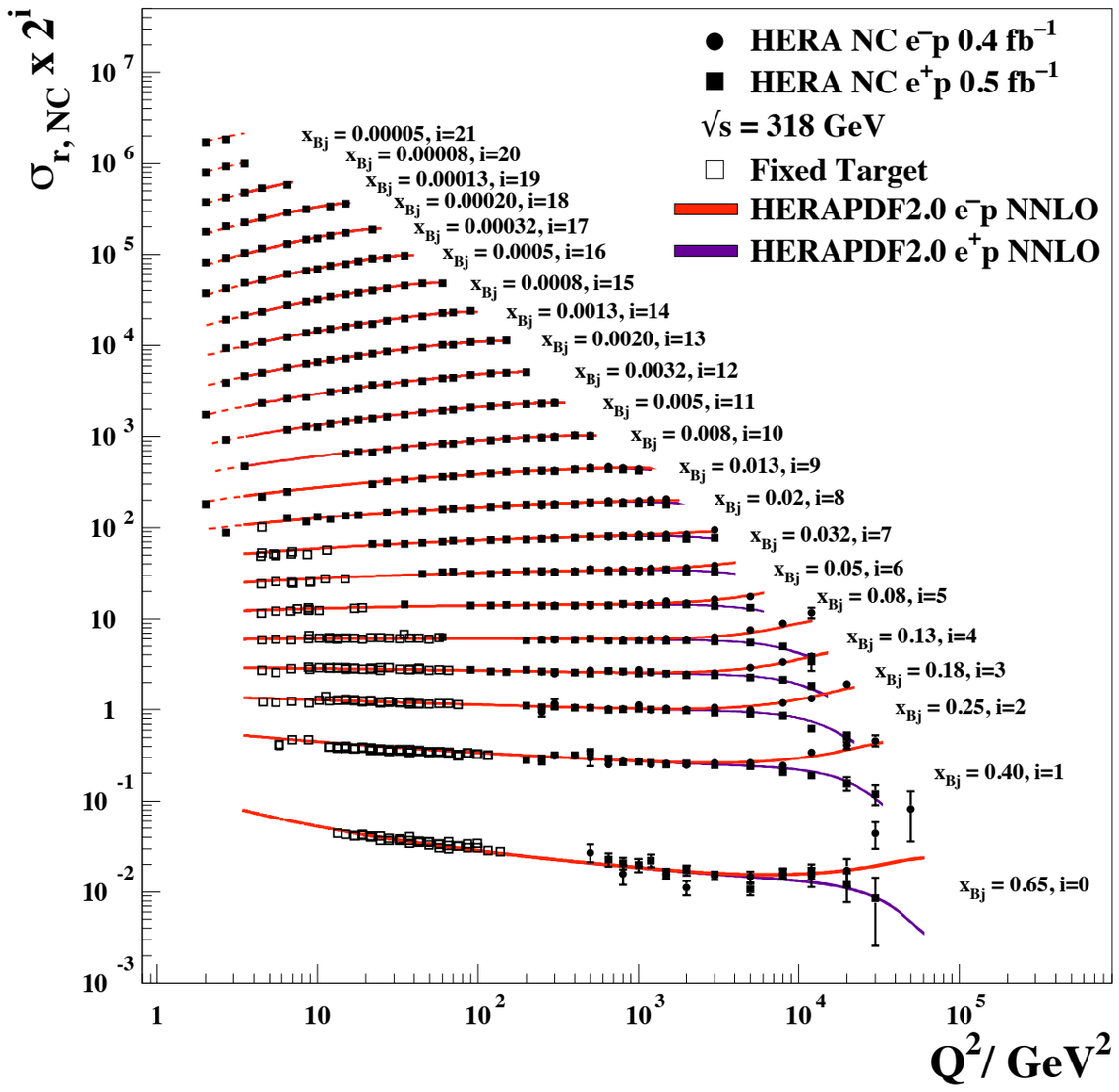

HERAPDF2.0 NLO (VFNS) vs HERAPDF2.0FF3B (FFNS)

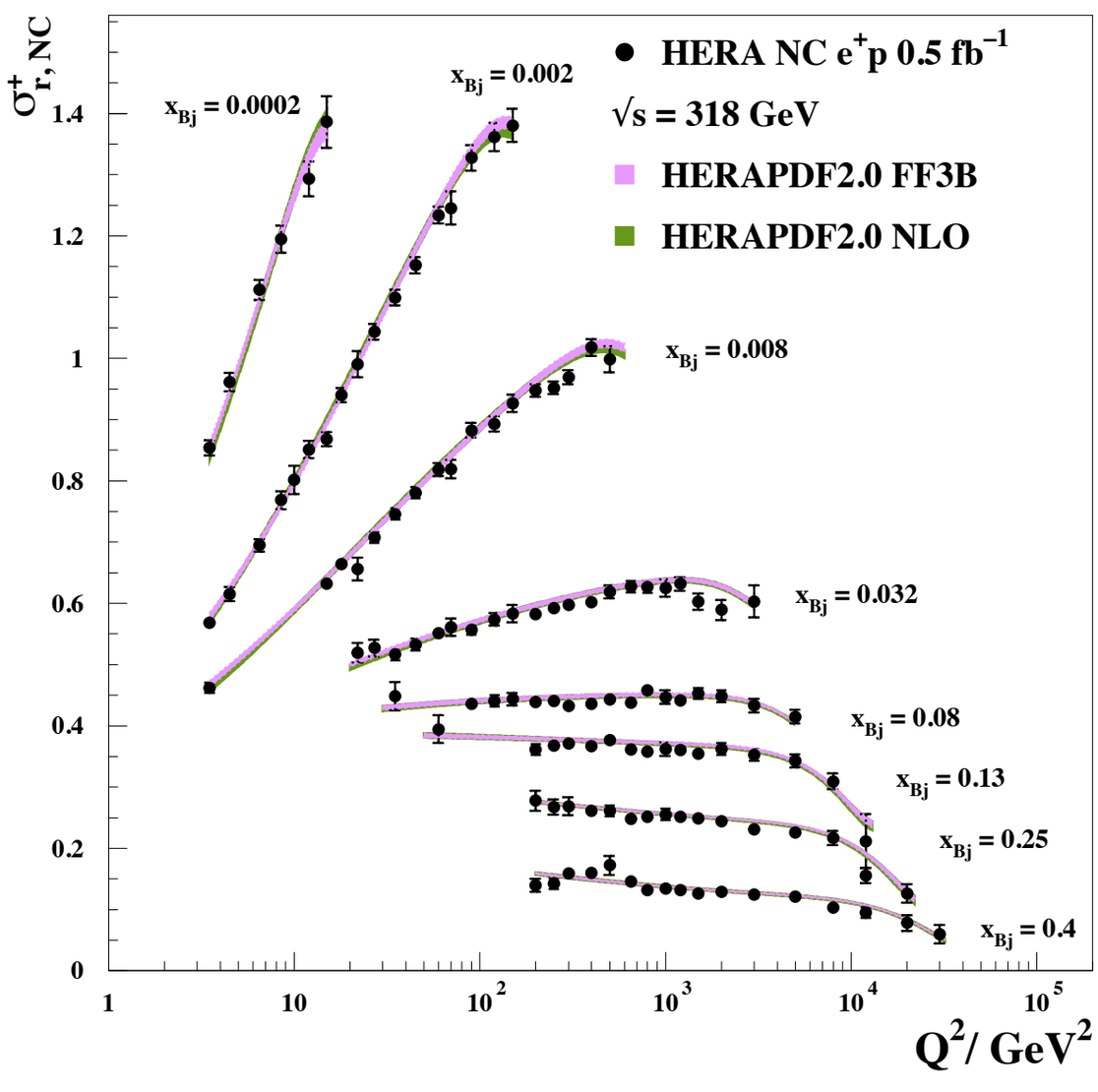

Textbook plots showing with great precision scaling violations patterns (and EW effects at high-Q^2 and high-x)

Rise of F_2

HERA F_2 (1993)

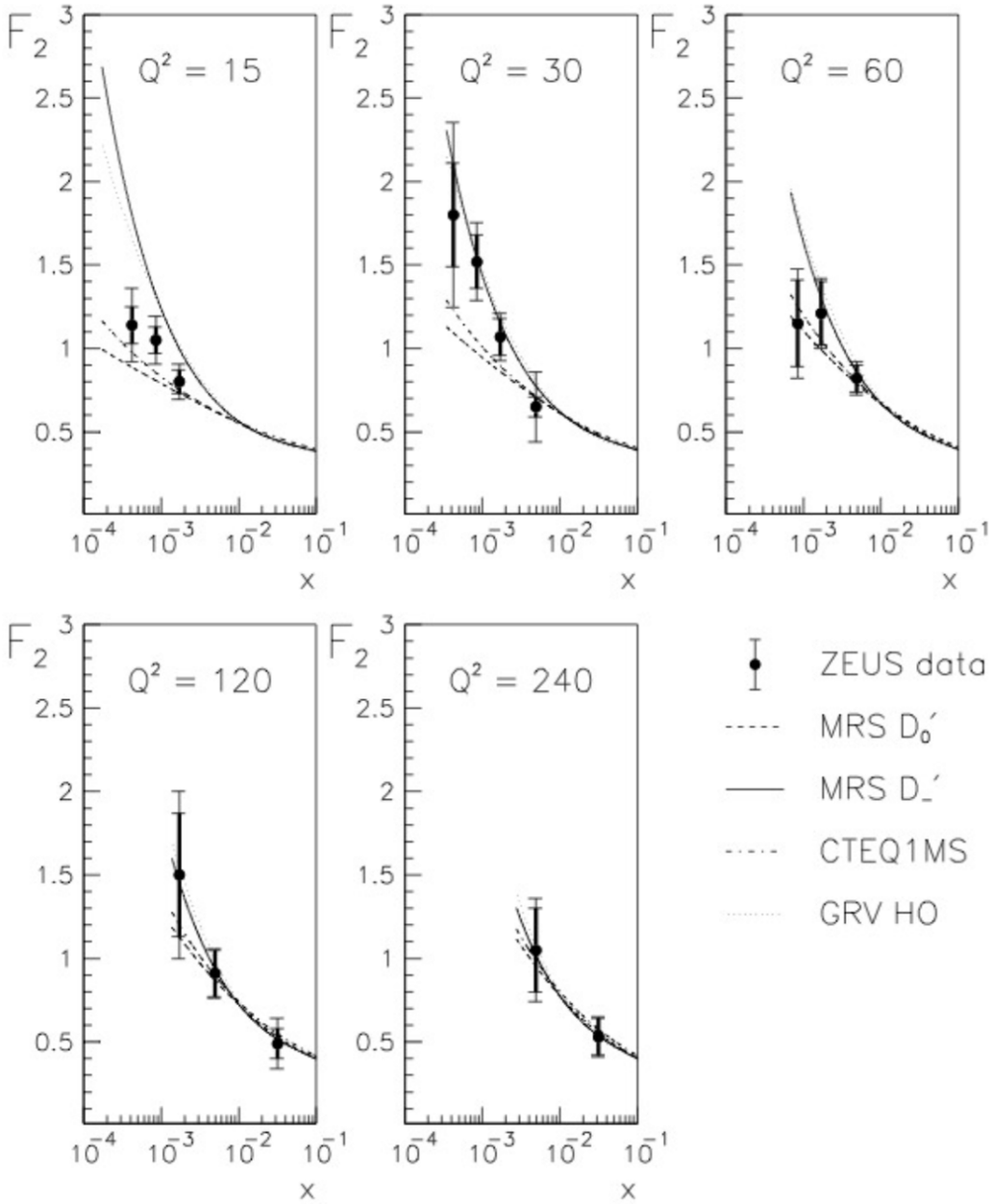

HERA F_2 (2015)

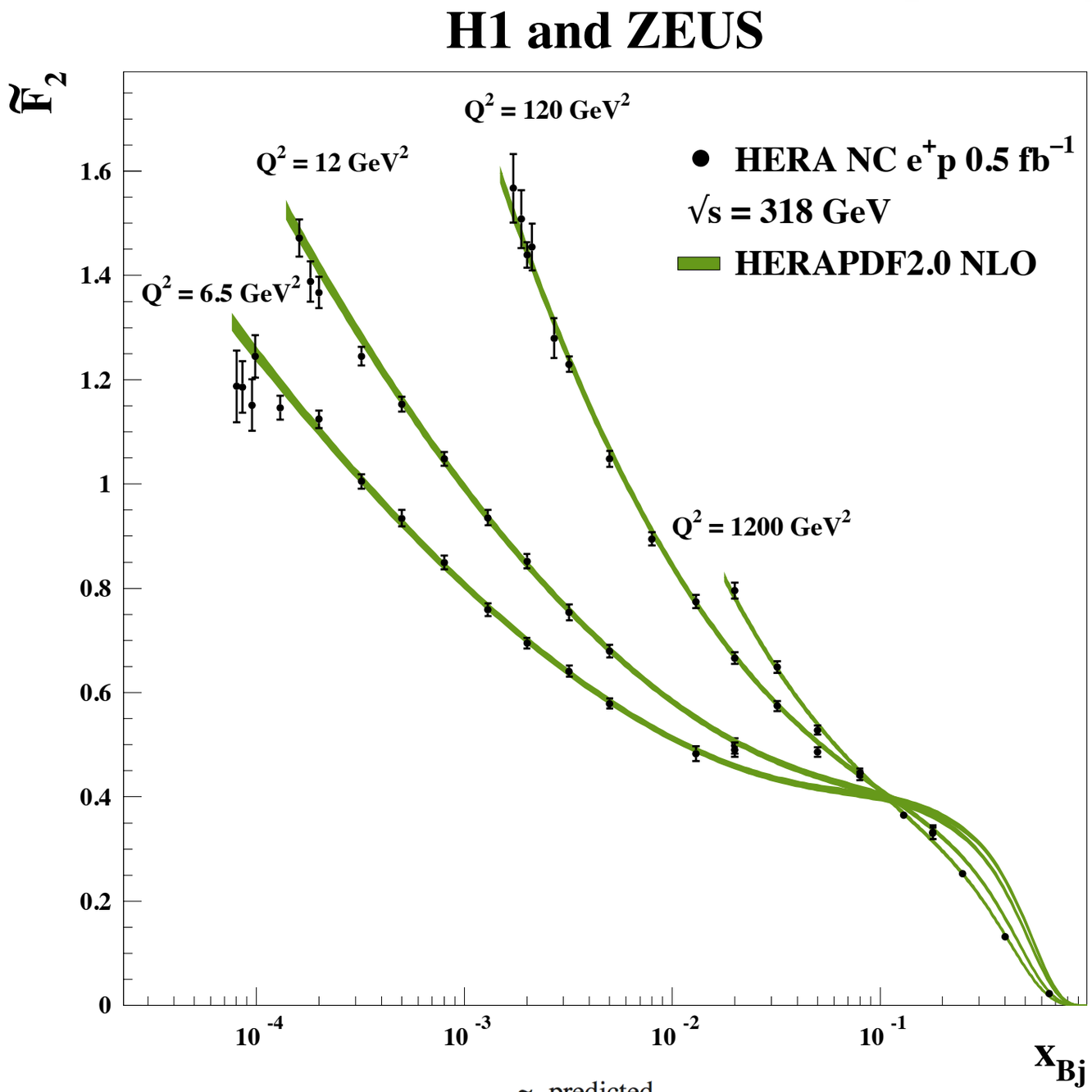

$$\tilde{F}_2 = \sigma^{\pm}_{r,\mathrm{NC}} \cdot \frac{\tilde{F}_2^{\ \mathrm{predicted}}}{\sigma^{\pm}_{r,\mathrm{NC}}{}^{\mathrm{predicted}}} = \sigma^{\pm}_{r,\mathrm{NC}} \cdot (1 + C_F)$$

Comparison to inclusive HERA data

CC $e^{\pm}p$, $\sqrt{s}$ =318 GeV

CC $e^{+}p$

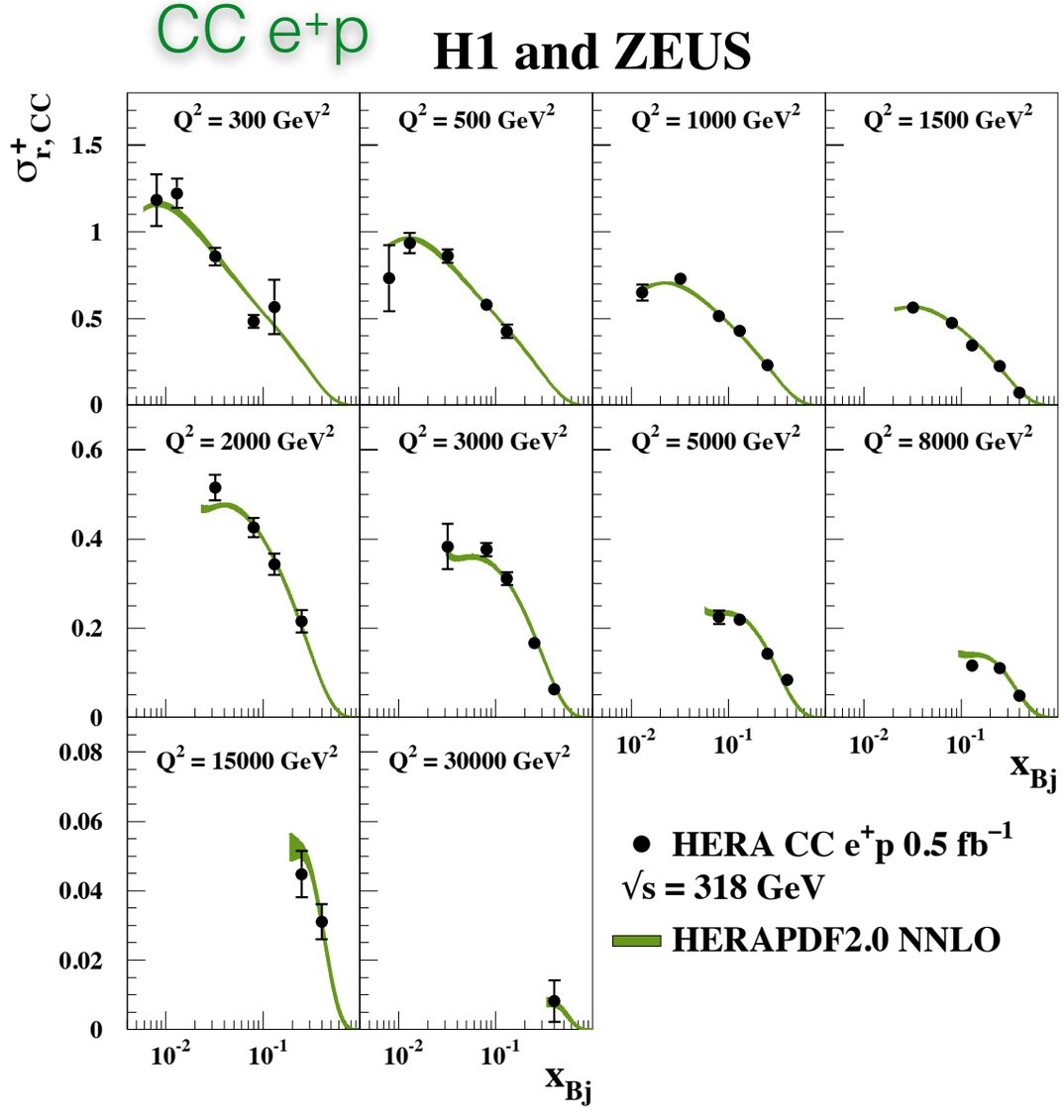

CC $e^{-}p$

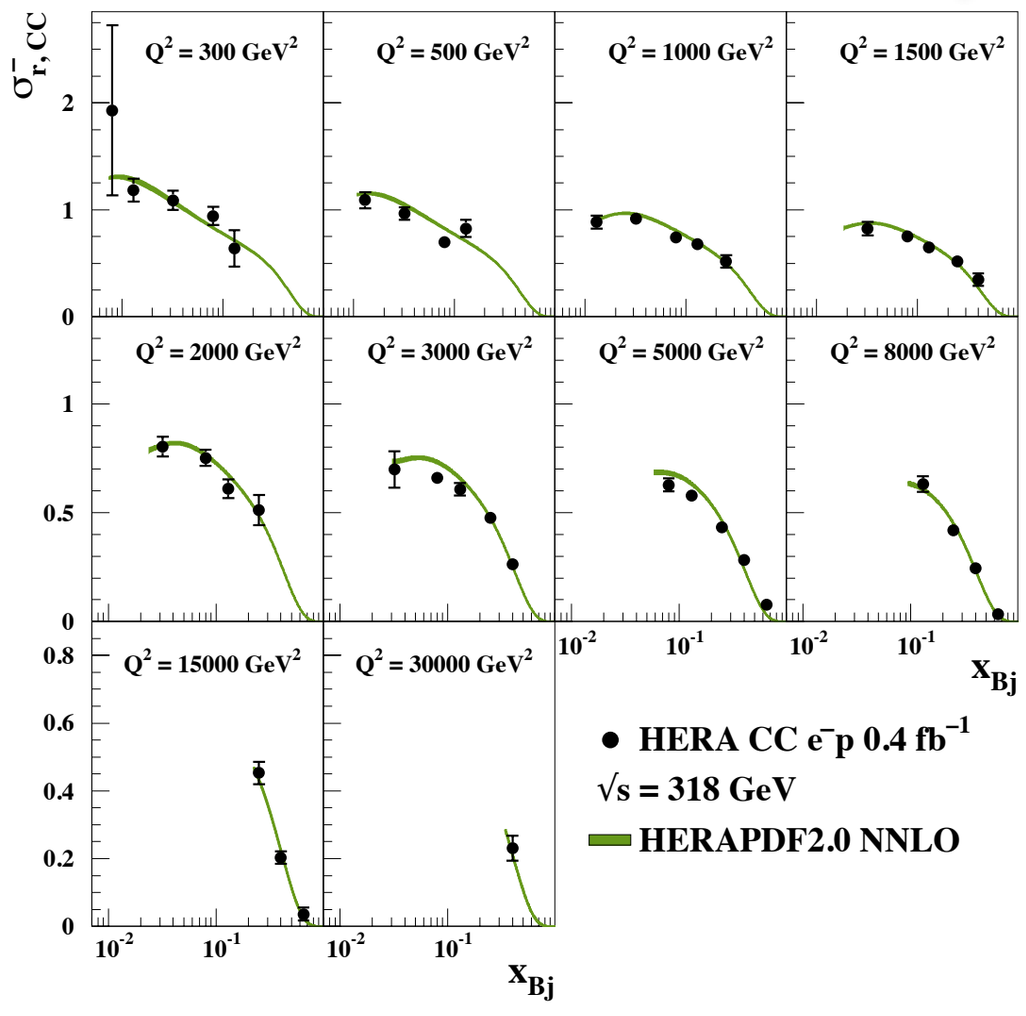

Improved precision due to higher statistics and combination

QCD and Electroweak Analyses

for additional details see arXiv:1506.06042

Electroweak Unification

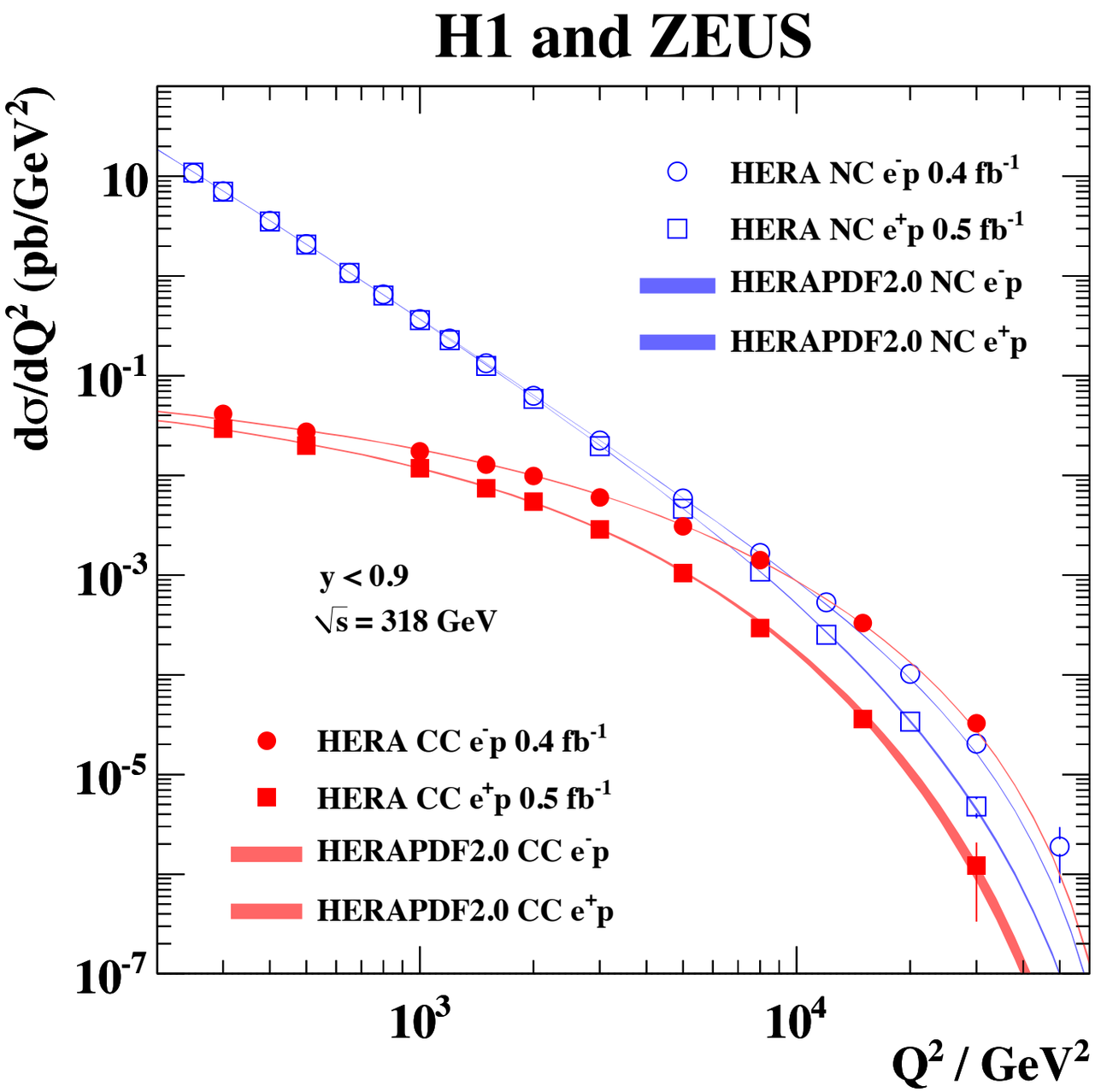

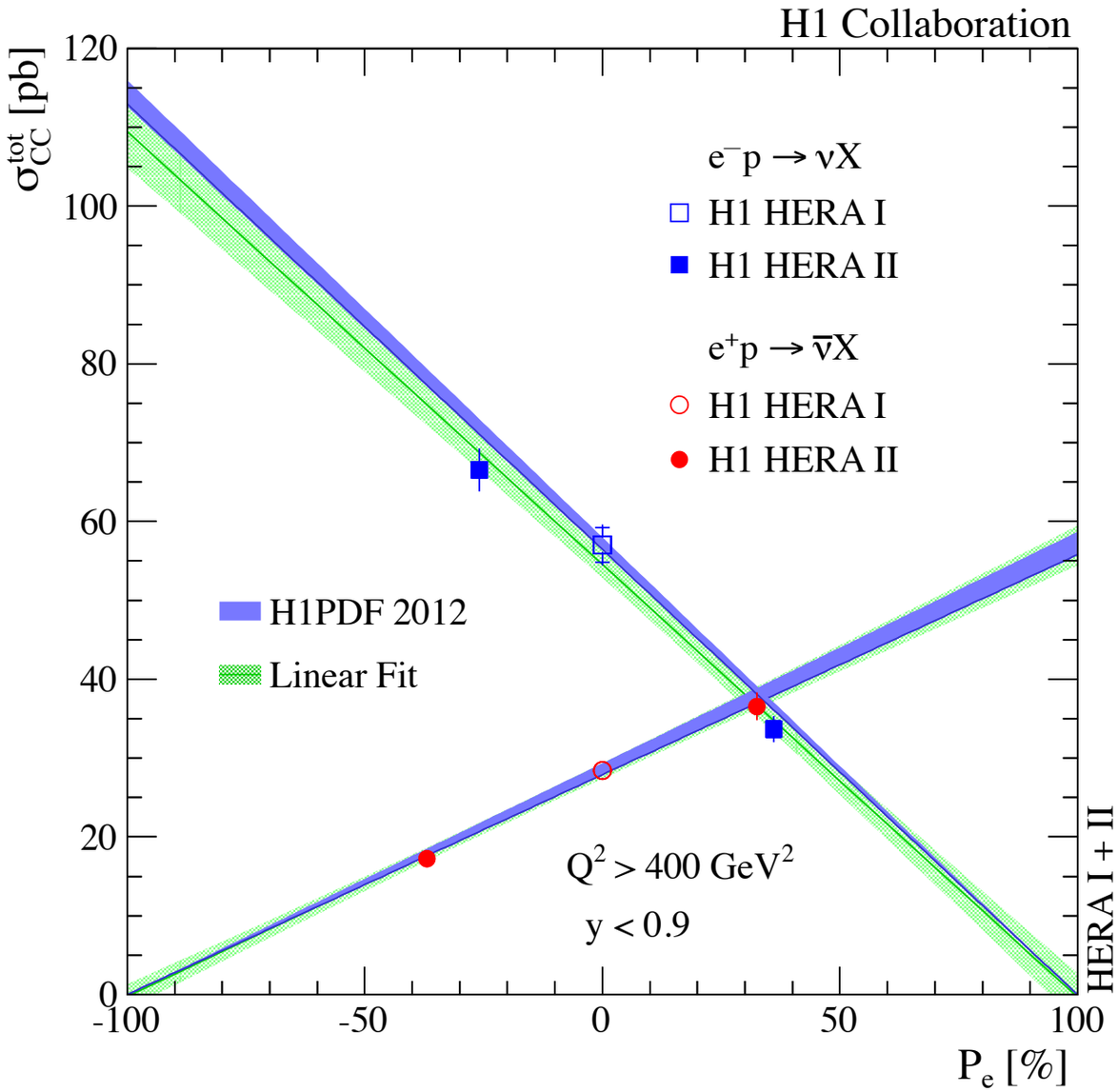

Beautiful textbook plots that show the unification of the NC and CC interactions at the EW scale and chiral structure of the SM.

Electroweak effects and $xF_3^{\gamma Z}$

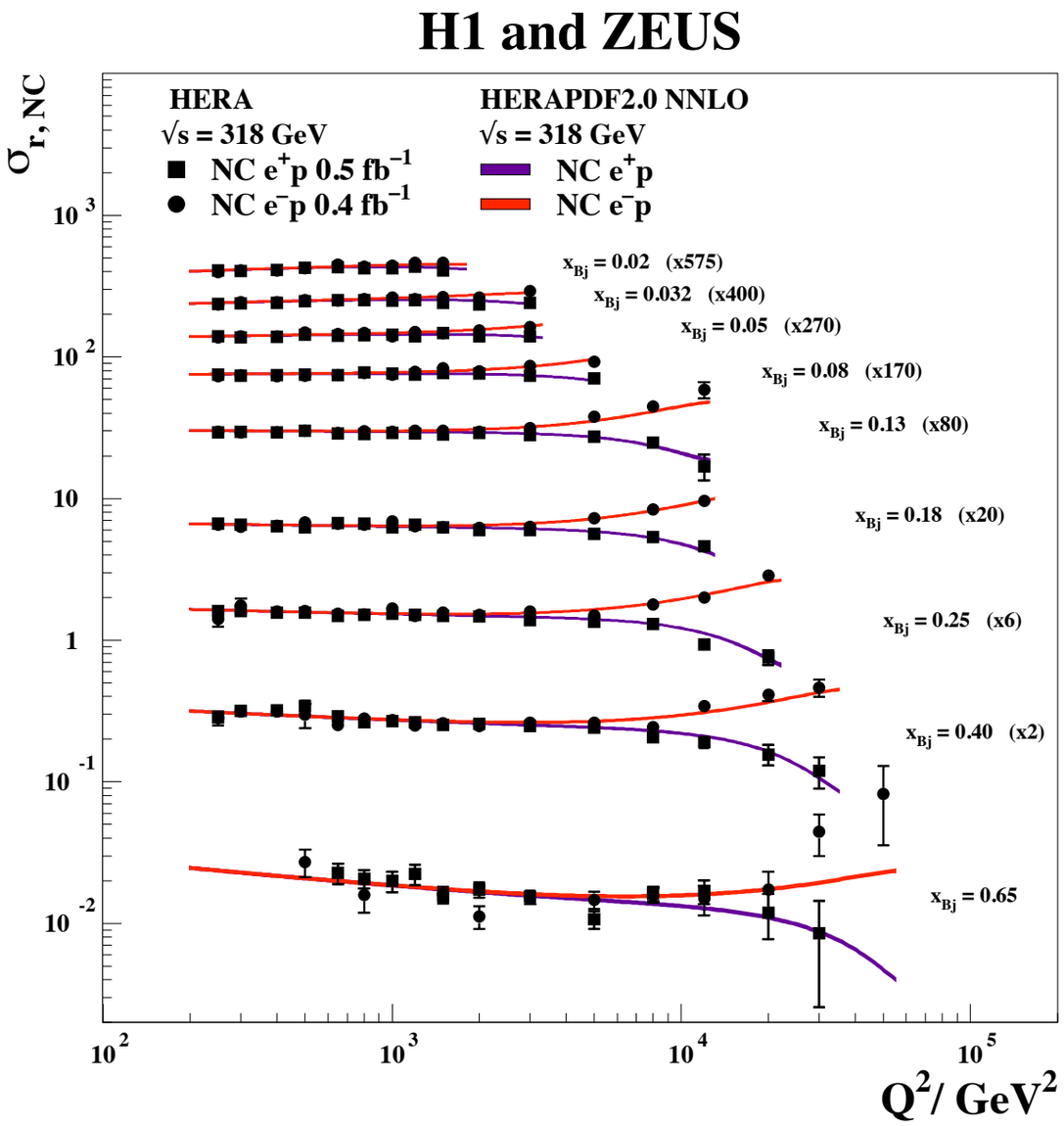

$$x\tilde{F}_3 = \frac{Y_+}{2Y_-}(\sigma^-_{r,\mathrm{NC}} - \sigma^+_{r,\mathrm{NC}})$$

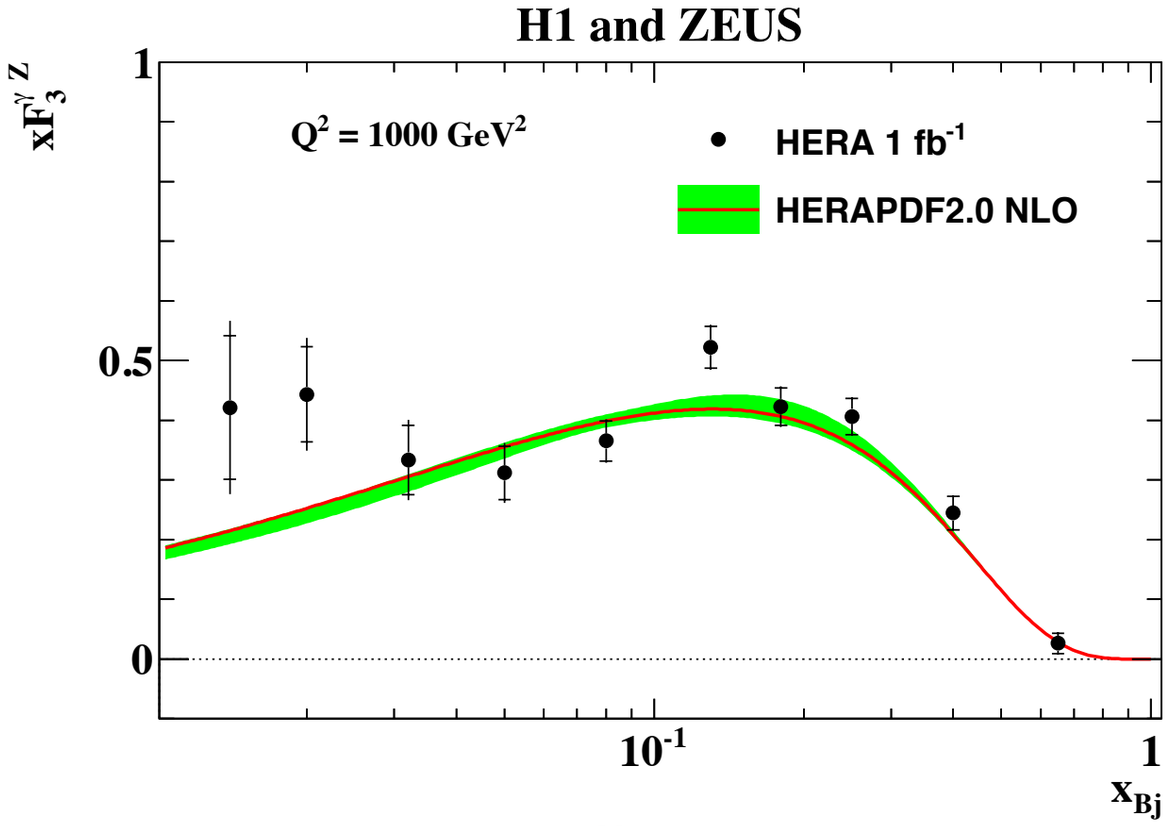

$$xF_3^{\gamma Z} \approx \frac{x}{3}(2u_v + d_v)$$

- Best determination of $xF_3^{\gamma Z}$
- Parity violation demonstrated down to scale of 10^{-18} m

Polarised DIS

NC & CC Cross sections

$$\frac{d^2\sigma^{\mathrm{NC}}(e^{\pm}p)}{dxdQ^2} = \frac{2\pi\alpha^2}{xQ^4}(Y_+\tilde{F}_2(x,Q^2) \mp Y_- x\tilde{F}_3(x,Q^2) - y^2\tilde{F}_L(x,Q^2))$$

$$\frac{d^2\sigma^{\mathrm{CC}}(e^{\pm}p)}{dxdQ^2} = \frac{1 \pm P}{2}\frac{G_F^2}{4\pi x}\left[\frac{M_W^2}{M_W^2+Q^2}\right]^2 [Y_+W_2^{\pm}(x,Q^2) \mp Y_- xW_3^{\pm}(x,Q^2) - y^2W_L^{\pm}(x,Q^2)]$$

Generalised Structure Functions:

$$\tilde{F}_2 = F_2^{\gamma} + \kappa_Z(-v_e \mp P_e a_e)F_2^{\gamma Z} + \kappa_Z^2(v_e^2 + a_e^2 \pm P_e v_e a_e)F_2^Z$$

$$x\tilde{F}_3 = +\kappa_Z(\pm a_e + P_e v_e)xF_3^{\gamma Z} + \kappa_Z^2(\mp 2v_e a_e - P_e(v_e^2 + a_e^2))xF_3^Z$$

Structure functions and couplings (QPM):

$$[F_2, F_2^{\gamma Z}, F_2^Z] = x\sum_q [e_q^2, 2e_q v_q, v_q^2 + a_q^2]\{q + \bar{q}\}$$

$$[xF_3^{\gamma Z}, xF_3^Z] = 2x\sum_q [e_q a_q, v_q a_q]\{q - \bar{q}\}$$

$$\kappa_Z(Q^2) = \frac{Q^2}{Q^2 + M_Z^2}\frac{G_F m_Z^2}{2\sqrt{2}\pi\alpha}$$

$$v_f = I_{f,L}^3 - 2e_f \sin^2\theta_W \quad (f = e, u, d, \ldots)$$
$$a_f = I_{f,L}^3$$

On-shell Scheme: $G_F = \frac{\pi\alpha}{\sqrt{2}M_W^2\left(1 - \frac{M_W^2}{M_Z^2}\right)}(1 + \Delta r)$

EW couplings and mixing angle

Simultaneous DGLAP and EW fit performed with the goal to measure PDFs and relevant EW parameters (quark couplings and mixing angle)

H1prelim-16-041
Zeus: PRD93(2016)092002

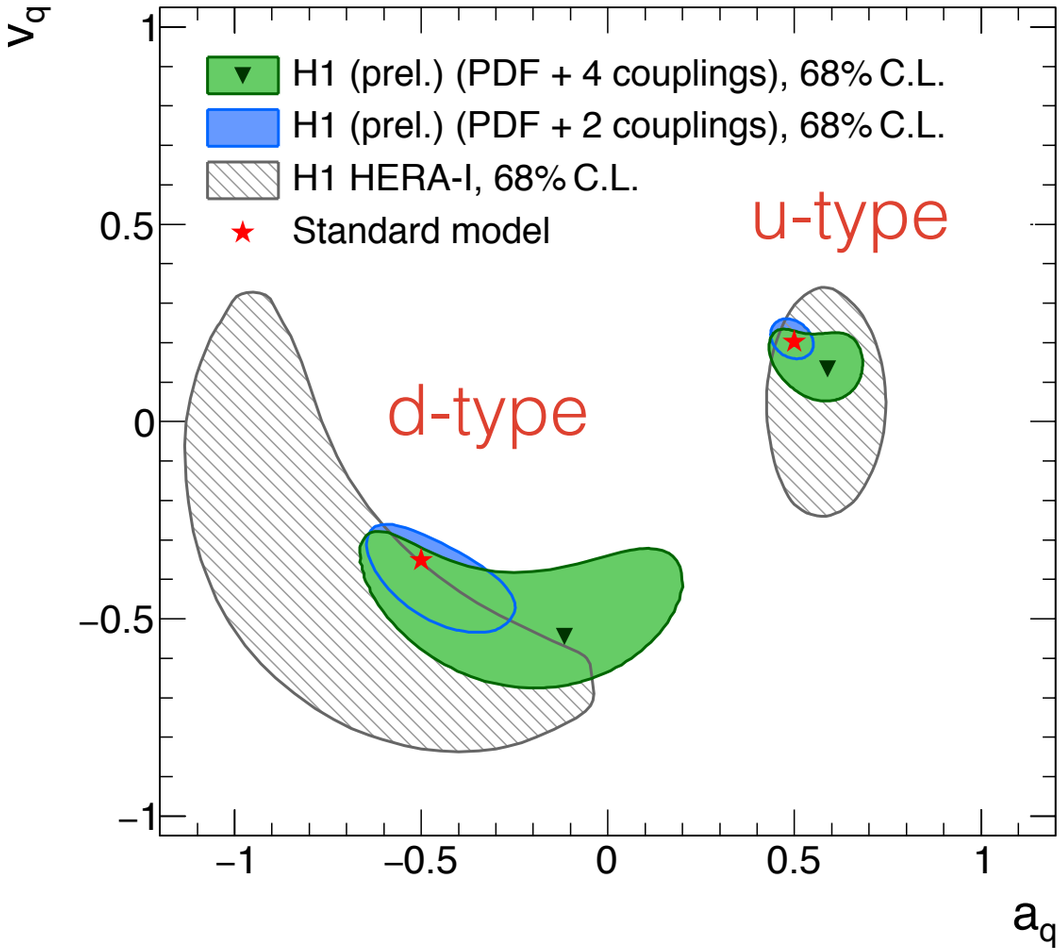

a_q, v_q couplings agree with world average
u-type coupling among the most accurate

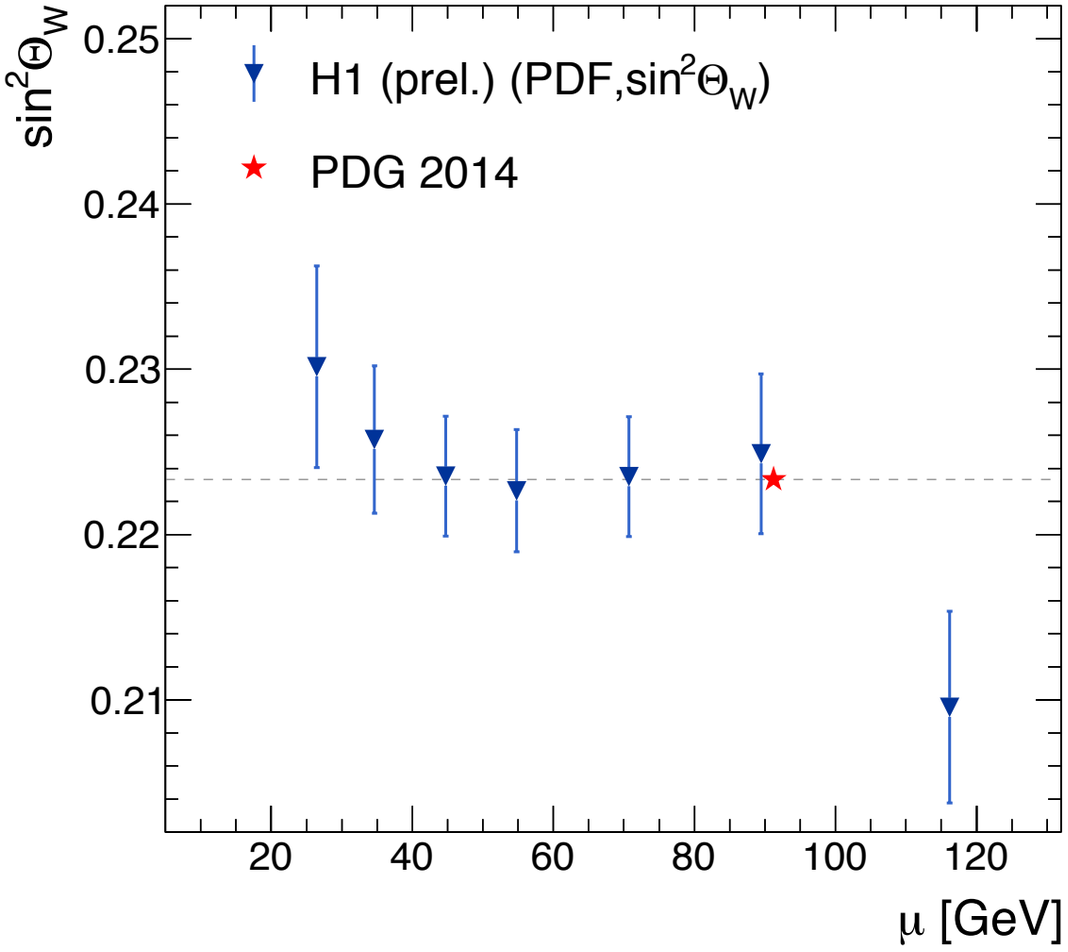

$\sin^2\vartheta_W$ determined at different scales

Very similar results from ZEUS - resulting PDFs very similar to HERAPDF2.0 (not shown)

Extended QCD analyses including HERA charm and jet production data

HERAPDF2.0Jets:
including charm and jet production data

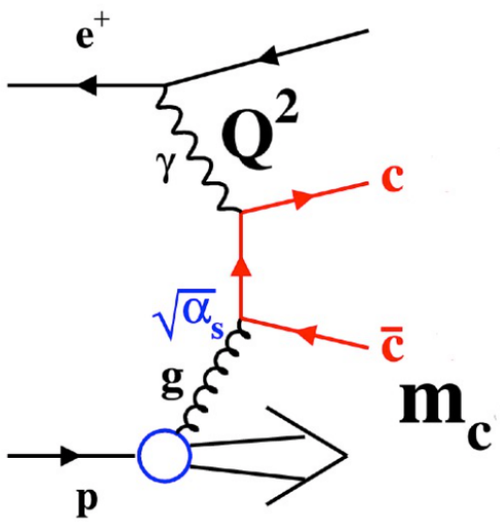

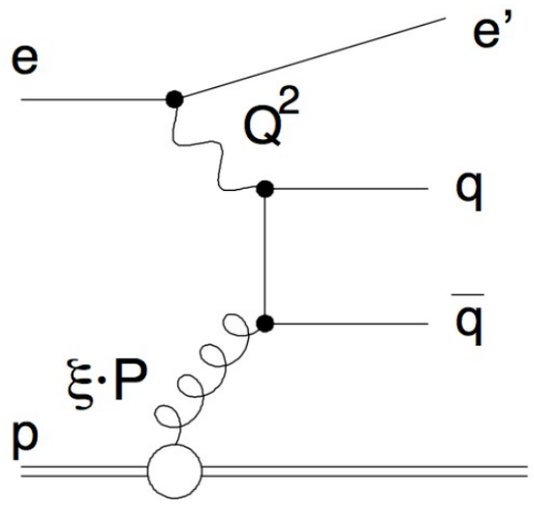

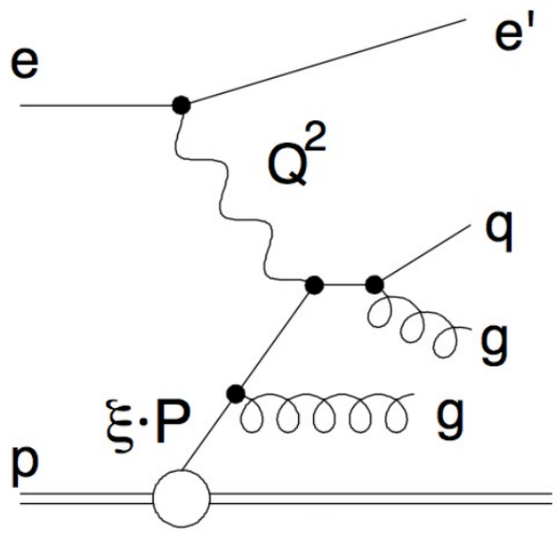

- The Hera charm and jet production measurements bring <u>direct sensitivity</u> to the gluon density *xg(x)* and the strong coupling α_s.

- In the HERAPDF2.0Jets fit the combination of the HERA charm measurements and a selection of H1 and ZEUS jet cross sections measurements (incl. jet, dijet, trijet) have been added to the combined inclusive cross sections
  - <u>stringent test of QCD factorisation and competitive determination of α_s</u>.

N.B. Although formally bottom production is not included in the HERAPDF2.0 fits HERA bottom measurements (together with charm data) from H1 and ZEUS have beam used (as described in the next slide) to determine the M_c and M_b mass parameters used in all the HERAPDF2.0 fits.

Charm and bottom masses

The values of the charm (M_c) and bottom (M_b) masses used in the DGLAP fits were determined after performing χ^2 scans of NLO and NNLO fits to the HERA combined inclusive cross sections and the HERA combined charm and the H1 and ZEUS bottom data

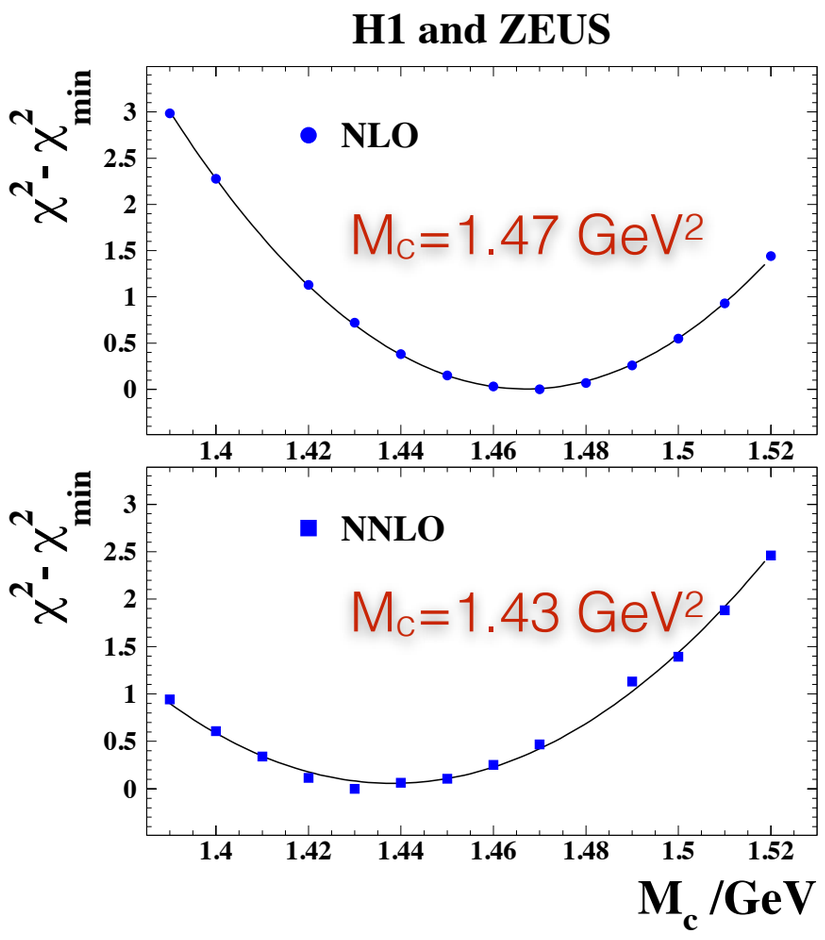

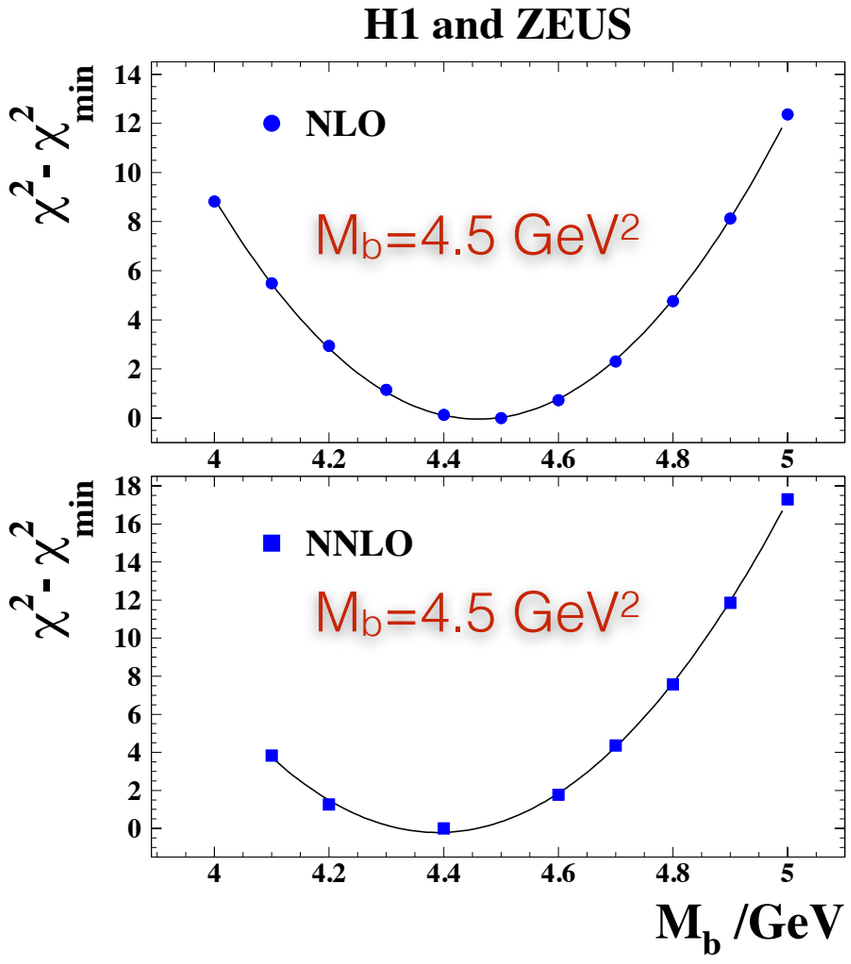

On HERA combined charm data see: EPJ C 73, 2311 (2013)

HERAPDF2.0Jets and $\alpha_s(M_Z)$

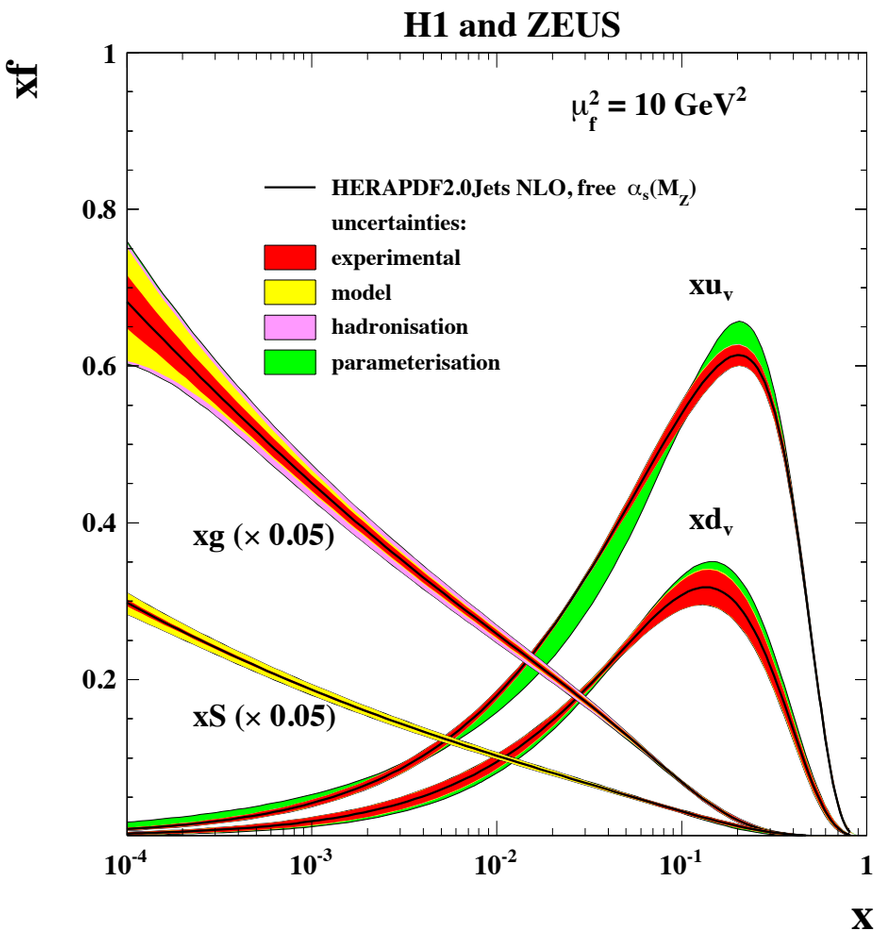

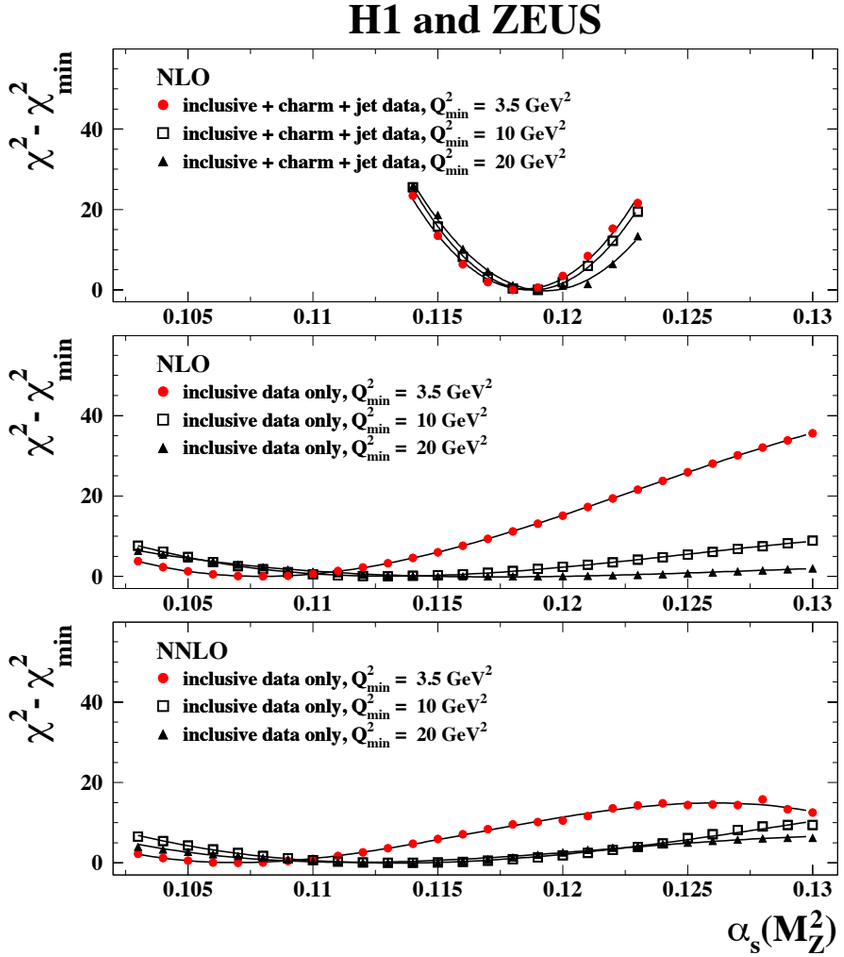

- Inclusion of jet (and only partially charm) data crucial for precise determination of α_s

$$\alpha_s(M_Z^2) = 0.1183 \pm 0.0009(exp) \pm 0.0005(model/param) \pm 0.0012(had)^{+0.0037}_{-0.0030}(scale)$$

- We need NNLO predictions for jet cross sections at HERA
- This study and fit validates (a posteriori) the choice α_s=0.118 adopted for the HERAPDF2.0 default fit

HERAPDF2.0Jets: Comparison to jet data

Dijet

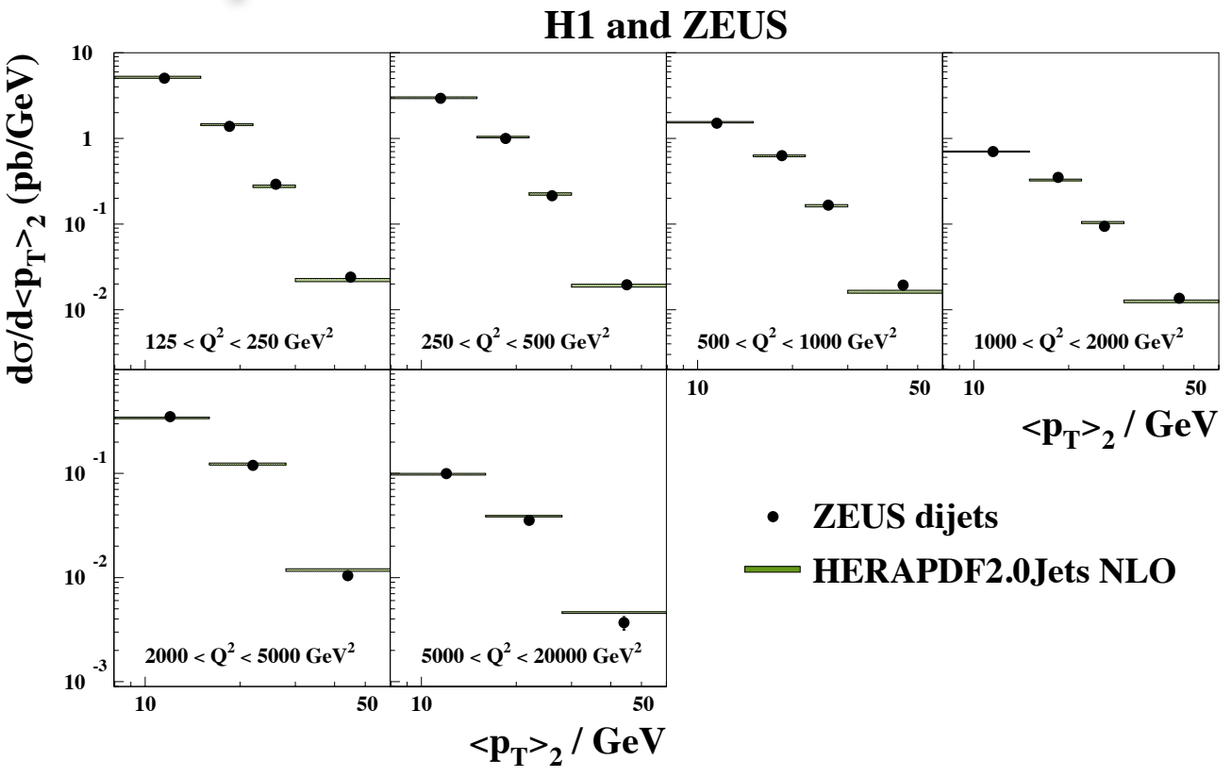

Trijet

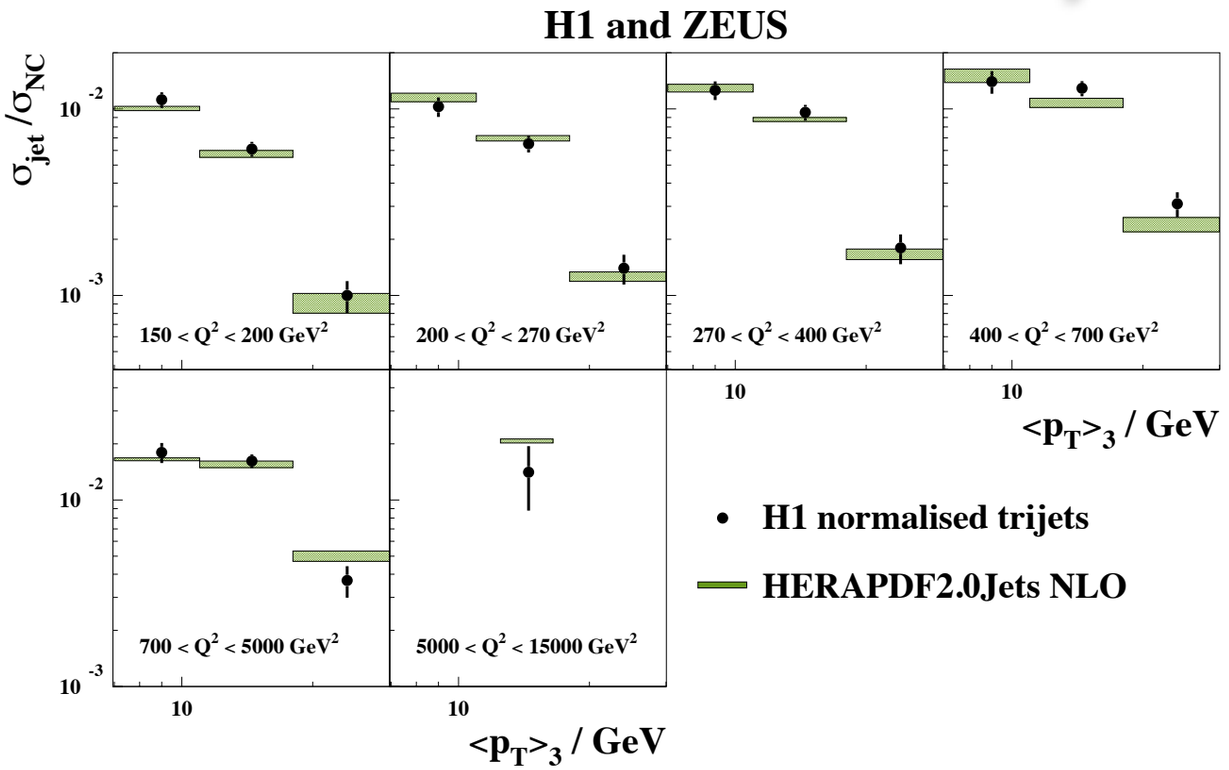

The description of all data on jet production by the HERAPDF2.0Jets PDFs is excellent.

HERAPDF2.0Jets: Comparison to charm data

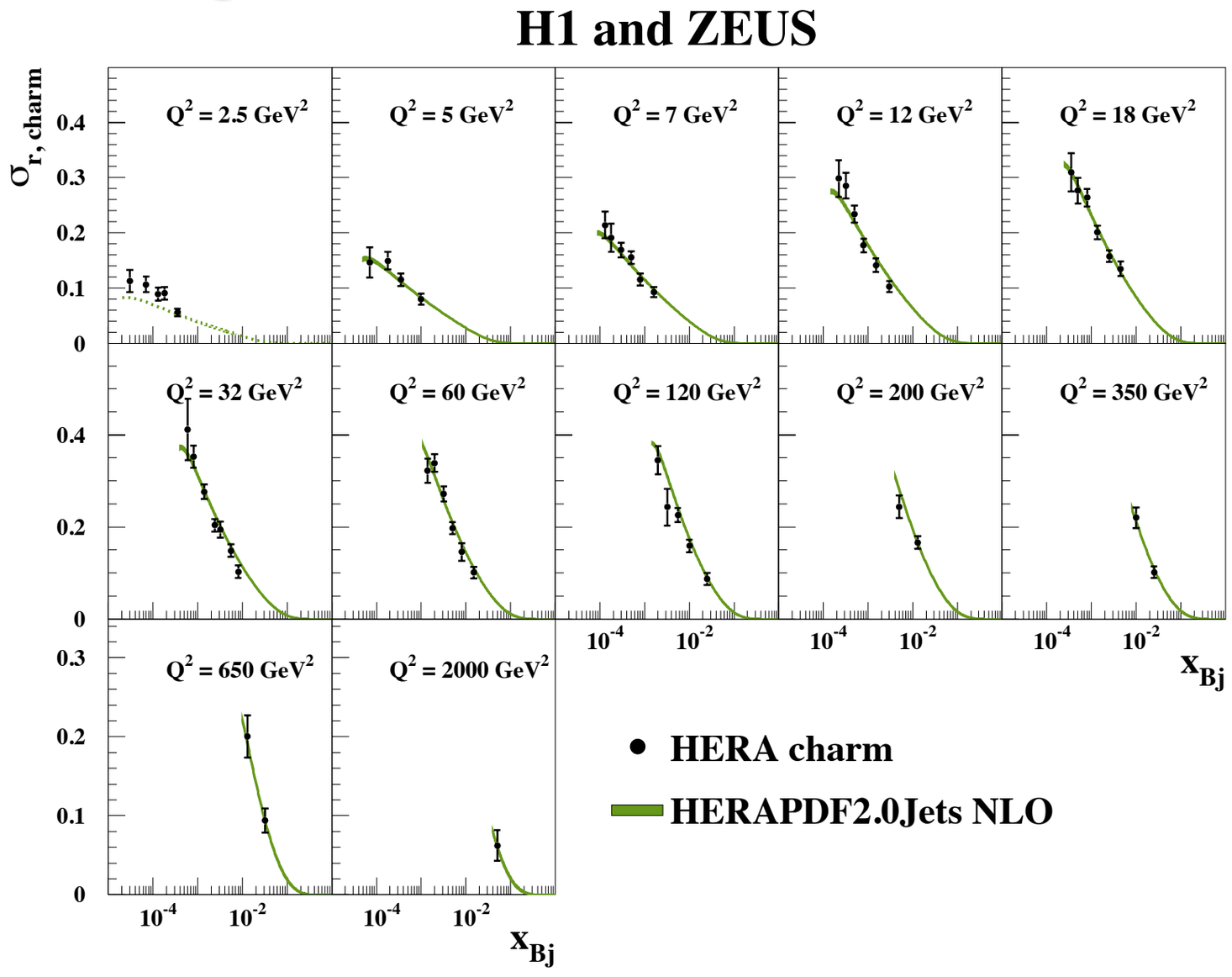

The description of charm cross sections is also very good.

Inclusive dijet production @ NNLO

J. Currie, T. Gehrmann, J. Niehues , arXiv:1606.03991

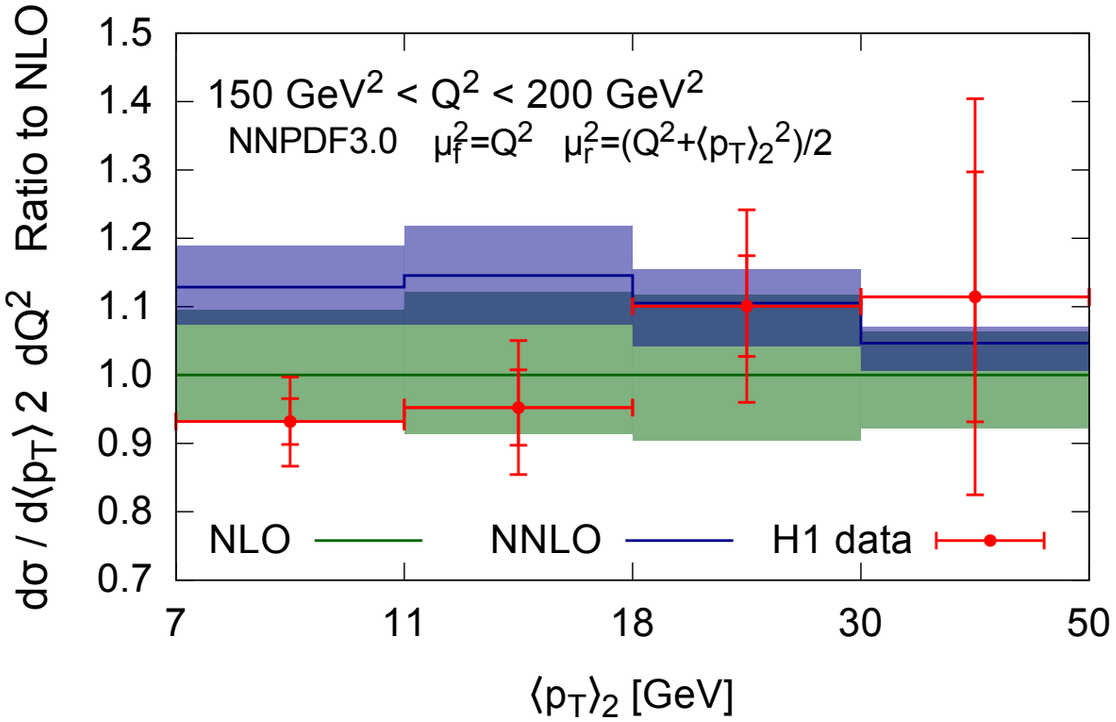

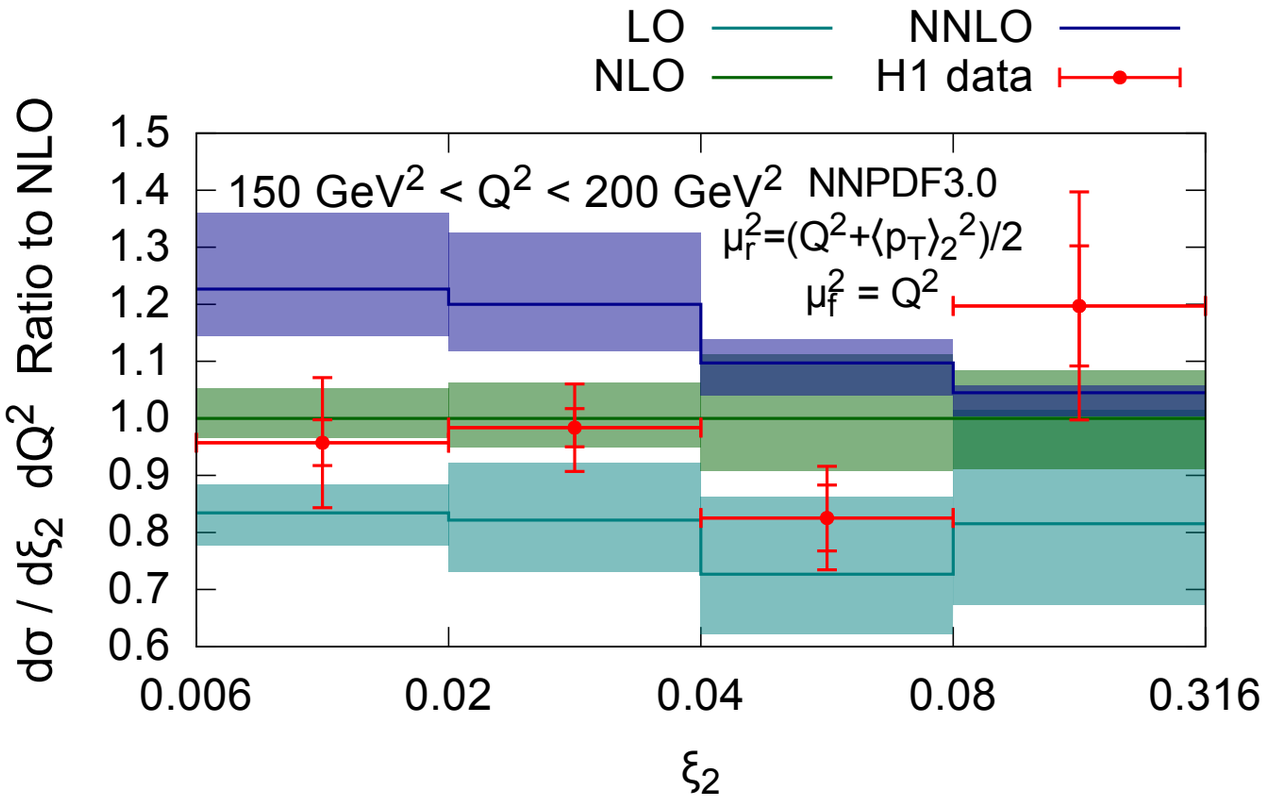

A very important result, will improve the determination of the strong coupling and trigger very interesting studies with DIS jet cross sections (test of pQCD, DGLAP fits and xg).

Multijet production at low Q^2

H1 measured multi-jet (incl, dijet, tri-jet) production at low Q^2 using 2006-2007 data (L=184 pb^{-1})

H1prelim-16-061

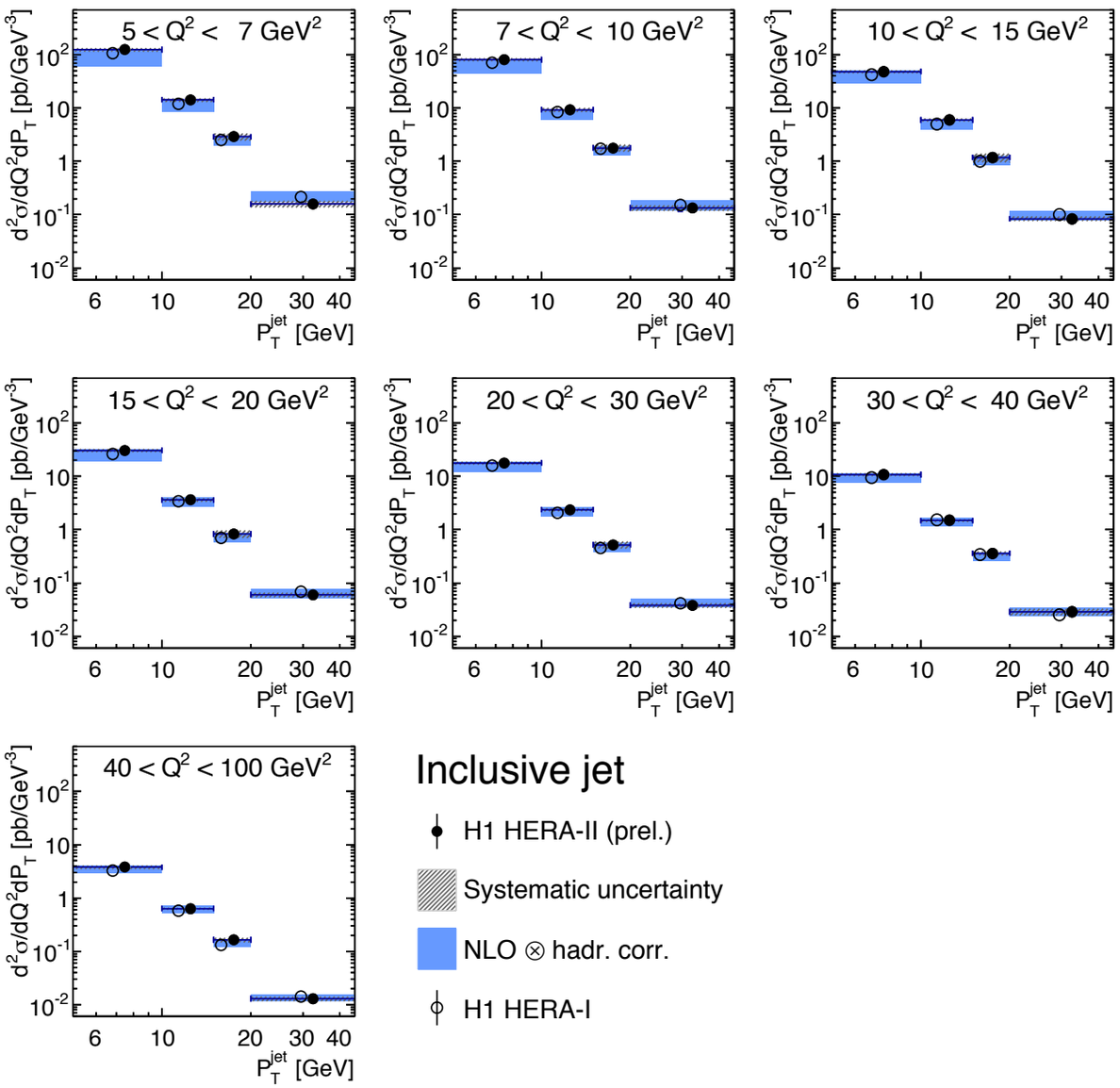

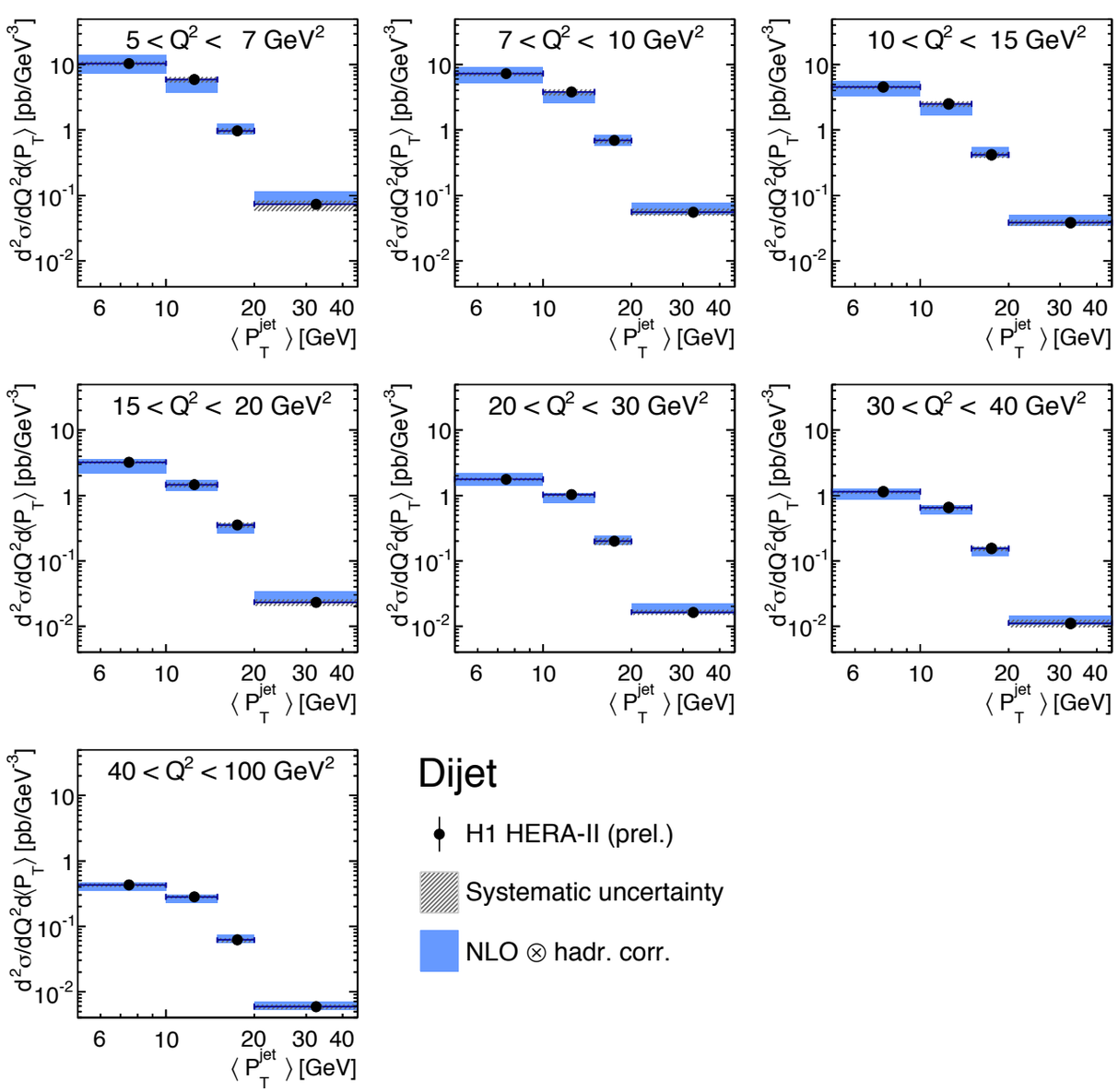

Summary

HERA is our main source of information on proton's structure.

The final combination of the complete H1 and ZEUS inclusive measurements, a major legacy of HERA, has allowed the determination of the proton's PDFs (HERAPDF2.0) with an unprecedented precision.

Most of the improvements in the understanding of the PDFs, described here, are very relevant for the physics programme being pursued at the LHC.

Backup Slides

Combination: Averaging Method

- Combination performed using the HERAverager package
- Averaging procedure take correlations of systematic unc. fully into account
- Multiplicative treatment of the systematic uncertainties (as a default choice)
- Minimisation procedure based on the following χ^2 definition:

$$\chi^2_{\mathrm{exp},ds}(\boldsymbol{m},\boldsymbol{b}) = \sum_i \frac{\left[m^i - \sum_j \gamma^i_j m^i b_j - \mu^i\right]^2}{\delta^2_{i,\mathrm{stat}}\,\mu^i\left(m^i - \sum_j \gamma^i_j m^i b_j\right) + \left(\delta_{i,\mathrm{uncor}}\,m^i\right)^2} + \sum_j b_j^2$$

- Procedural uncertainties:
  - Multiplicative vs additive nature of the systematic error sources
  - Correlations in photo-production background and hadronic energy scale across H1 and ZEUS measurements
  - Large pulls in correlated syst. uncert.

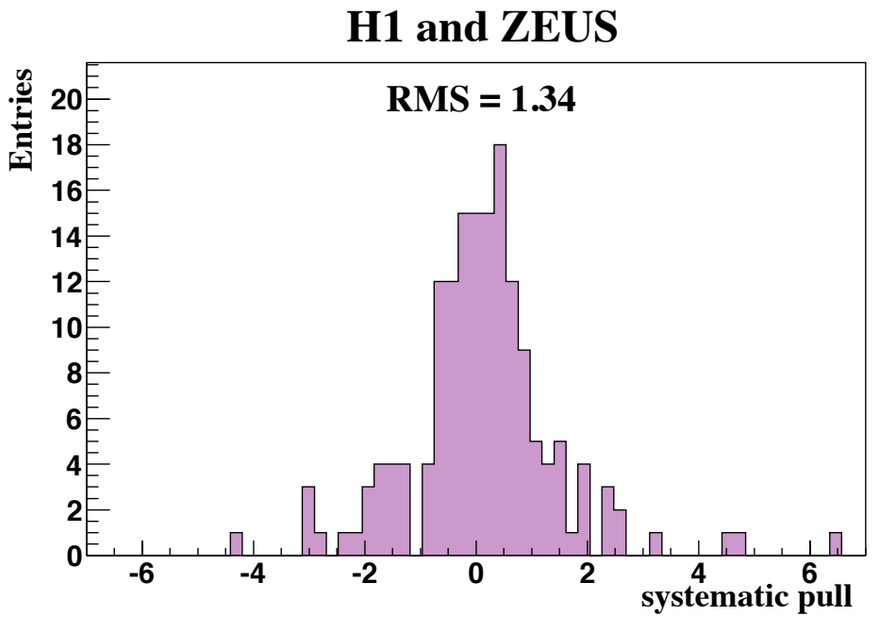

HERAFitter -> xFitter

experimental input

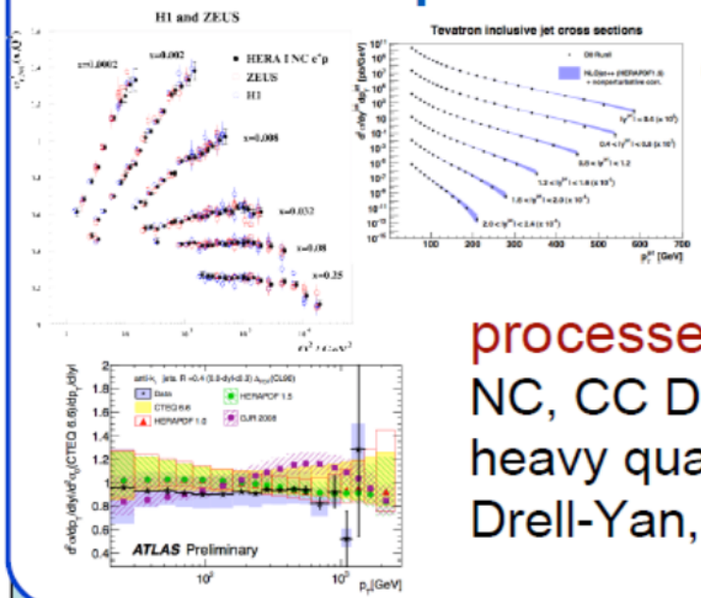

experiments:
HERA, Tevatron,
LHC, fixed target

processes:
NC, CC DIS, jets, diffraction,
heavy quarks (c,b,t)
Drell-Yan, W production

$\alpha_s(M_Z^2)=0.118$

theoretical calculations/tools

Heavy quark schemes:	MSTW, CTEQ, ABM
Jets, W, Z production:	fastNLO, Applgrid
Top production	NNLO (Hathor)
QCD Evolution	DGLAP (QCDNUM)
	k_T factorisation
Alternative tools	NNPDF reweighting
Other models	Dipole model

+ Different error treatment models
+ Tools for data combination (HERAaverager)

HERAFitter

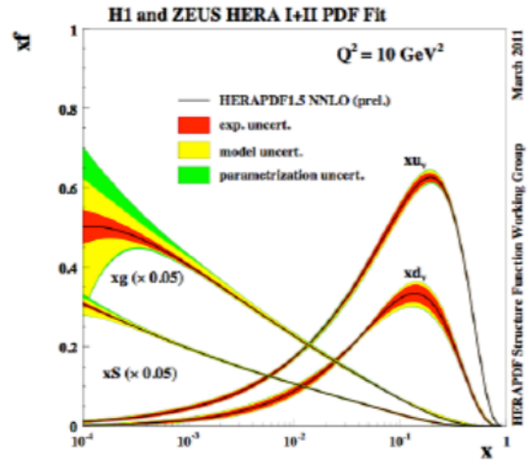

PDF or uPDF or DPDF

$\alpha_s(M_Z), m_c, m_b, m_t, f_s, ..$

Theory predictions

Benchmarking

Comparison of schemes

for more visit https://www.herafitter.org

HERAPDF2.0: Overview

HERAPDF approach:
DGLAP Analysis based only on HERA data. Several advantages:

- the final combined e±p NC and CC measurements are very precise
  so to allow the extraction of the parton densities at the starting scale

$$xd_v(x),\ xu_v(x),\ x\bar{U}(x),\ x\bar{D}(x) \text{ and } xg(x)$$

- the use of a single consistent data sample allows a more rigorous treatments of the experimental uncertainties

- because we do not use fixed target data there is no need for heavy-target/deuterium corrections or strong isospin assumptions

Previous HERAPDF Fits

Data	PDF Set
H1+ZEUS NC,CC - HERA I	***HERAPDF1.0 (NLO)***
H1+ZEUS NC,CC - HERA I +II (part)	***HERAPDF1.5 (NLO,NNLO)***

HERAPDF2.0: NLO and NNLO PDFs

NLO

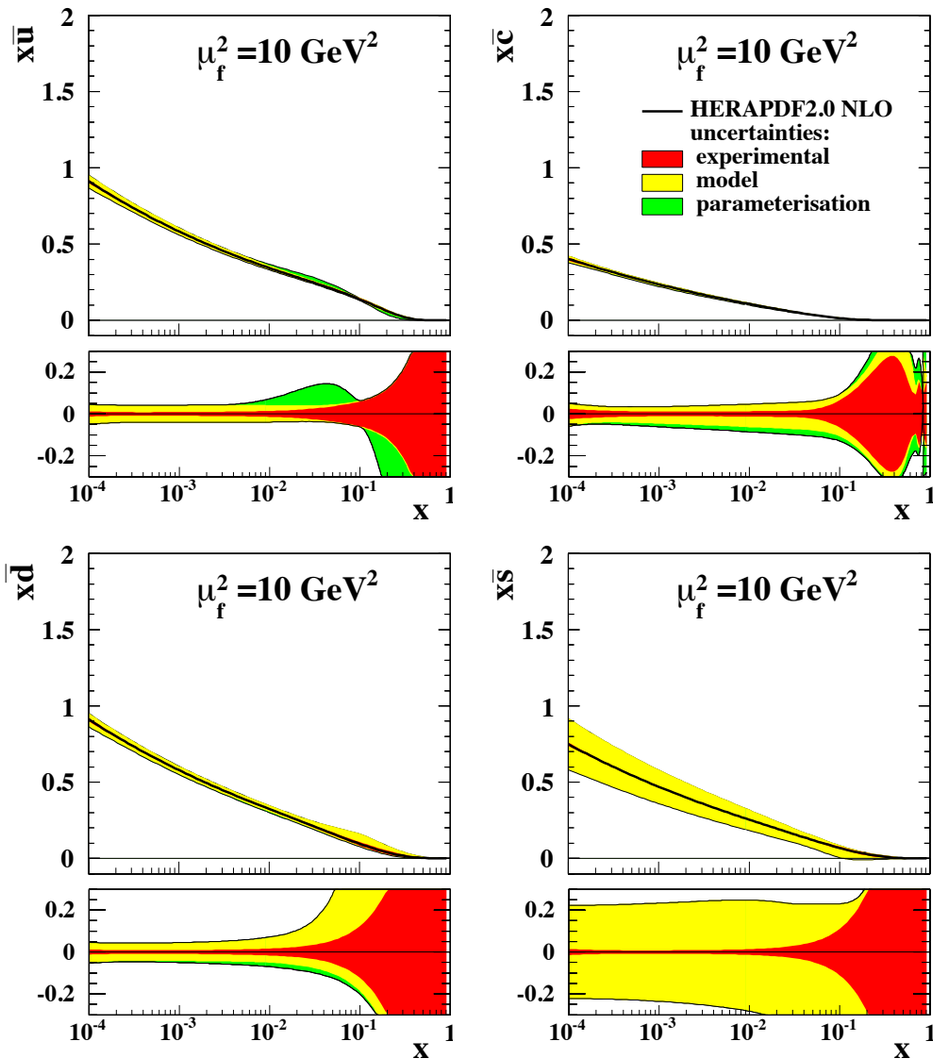

NNLO

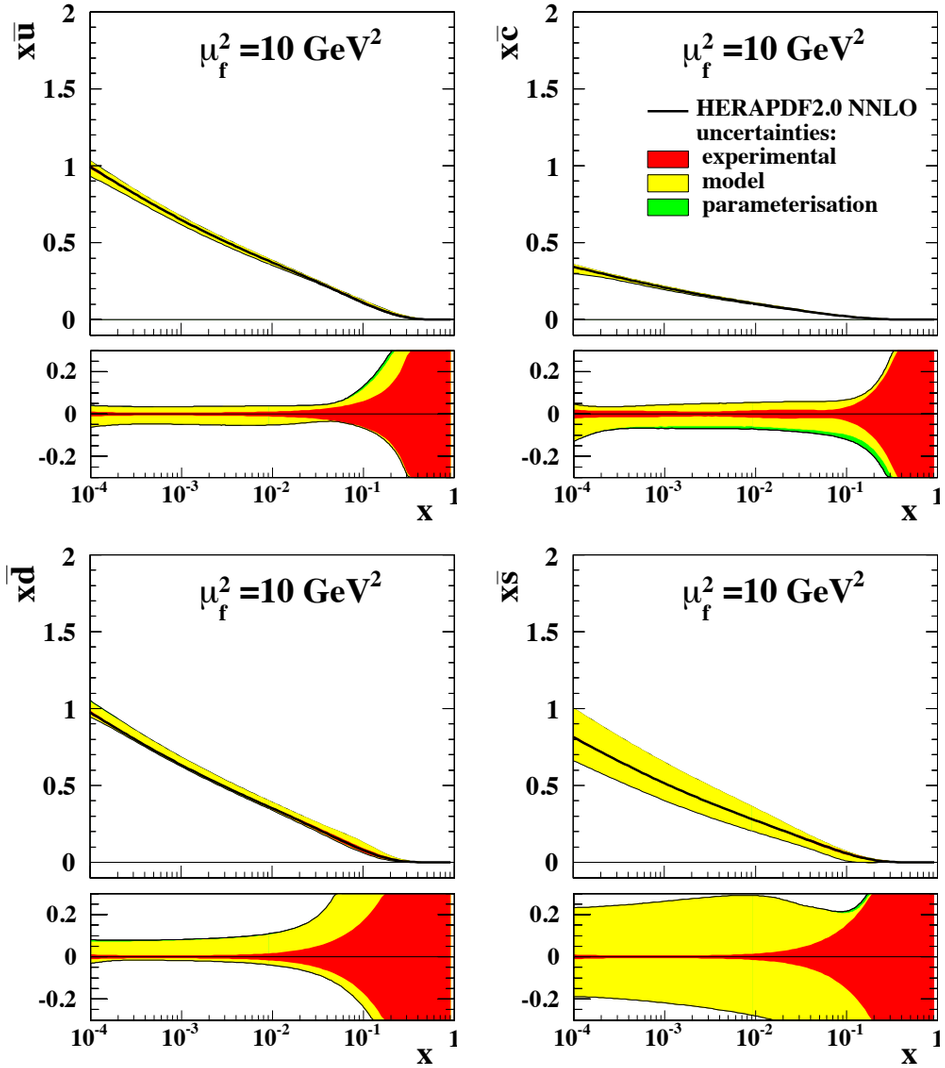

The flavour breakdown of the sea distribution

HERAPDF2.0: Comparison to other Global PDFs

NLO

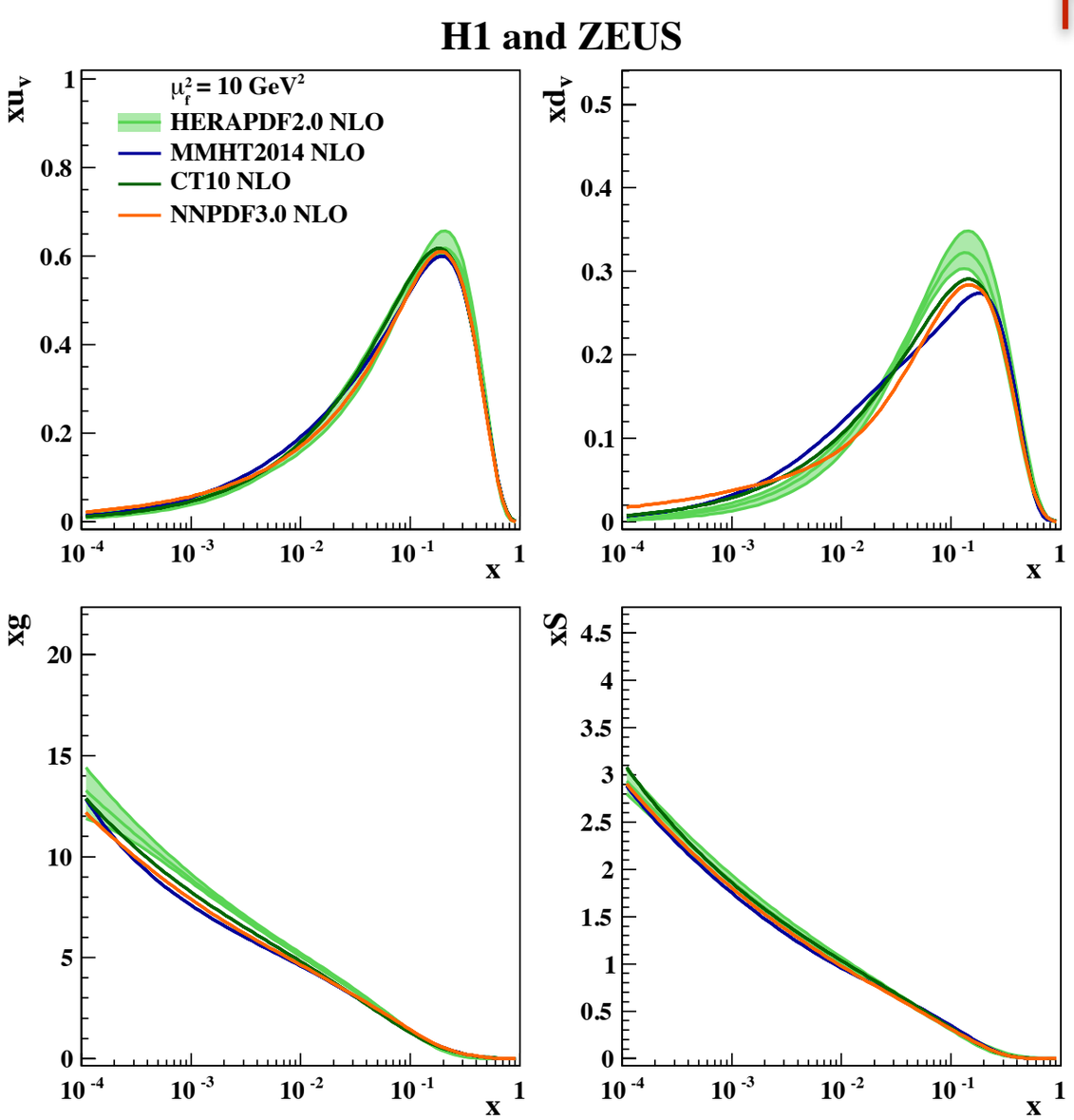

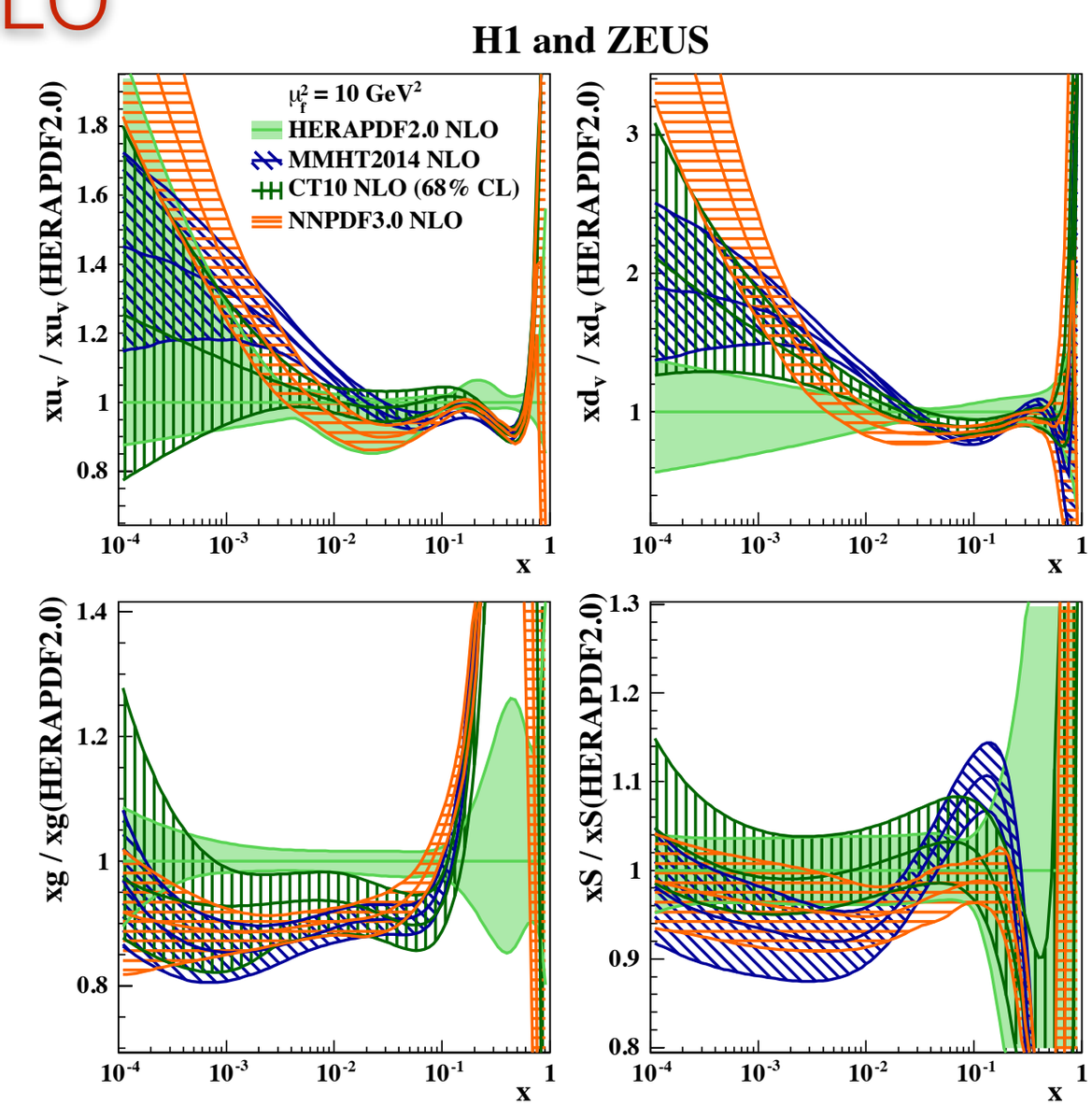

The HERAPDF2.0 are in general compatible with the global PDFs

- largest relative discrepancy (~2.5σ) in the shape of xu_v at x~0.4
- gluon distribution at high-x softer than that of the other PDFs

HERAPDF2.0:
Comparison to other Global PDFs (NNLO)

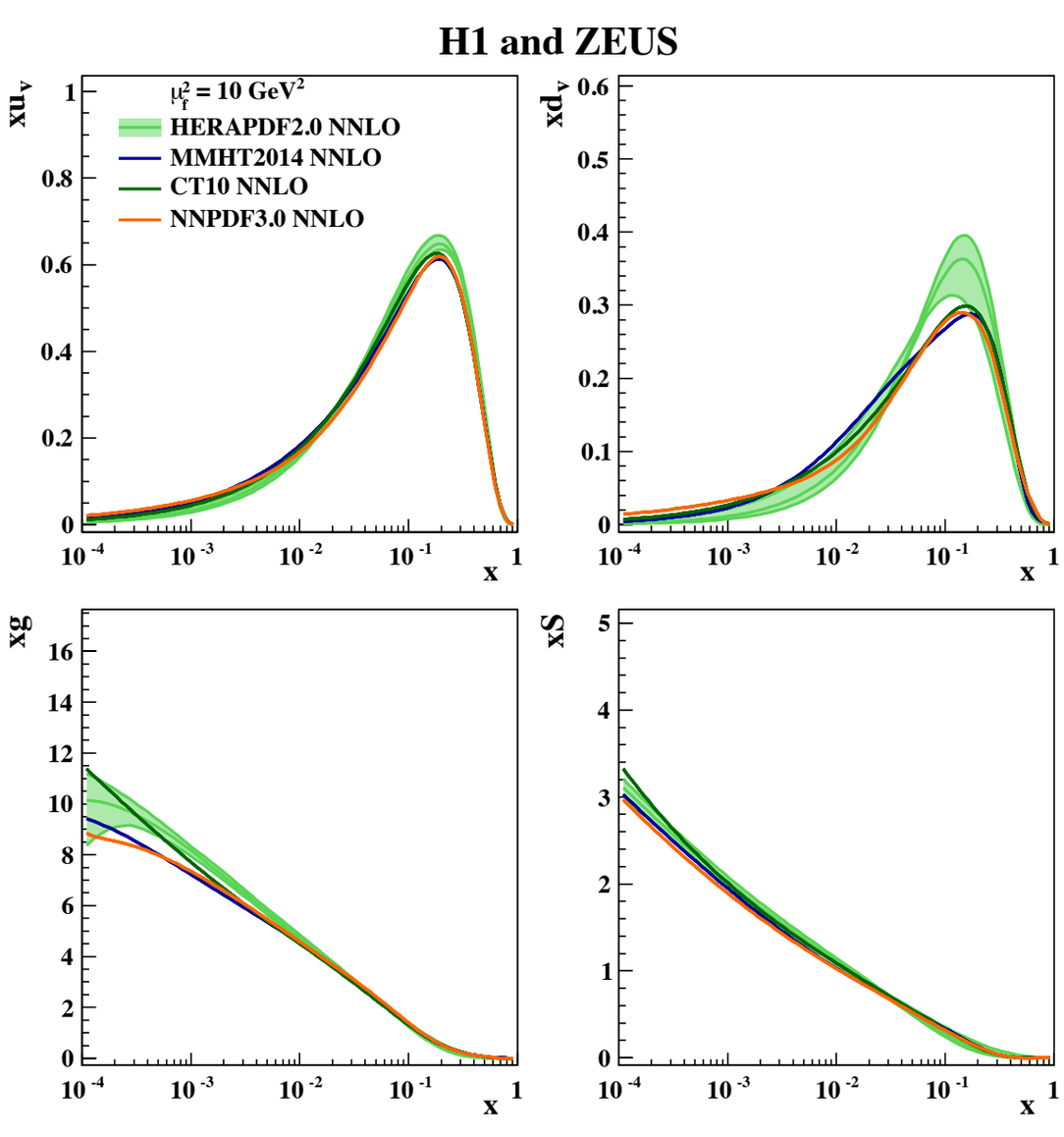

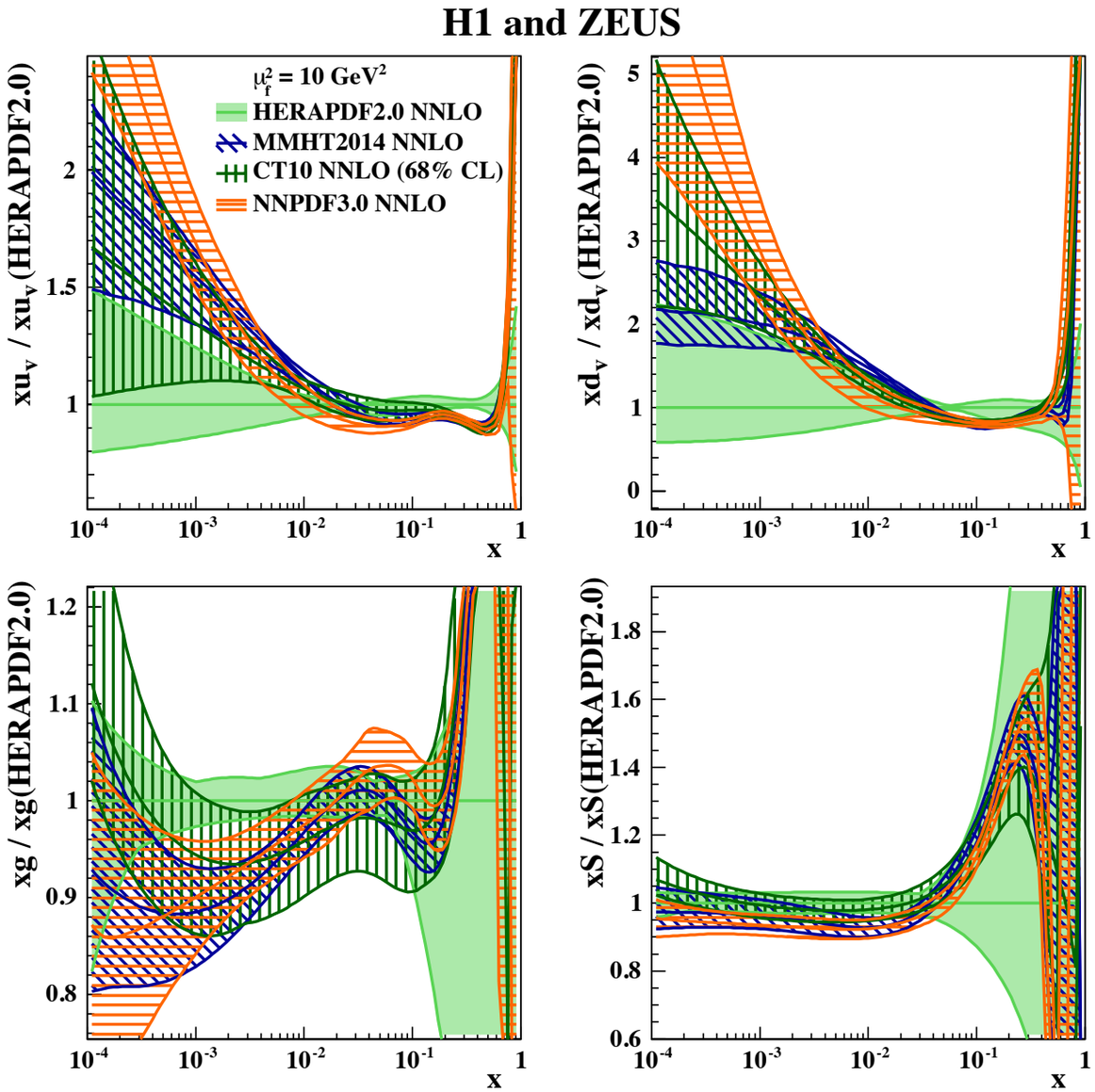

HERAPDF2.0AG LO vs NC e+p

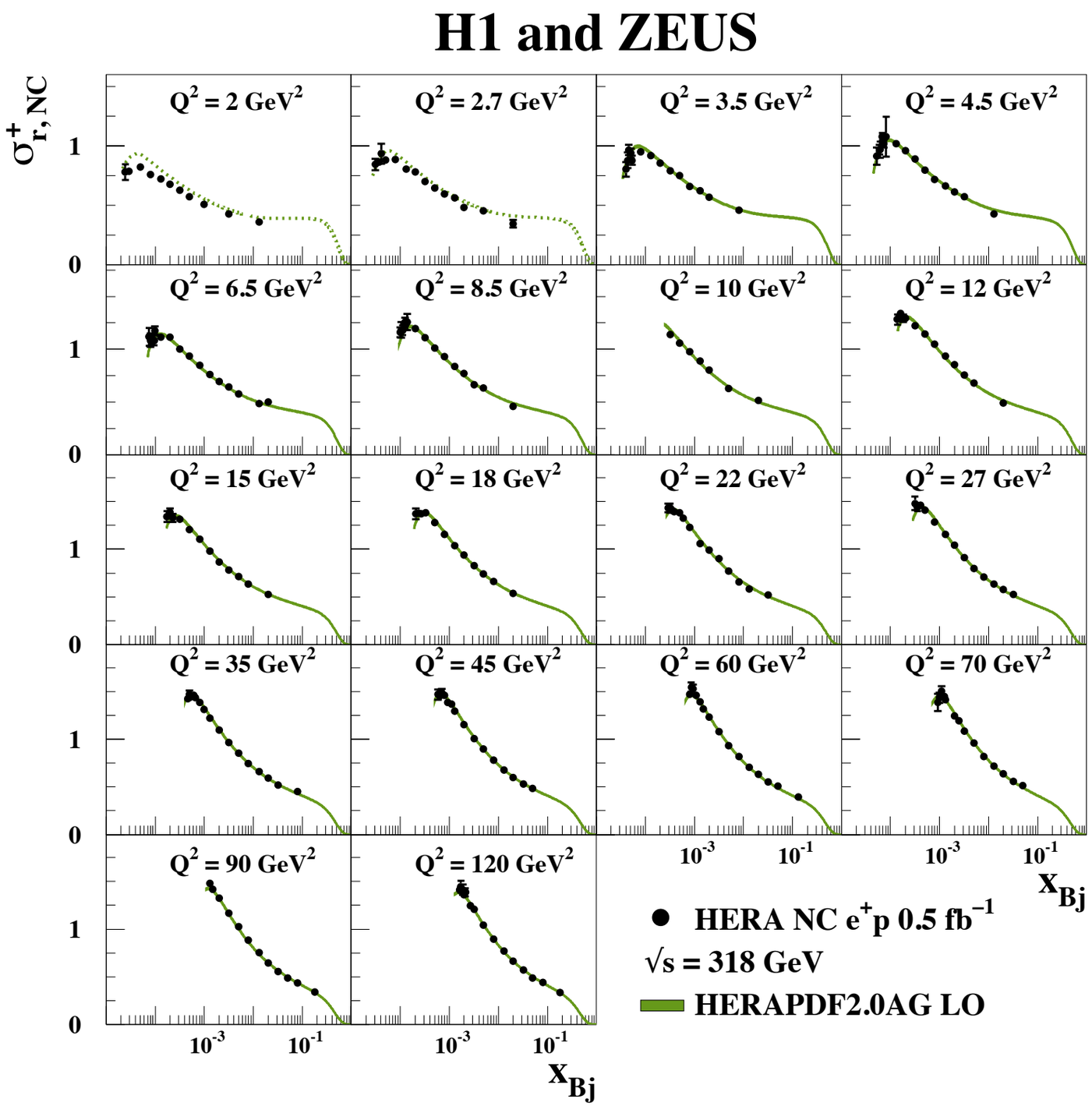

Comparison to inclusive HERA data

NC e^-p $\sqrt{s}$ =318 GeV

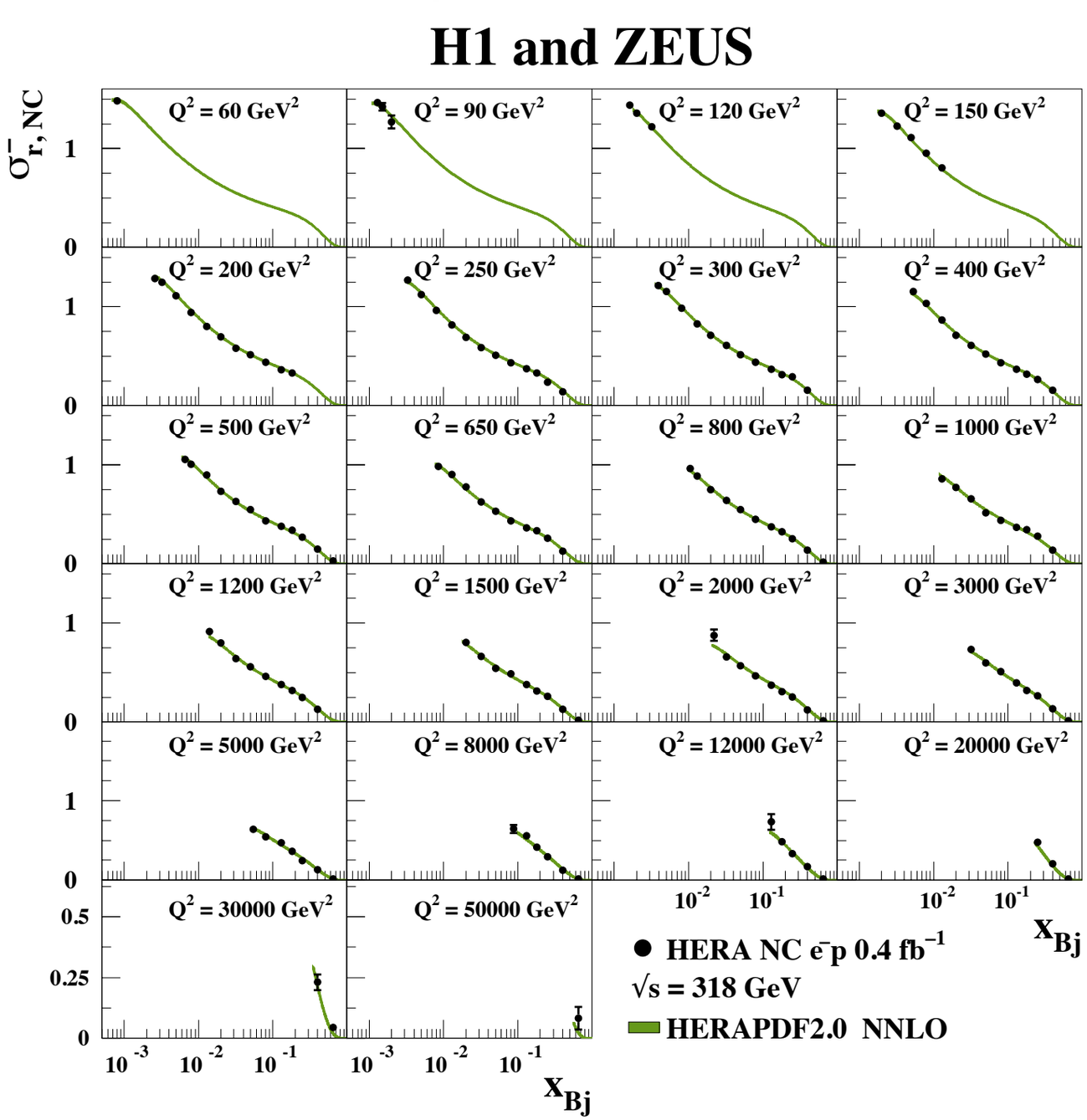

Very good description over entire probed phase space

HERAPDF2.0AG LO vs NC e+p

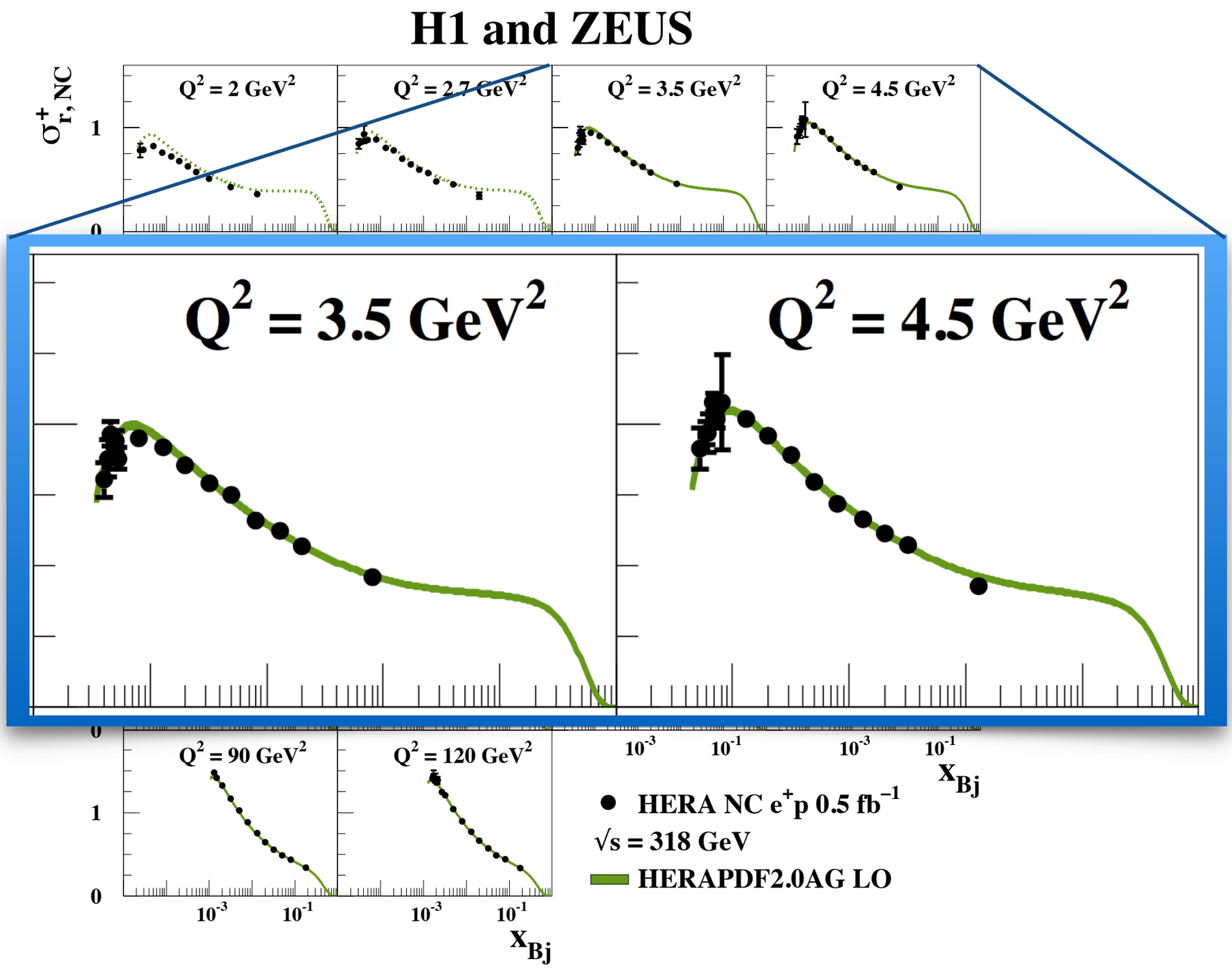

Helicity effects in CC interactions

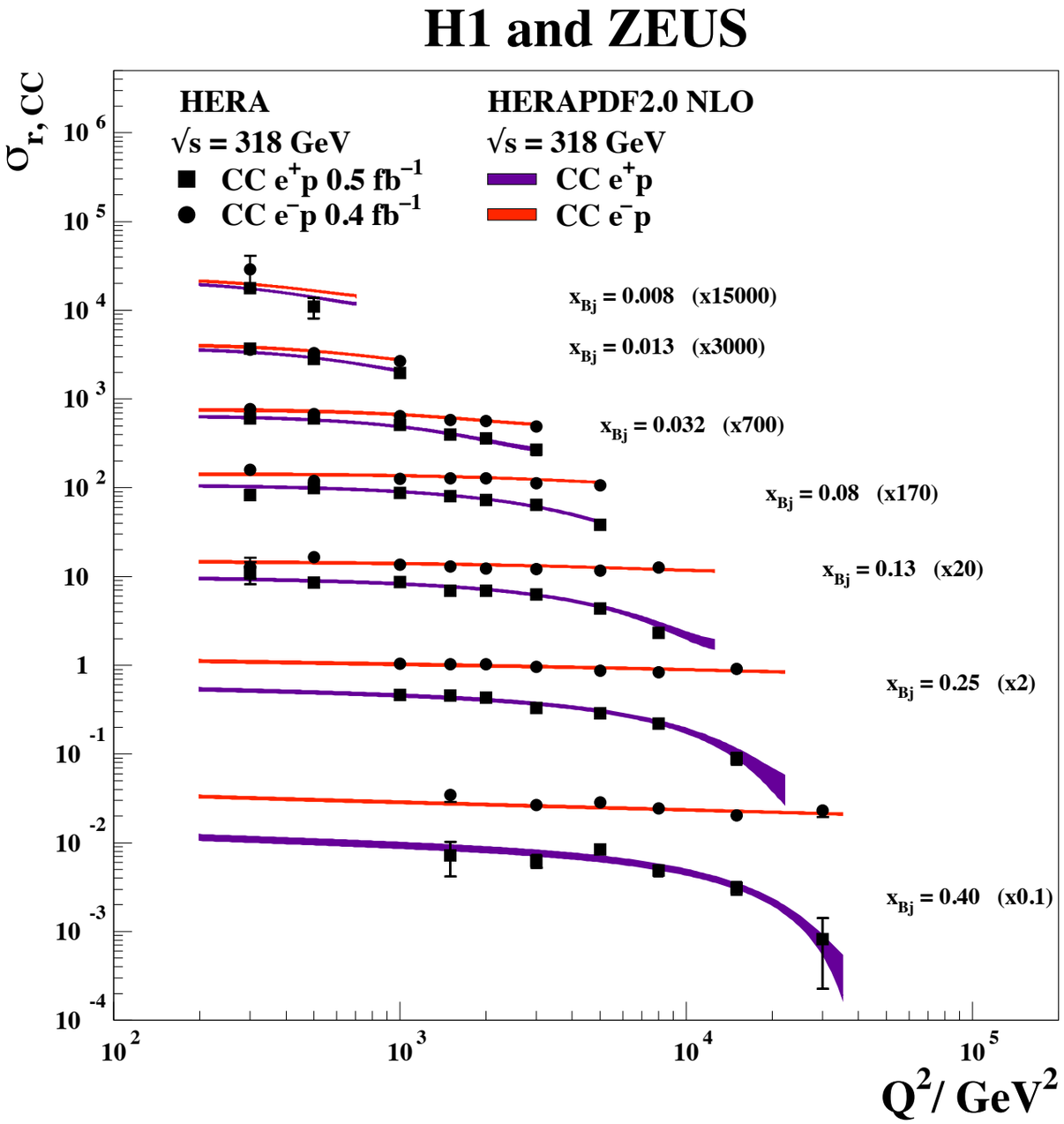

Reminder:

$$\sigma^{+}_{r,\mathrm{CC}} \approx (x\bar{U} + (1-y)^2 xD)$$

$$\sigma^{-}_{r,\mathrm{CC}} \approx (xU + (1-y)^2 x\bar{D})$$

The helicity factor $(1-y)^2$ affects differently the $e^{\pm}p$ CC cross sections:

- The $e^{+}p$ cross section is suppressed at high-y (high-Q^2)
- The $e^{-}p$ cross section is almost unaffected

The precision of the CC cross sections at high-Q^2 allow the study of these helicity effects.

HERAPDF2.0FF3A/3B

Two schemes with three active flavours in the PDFs:

- scheme FF3A:
  - Three-flavour running of α_S;
  - F_L calculated to $O(\alpha^2_S)$;
  - pole masses for charm, m_c^{pole}, and beauty, m_b^{pole};
- scheme FF3B:
  - Variable-flavour running of α_S .
  - massless (light flavour) part of the F_L contribution calculated to $O(\alpha_S)$
  - MSbar running masses for charm, $m_C(m_C)$, and beauty $m_b(m_b)$.